WISSENSCHAFTSZENTRUM WEIHENSTEPHAN
ENTWICKLUNGSBIOLOGIE DER PFLANZEN

TECHNISCHE UNIVERSITÄT MÜNCHEN

REGULATORY FEEDBACK BETWEEN AGC KINASES COORDINATING ARABIDOPSIS OVULE INTEGUMENT GROWTH

DISSERTATION

SEBASTIAN SCHOLZ

Freising

Januar 2018

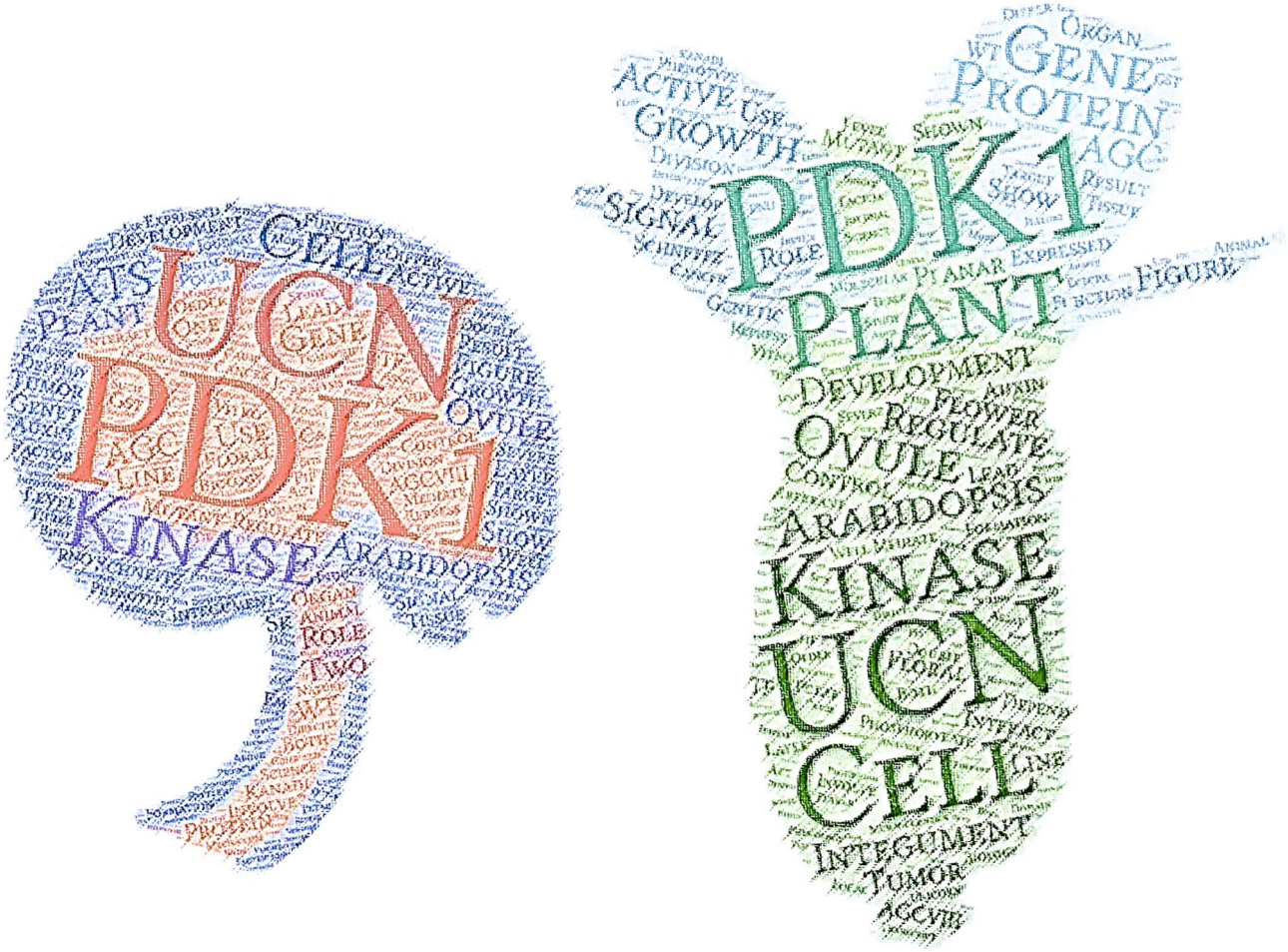

TECHNISCHE UNIVERSITÄT MÜNCHEN
Wissenschaftszentrum Weihenstephan
Professur für Entwicklungsbiologie der Pflanzen

Regulatory feedback between AGC kinases coordinating Arabidopsis ovule integument growth

SEBASTIAN SCHOLZ

Vollständiger Abdruck der von der Fakultät Wissenschaftszentrum Weihenstephan für Ernährung, Landnutzung und Umwelt der Technischen Universität München zur Erlangung des akademischen Grades eines

Doktors der Naturwissenschaften

genehmigten Dissertation.

Vorsitzender: Prof. Dr. ERWIN GRILL

Prüfer der Dissertation: 1. Prof. Dr. KAY H. SCHNEITZ

2. Prof. Dr. BRIGITTE POPPENBERGER-SIEBERER

Die Dissertation wurde am 18.01.2018 bei der Technischen Universität München eingereicht und durch die Fakultät Wissenschaftzentrum Weihenstephan für Ernährung, Landnutzung und Umwelt am 05.04.2018 angenommen.

"I AM A FIRM BELIEVER THAT WITHOUT SPECULATION THERE IS NO GOOD AND ORIGINAL OBSERVATION."

CHARLES DARWIN, 22 DECEMBER 1857

I. TABLE OF CONTENTS

I. TABLE OF CONTENTS 5

II. TABLE OF FIGURES 8

III. ABBREVIATIONS 10

IV. SUMMARY 13

V. ZUSAMMENFASSUNG 15

1 INTRODUCTION 17

1.1 Tissue morphogenesis and organogenesis in plants 17

1.1.1 Pattern formation during floral development 17

1.1.2 Ovule development 20

1.1.3 Arabidopsis ovules as model systems for organ development 22

1.1.4 Cell division plane and planar growth 23

1.1.5 Growth control and polarity determination: A concert of transcription factors 24

1.2 Protein kinases in plant development and physiology 25

1.2.1 AGC kinases and plant development 26

1.2.2 PDK1 – master of the AGCs? 27

1.2.3 UNICORN – a suppressor of ectopic growth 29

1.3 Tumorigenesis in animals and plants 31

1.3.1 Pathogen-induced tumors 32

1.3.2 Genetic tumors 33

1.3.3 (Phyto-) hormones in tumorigenesis 34

1.3.4 AGC kinases in tumorigenesis 35

1.4 Objectives 36

2 MATERIAL AND METHODS 37

2.1 Plant work, Plant Genetics and Plant Transformation 37

2.2 Recombinant DNA work 37

2.3 Quantitative real-time PCR 38

2.4 Reporter Constructs 38

2.5 CRISPR/Cas9 Constructs 38

2.6 Generation, Expression and Purification of Recombinant Proteins 39

2.7 In vitro kinase assay 40

2.8 Yeast Two-Hybrid assay 40

2.9 BiFC assay 40

2.10 In Situ Hybridization and Microscopy 41

2.11 Growth media, growth conditions and frequently used buffers 41

2.12 Bioinformatics 43

3 RESULTS 44

3.1 Characterization of the Arabidopsis AGC kinases PDK1.1 and PDK1.2 44

3.1.1 Structure-function properties of PDK1 and conservation between the two Arabidopsis PDK1 and PDK1 proteins of other plant species 44

3.1.2 PDK1 expression analysis 46

3.1.3 *pdk1* double knockout plants show a surprisingly mild phenotype 47

3.1.4 Subcellular distribution of PDK1:EGFP fusion proteins 49

3.2 Mechanism of *UCN*-mediated control of ovule and floral organ development via *PDK1* 52

3.2.1 The knockout of either *PDK1* gene almost completely rescues *ucn-1* 52

3.2.2 *PDK1* overexpression leads to a *ucn-1*-like phenotype 56

3.2.3 UCN regulates planar growth in ovule integuments and floral organ development through a direct negative regulation of PDK1 59

3.2.4 Relationship between *PDK1* and *ATS* 70

3.3 UCN phosphorylates serine residues of ATS in vitro 72

3.3.1 UCN still phosphorylates ATS-phosphomutants 73

3.3.2 UCN interacts with ATS-phosphomutants in plant cells 73

3.4 Generation of novel *ucn* alleles 77

3.4.1 Approach 77
3.4.2 Characterization of *ucn-11* 77

4 DISCUSSION 79

4.1 PDK1s – AGC master regulators of development? 79
4.1.1 Do other kinases substitute for the PDK1s? 80
4.1.2 PDK1 kinases control polarity in plant development 82

4.2 The role of *PDK1* in *UCN* signaling 83
4.2.1 How does *PDK1* relate to *ATS* with respect to *UCN* signaling? 85
4.2.2 PDK1 as a global player in UCN signaling 86

4.3 UCN-ATS interaction 88

4.4 CRISPR/CAS9 mediated genetic engineering – a powerful tool for the generation of novel mutants 88

5 CONCLUSION 90

6 REFERENCES 92

7 SUPPLEMENT 110

8 DANKSAGUNG 119

9 CURRICULUM VITAE 120

II. TABLE OF FIGURES

Figure 1-1 Overview of early flower development, the ABCE, and the quartet model of floral organ patterning. 19
Figure 1-2 Simplified cartoon depicting two stages of ovule development. 21
Figure 1-3 Planar growth aberrations in *ucn-1* ovules. 22
Figure 1-4 Phylogenetic tree of the Arabidopsis AGC kinase family. 27
Figure 1-5 Confocal micrographs of mPS-PI stained ovules depicting protrusion formation. 29
Figure 1-6 Floral phenotypes of *ap3 ucn*, *ag ucn* and *ap2 ucn* double mutants 30
Figure 1-7 *ucn ett* and *ucn ett arf4* ovules depict additive phenotypes 31
Figure 3-1 Schematic depiction of PDK1 domain structure. 44
Figure 3-2 Alignment of PDK1 protein sequences of different plant species. 45
Figure 3-3 Mean-normalized and absolute expression levels of *PDK1.1* (*At5g04510*) and *PDK1.2* (*At3g10540*). 46
Figure 3-4 Phenotypic characterization of *pdk1* T-DNA lines. 47
Figure 3-5 Subcellular localization of PDK1.2:EGFP fusion proteins in different tissues. 49
Figure 3-6 Subcellular localization of PDK1:EGFP 51
Figure 3-7 Restoration of floral and ovule phenotypes in *pdk1 ucn-1* double mutants. 53
Figure 3-8 *PDK1.1* and *PDK1.2* expression levels in flowers and stems of L*er* and *ucn-1*. 54
Figure 3-9 Whole mount in situ hybridizations. Stages of ovule organogenesis (anti-sense, from left to right): 2-V, 3-I to 3-II, and 3-VI; stages according to Schneitz et al. (1995). 55
Figure 3-10 Morphological phenotypes of *PDK1* over-expressors. 56
Figure 3-11 *PDK1.1* and *PDK1.2* expression in flowers of overexpression lines 58
Figure 3-12 Microscale thermo-phoresis (MST) measurements of MBP:PDK1$_{labeled}$ and GST:UCN. 60
Figure 3-13 Basic structure of UCN and PDK1 proteins. 61
Figure 3-14 In vitro kinase assays of active PDK1.1, PDK1.2 and five different UCN versions. 62
Figure 3-15 In vitro kinase assays of inactive PDK1 and active UCN. 63
Figure 3-16 Influence of increasing amounts of UCN on PDK1 activity. 65
Figure 3-17 Relative PDK1 phosphorylation with respect to UCN$_x$ levels. 66
Figure 3-18 PDK1-dependent UCN phosphorylation sites in vitro. 67
Figure 3-19 Yeast two-hybrid assay of AD:PDK1 versions combined with DB:UCN versions. 68
Figure 3-20 Bimolecular fluorescence comple-mentation assays in Arabidopsis mesophyll protoplasts 69
Figure 3-21 Confocal micrographs of mature ovules of (A) *sk21-D*, (B) *pdk1.1 sk21-D,* and (C) *pdk1.2 sk21-D.* 71
Figure 3-22 ATS phosphosites determined in a LC-MS/MS approach 72
Figure 3-23 UCN-mediated phosphorylation of ATS-phosphomutants. 73
Figure 3-24 Bimolecular fluorescence complemen-tation assays between UCN$_x$, PDK1 and ATS phosphomutants in Arabi-dopsis mesophyll protoplasts. 75
Figure 3-25 Stereo- and confocal micrographs depicting *ucn-11* phenotype, and *UCN* gene structure. 78

Figure 4-1 Simplified models of TOR signaling pathways in animals and plants. 81
Figure 4-2 Negative feedback loop of UCN activation and PDK1 repression. 84
Figure 4-3 Hypothetical model of the molecular mechanisms underlying the *UCN* signaling pathway in the control of planar growth. 87
Figure 7-1 Alignment of 29 PDK1 protein sequences of 27 different plant species. 112
Figure 7-2 *PDK1.1, PDK1.2* and *ACT8* transcript amounts in *pdk1* T-DNA lines and Col-0. 116
Figure 7-3 Root hair phenotypes. 117
Figure 7-4 Protein alignment of PDK1.1, PDK1.2, and At2g20050. 118

III. ABBREVIATIONS

3-AT	3-amino-1,2,4-triazole
AA	Amino acid
ab	abaxial
ad	adaxial
AD	Activation domain (of GAL4)
AGC	cAMP-, cGMP- and lipid-dependent protein kinases; named after PKA, PKG, and PKC
AIL6/PLT3	AINTEGUMENTA-LIKE 6/PLETHORA 3
ANT	AINTEGUMENTA
AP1, AP2, AP3	APETALA 1, 2, and 3
ARF	AUXIN RESPONSE FACTOR
ATS	ABERRANT TESTA SHAPE
ATXR7	ARABIDOPSIS TRITHORAX-RELATED 7
BiFC	Bimolecular fluorescence complementation
ca	Carpel
CaM	Calmodulin
CaMK	Ca2+/Calmodulin-dependent
cAMP	cyclic adenosine monophosphate
CBB	Coomassie brilliant blue
CDK	Cyclin-dependent kinase
cGMP	cyclic guanosine monophosphate
CLV1, CLV3	CLAVATA1, and 3
CMGC	Kinase group, named after CDK, MAPK, GSK, and Casein kinase
CNA	CORONA
Col-0	Columbia-0
CRISPR	Clustered regularly interspaced short palindromic repeats
CZ	Central zone
D6PK	D6 PROTEIN KINASE
DB	DNA-binding domain (of GAL4)
DIL	Double insertion line
DNA, cDNA, gDNA, T-DNA	Deoxyribonucleic acid, complementary DNA, genomic DNA, transfer DNA
DSB	Double strand break
EDTA	Ethylenediaminetetraacetic acid
EGFP	enhanced green fluorescent protein
ELA1	EUI-LIKE P450 A1
ETT	ETTIN
F1, F2, F3	Filial generations
FLC	FLOWERING LOCUS C
FM	Floral meristem
FT	FLOWERING LOCUS T
GA	Gibberellic acid
GAP	GTPase-activating protein
GDF	GDI-displacement factor
GDI	GDP dissociation inhibitor
GDP	Guanosine diphosphate
GEF	Guanosine exchange factor
gk	gurke
GSK	Glycogen synthase kinase
GST	Glutathione transferase
GTP	Guanosine triphosphate
HD-ZIPIII	Class III HOMEODOMAIN-LEUCINE ZIPPER
HMK	HEPES Magnesium chloride Kinase
ii	inner integument
IM	Inflorescence meristem
INO	INNER NO OUTER
IPTG	Isopropyl β-D-1-thiogalactopyranoside
K	Kelvin
KAN	KANADI
KD	Kinase deficient
Kn-1	Knotted-1
KO	Knockout
LB	Lysogeny broth
LC-MS/MS	Liquid chromatography-mass spectrometry/mass spectrometry
Ler	Landsberg erecta
LFY	LEAFY
LRR	Leucine rich repeat
MAPK	Mitogen-activated protein kinase
MBP	Maltose-binding protein

MMC	Megaspore mother cell
MP	MONOPTEROS
mPS-PI	modified Pseudoschiff-Propidium iodide
MS	Murashige Skoog
MST	Microscale thermophoresis
(m)TOR	(mammalian) TARGET OF RAPAMYCIN
(m)TORC	(mammalian) TOR complex
NDR	Nuclear dbf2-related kinases
NHEJ	Non-homologous end joining
OAK	OUTGROWTH ASSOCIATED KINASE
OC	Organizing center
OD	Optical density
oi	Outer integument
OX	Overexpression/overexpressor
OXI1	OXIDATIVE SIGNAL INDUCIBLE 1
p16	Promoter of AtRPL37aC gene (At3g60245)
PA	Phosphatidic acid
PAM	Protospacer adjacent motif
pas	pasticcino
PBP1	PID-BINDING PROTEIN 1
PBS	Phosphate buffered saline
pCaMV35S	Cauliflower mosaic virus 35S promoter
PCR, qPCR, RT-PCR	Polymerase chain reaction, quantitative PCR, reverse transcription PCR
PD	Plasmodesmata
PDK1	3-PHOSPHOINOSITIDE-DEPENDENT KINASE 1
pe	Petal
pEC	Eggcell specific promoter
pep	pepino
PH	Pleckstrin homology
PHB	PHABULOSA
PHOT	PHOTOTROPIN
PHV	PHAVOLUTA
PID	PINOID
PIF	PDK1-interacting fragment
PIN	PIN-FORMED
PK	Protein kinase
PKA	Protein kinase A
PKB	Protein kinase B
PKC	Protein kinase C
PKG	Protein kinase G
PPB	Pre-prophaseband
pUBQ	UBIQUITIN promoter
PZ	Peripheral zone
QUA2	QUASIMODO2
Rb	Retinoblastoma
RBR	RETINOBLASTOMA-RELATED
REV	REVOLUTA
RLCK	Receptor-like cytoplasmic kinase
RLK	Receptor-like kinase
RNA, mRNA, miRNA, sgRNA	Ribonucleic acid, messenger RNA, micro RNA, single guide RNA
RNO	RHINO
ROP	Rho of plants
S6K	40S ribosomal S6 kinase
SAM	Shoot apical meristem
SD	Synthetic defined
SDS	Sodium dodecylsulfate
se	Sepal
SEP	SEPALLATA
SHP1, SHP2	SHATTERPROOF1, and 2
SOC	Super optimal broth
st	Stamen
STK	SEEDSTICK
T1, T2, T3	Transgenic generations
TB	Terrific broth
TBE	Tris/Borate/EDTA
TF	Transcription factor
Trx	Thioredoxin
TSD/KOR	TUMOROUS SHOOT DEVELOPMENT/KORRIGAN
TUM	Technische Universität München
UCN	UNICORN
UTR	Untranslated region

VLCFA	Very-long-chain fatty acid
WT	Wildtype
WUS	WUSCHEL
Y2H	Yeast Two-Hybrid
YPD	Yeast extract peptone dextrose
ΔPIF	deleted PIF motif

IV. SUMMARY

The spatiotemporal orchestration of proliferation and growth is of paramount importance for the maintenance of distinct cell layers and tissue morphogenesis in plants. Single cell layers are maintained by proliferative cell divisions with the cell division plane stereotypically oriented in a strictly anticlinal fashion. This is referred to as planar growth. Disturbance of this process leads to periclinal or oblique divisions, which in turn introduce new cell layers and can result in tumor formation. The molecular mechanisms underlying planar growth control are poorly understood. Arabidopsis ovule integuments were shown to be excellent model tissues to study planar growth. Major advantages are their good accessibility, the relatively simple structure of the four integumental layers, and the high numbers of ovules per pistil. The AGCVIII kinase UNICORN (UCN) was shown to be of critical importance in the suppression of ectopic growth. The *ucn-1* mutant exhibits aberrant cell divisions in the ovule integuments eventually resulting in protrusion formation (Schneitz et al. 1997, Enugutti et al. 2012). Similar alterations can be observed in petals and stamens of *ucn-1* mutants (Enugutti et al. 2012). UCN was shown to suppress protrusion formation in integuments by directly repressing the KANADI transcription factor ABERRANT TESTA SHAPE (ATS) (Enugutti et al. 2012, Enugutti and Schneitz 2013). Other molecular components participating in the *UCN* signaling pathway have not been identified so far.

In this study, I present evidence that the two Arabidopsis 3-PHOSPHOINOSITIDE DEPENDENT KINASEs 1 (PDK1s) are components, which need to be repressed in the *UCN*-mediated signaling pathway. PDK1 is a central regulator of AGC kinases in animals and at least for some plant AGC kinases. Genetic analyses of *ucn pdk1* double mutants reveal that UCN acts as a negative regulator of both PDK1s. Interestingly, overexpression of either *PDK1* leads to *ucn-1*-like phenotypes with respect to integuments and petals. Furthermore, I demonstrate that both PDK1 proteins interact directly with UCN in vitro and in vivo.

My further findings indicate that PDK1 is able to phosphorylate UCN and vice versa. PDK1 is able to activate UCN through phosphorylation, and subsequent UCN-mediated PDK1 phosphorylation results in decreased PDK1 activity, which in turn is crucial for the ectopic growth suppression in ovule integuments and petals. Direct PDK1 suppression by another AGC kinase is a novel and unique feature in AGC kinase regulation. While ATS is only involved in the ovular aspect of *UCN* signaling, PDK1 plays a more global role. UCN mediated repression of ATS and PDK1 leads to the question about the relation between ATS and PDK1. I can demonstrate that PDK1 and ATS

do not interact directly in vivo most likely due to their spatial separation (ATS in the nucleus, PDK1 in the cytosol/at the plasma membrane). In addition, I propose a model for integument growth, in which ATS induces the expression of a gene whose resulting protein is a downstream target of PDK1.

V. ZUSAMMENFASSUNG

Die räumlich-zeitliche Koordination von Proliferation und Wachstum ist von entscheidender Bedeutung für die Aufrechterhaltung einzelner Zellschichten und die Gewebemorphogenese in Pflanzen. Einzelzellschichten werden durch proliferative Zellteilungen aufrechterhalten, wobei die Zellteilungsebene strikt antiklin orientiert ist. Dies wird als planares Wachstum bezeichnet. Eine Störung dieses Prozesses führt zu periklinen oder schrägen Zellteilungen, die wiederum neue Zellschichten einführen und zur Tumorbildung führen können. Die molekularen Mechanismen, die der planaren Wachstumskontrolle zugrunde liegen, sind nur wenig verstanden. Die Integumente der Samenanlage von *Arabidopsis* sind ausgezeichnete Modellgewebe, um planares Wachstum zu studieren. Große Vorteile sind die gute Zugänglichkeit und die relativ einfache Struktur der vier Integumentschichten, sowie die hohe Anzahl an Samenanlagen pro Fruchtknoten. Es wurde gezeigt, dass die AGCVIII-Kinase UNICORN (UCN) von entscheidender Bedeutung für die Unterdrückung ektopischen Wachstums ist (Schneitz et al. 1997, Enugutti et al. 2012). Die *ucn-1*-Mutante zeigt abweichende Zellteilungen in den Integumenten, was schließlich zu tumorähnlichen Auswüchsen führt. Ähnliche Veränderungen können in den Petalen und Stamina beobachtet werden (Enugutti et al. 2012). Es wurde gezeigt, dass UCN die Bildung der Auswüchse in den Integumenten durch direkte Repression des KANADI-Transkriptionsfaktors ABERRANT TESTA SHAPE (ATS) unterdrückt (Enugutti et al. 2012, Enugutti und Schneitz 2013). Andere am *UCN*-Signalweg beteiligte molekulare Komponenten wurden bislang nicht identifiziert.

In dieser Arbeit zeige ich, dass die beiden 3-Phosphoinosotid-abhängigen Kinasen (PDK1) Komponenten sind, die im *UCN*-vermittelten Signalweg reprimiert werden müssen. Genetische Analysen von *ucn-pdk1*-Doppelmutanten zeigen, dass UCN als negativer Regulator beider PDK1-Proteine fungiert. Interessanterweise führt die Überexpression beider *PDK1*-Gene unabhängig voneinander zu einem *ucn-1*-ähnlichen Phänotypen in Bezug auf die Integumente und Petalen. PDK1 ist ein zentraler Regulator von AGC-Kinasen in Tieren und zumindest für einige pflanzliche AGC-Kinasen. Darüber hinaus zeige ich, dass beide PDK1-Proteine *in vitro* und *in vivo* direkt mit UCN interagieren.

Meine Ergebnisse zeigen, dass PDK1 UCN phosphorylieren kann und umgekehrt. PDK1 ist in der Lage UCN durch Phosphorylierung zu aktivieren, und die darauffolgende UCN-vermittelte PDK1-Phosphorylierung führt zu einer verminderten PDK1-Aktivität, was wiederum entscheidend für die Suppression ektopischen Wachstums in den Integumenten und Petalen ist. Die direkte

PDK1-Unterdrückung durch eine andere AGC-Kinase ist ein neues und einzigartiges Merkmal der AGC-Kinase-Regulation. Während ATS nur in der Samenanlage in den *UCN*-Signalweg involviert ist, spielt PDK1 im Vergleich eine globalere Rolle. Die UCN-vermittelte Repression von ATS und PDK1 führt zu der der Frage nach der Beziehung zwischen ATS und PDK1. Ich kann zeigen, dass PDK1 und ATS in vivo nicht miteinander interagieren, höchstwahrscheinlich auf Grund ihrer räumlichen Trennung (ATS im Zellkern und PDK1 im Cytosol/an der Plasmamembran). Zusätzlich schlage ich ein Modell für das Wachstum von Integumenten vor, bei dem ATS die Expression eines Gens induziert, deren resultierendes Protein nachgeordnetes Ziel von PDK1 ist.

1 INTRODUCTION

1.1 Tissue morphogenesis and organogenesis in plants

Plant organogenesis occurs mostly in a post-embryonical fashion. In contrast to animals, the plant embryo develops into a seedling with simple architecture. Aboveground lateral organs ultimately originate from the shoot apical meristem (SAM), which gives rise to leaves, shoot branches and, once switched to the reproductive phase of the plant's life cycle, eventually to flowers. The spatiotemporal coordination of cell elongation and proliferation is of crucial importance for the maintenance of distinct cell layers and tissue morphogenesis.

1.1.1 Pattern formation during floral development

The outgrowth of primordia and the determination of organ identity is strictly controlled. The SAM develops into an inflorescence meristem (IM), producing floral primordia that develop into floral meristems (FMs), from which floral organs, such as sepals, petals, stamens and carpels, finally arise ((Miksche and John 1965, Coen and Meyerowitz 1991), Figure 1-1, a). Shoot and floral meristems are organized into several distinct zones. The central zone (CZ) comprises infrequently dividing stem cells that are innately undifferentiated. The organizing center (OC) beneath the stem cells supplies a cell niche necessary for stem cell induction and maintenance. At the flanks of the CZ, progeny of the stem cells ends up in the peripheral zone (PZ) where cell division occurs at higher rates and floral organs arise (Figure 1-1, b). Moreover, the meristems consist of three distinct cell layers (Satina et al. 1940) that are maintained by certainly oriented cell division. The two outermost layers, i.e. L1 (epidermal) and L2 (sub-epidermal), divide strictly perpendicular to the surface of the meristem (anticlinal cell division), the innermost L3 core divides in an apparently rather random fashion (Figure 1-1, b). Organ formation is triggered by local auxin maxima in the L1 of the PZ (Reinhardt et al. 2000, Reinhardt et al. 2003, Heisler et al. 2005). Auxin is produced throughout the meristem (Pinon et al. 2013) and actively redistributed in a PIN-FORMED (PIN)-dependent polar fashion to the sites of organ initiation (Grunewald and Friml 2010). The PINs are activated through phosphorylation by plasma membrane (PM)-associated AGCVIII kinases, such as PINOID (PID) and D6 PROTEIN KINASE (D6PK) (Zourelidou et al. 2014). Basipetal reorganization

of the PINs leads to the formation of an auxin sink, and auxin accumulation in the interior of the initiated floral primordium (Heisler et al. 2005, Bayer et al. 2009).

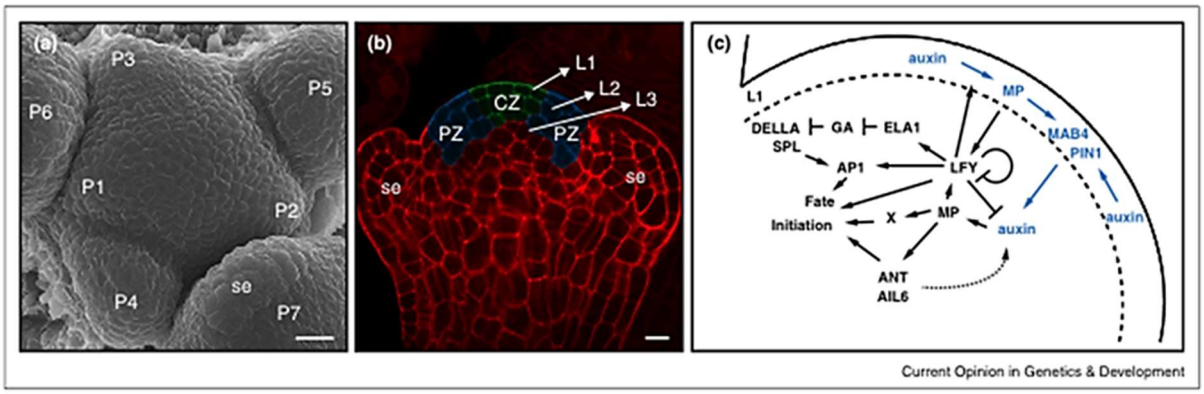

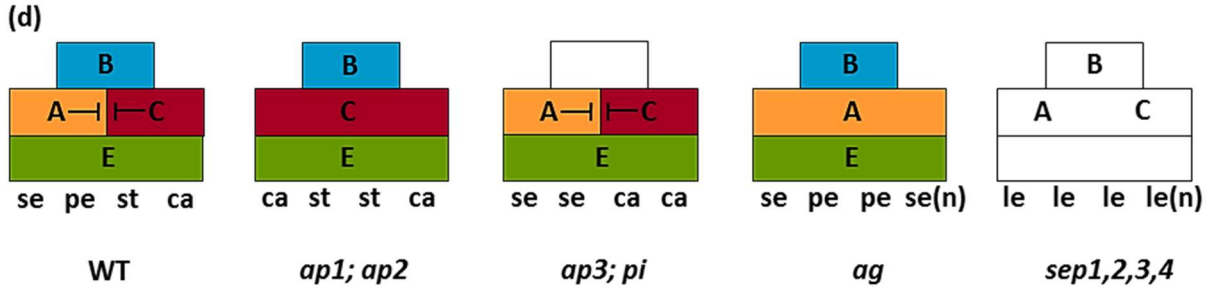

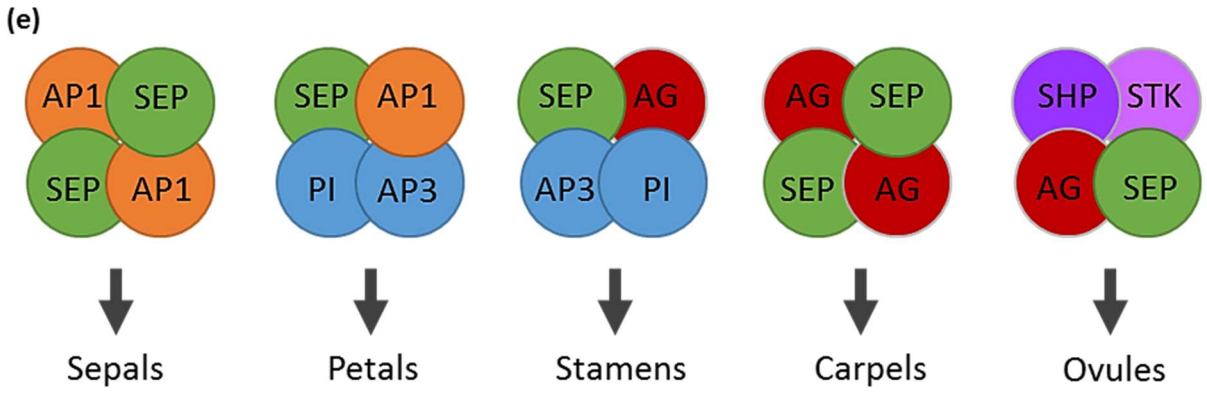

Figure 1-1 Overview of early flower development, the ABCE, and the quartet model of floral organ patterning.

(a) Scanning electron micrograph of an Arabidopsis shoot apical meristem with indicated floral primordia of different stages (youngest P1 to oldest P7). A sepal (se) primordium is shown in P7. (b) Confocal micrograph of a mid-optical vertical section of a stage 3 floral meristem. Sepal (se) primordia at the flanks are indicated. CZ, central zone; PZ, peripheral zone; cell layers L1 – L3 are indicated. Scale bars: 10 µm. (c) Cartoon depicting floral fate initiation by the interplay of auxin, MP, LFY, and GA. (a – c) from Vaddepalli et al. (2015). (d) The ABCE model of floral organ patterning, adapted from Krizek and Fletcher (2005). Arabidopsis WT flowers consist of four whorls. In the first whorl, class A activity confers sepal (se) identity, petal (pe) identity is conferred by class A and B activity, class B and C activity confers stamen (st) identity, and carpel (ca) identity is conferred by class C activity. Class A and C repress each other as indicated. Loss of class A identity in *apetala1* (*ap1*) or *ap2* mutants leads to expansion of class C activity, and transforms se into ca and pe into st. Loss of class B activity in *ap3* or *pistillata* (*pi*) mutants transforms pe into se and st into ca. Flowers of the *agamous* (*ag*) mutant lacking class C activity consist of reiterative patterns of se, pe, pe, se by expansion of class A activity and loss of floral determinacy. The *sepallata1 – 4* (*sep1,2,3,4*) quadruple mutant consists of reiterations of leaf-like (le) organ whorls. Loss of class E activity results in impaired class A, B, C functions and loss of floral determinacy. *SEEDSTICK* (*STK*), *SHATTERPROOF1* (*SHP1*) and *SHP2* were identified as ovule-specifying factors (D function). (e) Floral quartet model, adapted from Theißen et al. (2016). Floral organ identity is specified by the formation of organ-specific tetrameric complexes, which bind to two adjacent *cis*-regulatory elements of the DNA.

As shown in Figure 1-1c, the auxin response transcription factor (TF) MONOPTEROS (MP) activates several genes, including the transcription factors LEAFY (LFY), AINTEGUMENTA (ANT) and AINTEGUMENTA-LIKE6/PLETHORA3 (AIL6/PLT3), in an auxin-dependent fashion (Yamaguchi et al. 2013). In turn, LFY activates a central regulator of flower identity, the MADS-domain transcription factor APETALA1 (AP1) (Wagner et al. 1999), and represses the negative effect of gibberellic acid (GA) by positively regulating EUI-LIKE P450 A1 (ELA1) (Yamaguchi et al. 2014). Moreover, LFY, ANT and AIL6 share overlapping functions in floral fate determination (Weigel et al. 1992, Weigel and Nilsson 1995, Krizek 1999, Mizukami and Fischer 2000, Krizek and Eaddy 2012). The initiated FM is organized through a negative feedback loop (Fletcher et al. 1999, Brand et al. 2000). *WUSCHEL* (*WUS*), a homeodomain TF gene, is expressed in the OC and the WUS protein moves to the CZ, where it specifies stem cell fate in a non-cell autonomous manner (Yadav et al. 2011). WUS directly represses expression of the receptor-like kinase (RLK) gene *CLAVATA1* (*CLV1*), and activates its own negative regulator, the signal peptide CLAVATA3 (CLV3) (Busch et al. 2010, Yadav et al. 2011). Furthermore, WUS affects cytokinin signaling (Leibfried et al. 2005), and represses several differentiation-promoting TFs (Yadav et al. 2013).

Floral organ identity is conferred through the combinatorial action of a set of transcription factors, which except for *APETALA2* (*AP2*) belong to the MIKC-type MADS-domain TFs (Irish 2010). The ABCE-model in Figure 1-1d depicts the interplay between those TFs in floral organ

specification. *APETALA1* (*AP1*) and *AP2* provide class A function, B function is mediated by *AP3* and *PISTILLATA* (*PI*), and C function by *AGAMOUS* (*AG*) (Yanofsky et al. 1990, Mandel et al. 1992, Jack et al. 1992, Goto and Meyerowitz 1994, Jofuku et al. 1994). *SEEDSTICK* (*STK*), *SHATTERPROOF1* (*SHP1*) and *SHP2* mediate class D function for ovule identity (Angenent and Colombo 1996, Favaro et al. 2003, Pinyopich et al. 2003). As shown in Figure 1-1e, The *SEPALLATA* genes *SEP1, SEP2, SEP3* and *SEP4* contribute to the identity of all floral organs (Pelaz et al. 2000, Pelaz et al. 2001, Ditta et al. 2004). Class A and E activity results in sepal (se) identity, petals (pe) are determined by the activity of classes A, B, E. Stamina are specified by B, C and E activity, C and E specify carpels and C, D, and E specify ovules (reviewed in Theißen (2001), Krizek and Fletcher (2005), Ó'Maoiléidigh et al. (2014), Theißen et al. (2016).

1.1.2 Ovule development

The plant's life cycle is alternating between a haploid (gametophyte) and a diploid generation (sporophyte). Meiosis in plants generates haploid spores, which undergo differentiation and proliferation to give rise to the gametophytes. In turn, the gametophytes produces haploid gametes. The life cycle is completed by the fusion of egg cell and sperm cell producing the sporophyte (Raven et al. 1992). The ovule represents the major female reproductive organs in spermatophytes, and consists in principle of three functional domains: the nucellus containing the female gametophyte, the chalaza that gives rise to the integuments eventually surrounding the nucellus, and a stalk, called funiculus, representing the connective tissue to the placenta. Since the ovule contains the egg cell, and upon fertilization, it develops into seeds, the understanding of the molecular mechanisms controlling ovule development is of pivotal importance. Ovule ontogenesis has been well described during the last decades of research (Mansfield and Briarty 1991, Robinson-Beers et al. 1992, Modrusan et al. 1994, Schneitz et al. 1995, Schneitz et al. 1997, Grossniklaus and Schneitz 1998, Drews et al. 1998, Schneitz et al. 1998, Gasser et al. 1998, Schneitz 1999, Truernit and Haseloff 2008, Cucinotta et al. 2014), and a staging system has been conceived (Schneitz et al. 1995).

The ovule originally arises as a finger-like protuberance from the placental tissue (stages 1-I/II of ovule development, stages according to Schneitz et al. (1995)). At the distal end of the primordium (nucellus), a single hypodermal cell develops into the megaspore mother cell (MMC) (stage 2-I). Subsequently, the MMC undergoes meiosis in order to form a tetrad of haploid megaspores (stage 2-V). The three distal ones degenerate resulting in a single viable megaspore that gives rise to a multicellular embryo sac or female gametophyte (including the egg cell). During stages 2-II/III an outer and an inner integument initiate, which are of epidermal origin and will form two sheets each consisting of two layers (an adaxial and an abaxial cell layer), and eventually enclosing the nucellus completely. Embryo sac formation within the nucellus and integument maturation take place during stages 3-I to 3-VI. As described before, only the most proximal megaspore survives and forms the embryo sac comprising seven cells (three antipodal cells, a central cell and an egg cell, and two synergids). The asymmetric growth of the integuments determines the typical curvature and therefore the final amphitropous configuration of the ovule (Figure 1-2). The vasculature within the funiculus has emerged by the end of stage 3. The last main stage 4 (stages 4-I to 4-V) involves fertilization, as well as initial parts of endosperm development and embryogenesis.

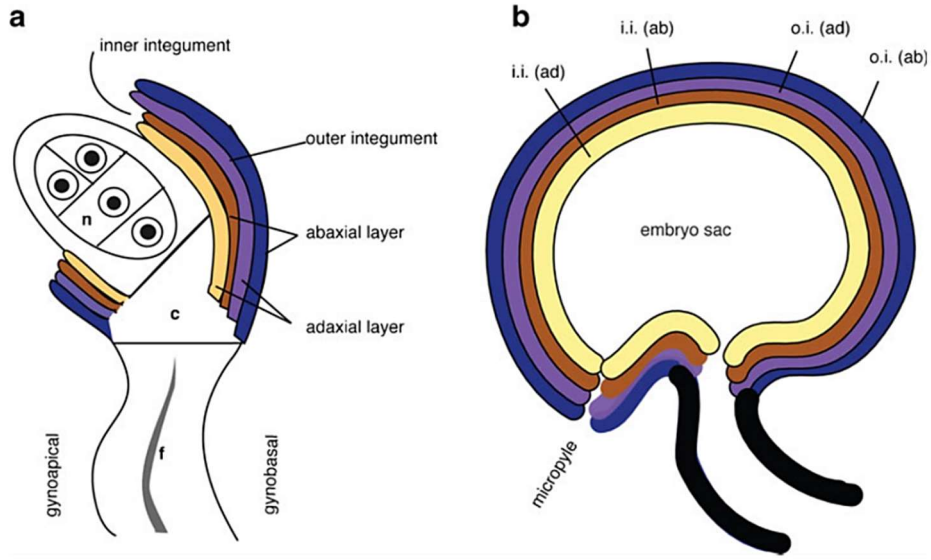

Figure 1-2 Simplified cartoon depicting two stages of ovule development.

(a) Ovule at stage 2-V (Schneitz et al. 1995). Two layers of each, inner and outer integument, initiated from the chalazal flanks and continue growth to eventually surrounding the nucellus. (b) Mature ovule displaying the typical amphitropous shape. Integuments envelop the embryo sac. *c* chalaza, *f* funiculus, *n* nucellus, *i.i.* inner integument, *o.i.* outer integument, *(ab)* abaxial, and *(ad)* adaxial cell layer. Figure from Enugutti et al. (2013), adapted from Truernit and Haseloff (2008).

1.1.3 Arabidopsis ovules as model systems for organ development

Due to their good accessibility, their relatively simple structure and the high number of developmentally independent organs (~ 50 ovules per WT pistil), Arabidopsis ovules are an excellent model system to study organ development, and their integuments represent excellent tissues to investigate planar growth. The ovule comprises two integuments each consisting of two layers eventually giving rise to the seed coat. An initial asymmetric division at the flanks of the chalazal region of the young ovule is followed by subsequent symmetric and strictly anticlinal cell division events generating the four single cell layers of integuments. In the last stage (3-VI) of ovule development before fertilization cells of the adaxial inner integument undergo periclinal divisions to give rise to an additional single cell layer, the inner integument 1' (ii1') (Schneitz et al. 1995). 35% of Col-0 and 70% of Wassilewskija ovules exhibit a sixth integument cell layer (ii1''), which derives from additional periclinal divisions in ii1' at stage 3-VI/4-I transition (Coen et al. 2017). Mutants impaired in correct cell division orientation can help to elucidate the underlying molecular mechanisms coordinating planar growth. Initially discovered in an EMS screen for identifying ovule mutants (Schneitz et al. 1997), *UNICORN* (*UCN, At1g51170*) was found to encode for an active AGCVIII protein kinase suppressing aberrant cell divisions in integuments (confer Figure 1-3), and other lateral organs by directly repressing the KANADI TF ABERRANT TESTA SHAPE (ATS) (Enugutti et al. 2012, Enugutti et al. 2013).

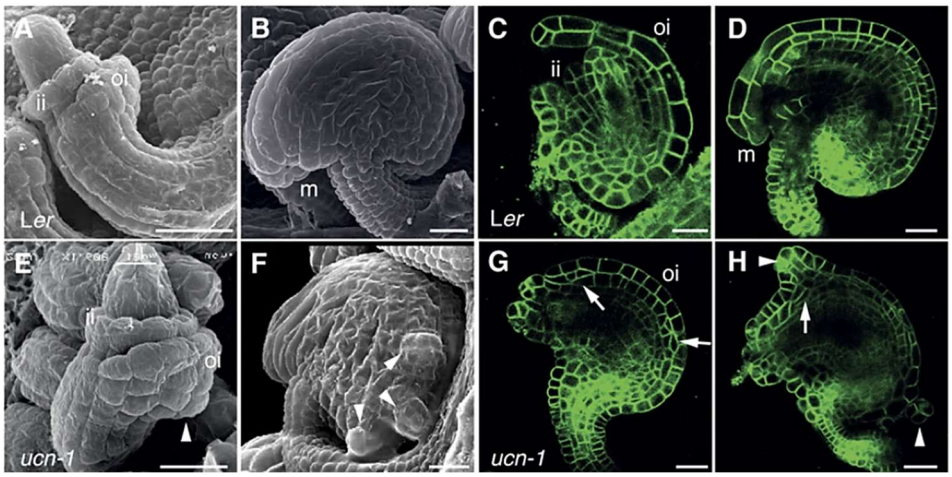

Figure 1-3 Planar growth aberrations in *ucn-1* ovules.

(A - D) L*er* WT. (A and B) Scanning electron micrographs of (A) stage 2-VI and (B) stage 4 WT ovules. (C and D) Confocal micrographs of (C) stage 3-I, and (D) stage 4 WT ovules expressing the plasma membrane marker *pUBQ::EGFP:LTI6B;* ii, inner integument; oi, outer integument; m, micropyle. (E – H) *ucn-1* ovules of similar stages as in A – D. Arrowheads indicate protrusions, and arrows indicate aberrant cell divisions in the integuments. Scale bars: 20 µm. Figure from Enugutti et al. (2012).

1.1.4 Cell division plane and planar growth

Planar growth crucially depends on cell divisions and molecular mechanisms correctly orienting the division plane relative to the surrounding cell layers. In contrast to animal cells, plant cells are surrounded by a rigid cell wall and therefore immobile. Novel cell layers needs to be initiated by defined orientations of the division planes (parallel or oblique to the surface of the tissue). The same holds true for the maintenance of distinct cell layers but, in contrast, the division plane needs to be oriented perpendicular to the surface. This strictly anticlinal and symmetric division behavior, in which periclinal and oblique divisions are repressed, leads to the propagation of a certain cell layer, for which cell division is oriented within the plane of the layer (planar growth) (Tilney-Bassett 1986). In the last decade, impressive progress in understanding the control of asymmetric cell division has been made (Abrash and Bergmann 2009, Petricka et al. 2009, De Smet and Beeckman 2011). The division plane orientation in symmetrically dividing cells can be predicted by mathematical models involving cytoskeleton dynamics and cell geometry (Besson and Dumais 2011). Cell geometry and the behavior of adjacent cells lead to distinct tensile stress patterns, and cortical microtubules align along maximal tensile stress in cell walls (Hamant et al. 2008, Besson and Dumais 2011, Sampathkumar et al. 2014). The future plane of division correlates with the orientation of the preprophase band (PPB), which consists of actin filaments, the ring of aligned cortical microtubules, organelles, and various proteins associated with organelles or the cytoskeleton appears at the position of the division plane. The PPB emerges in G2 phase of the cell cycle as a broad band of microtubules, and narrows during prophase by actin-mediated connection of adjacent microtubules (Mineyuki and Palevitz 1990, Takeuchi et al. 2016). It remains unknown if the PPB itself actively determines the division plane or if yet unidentified signals locate the PPB to the position of the later division plane. It was shown recently, that the PPB controls the robustness of division orientation by increasing the accuracy of spindle adjustment (Ambrose and Cyr 2008, Schaefer et al. 2017). Furthermore, the PPB positioning is directly dependent on the position of the nucleus within the mother cell (Murata and Wada 1991, Mineyuki et al. 1991). In late prophase, the nuclear membrane disassembles and acentriolar spindle formation occurs. Subsequently, the chromosomes align at the division plane in metaphase, and the central spindle emerges in anaphase at the position of the metaphase chromosomes. Detailed information is reviewed in, e.g. Lipka et al. (2015), Smertenko et al. (2017).

1.1.5 Growth control and polarity determination: A concert of transcription factors

The development of lateral organs is characterized by a distinct abaxial-adaxial polarity. Removal of leaf primordia from the meristem leads to the development of radial abaxialized structures suggesting that signals from the meristem are required for abaxial-adaxial polarity, and that abaxial cell fate might be the default state (Sussex 1954). Antagonistic effects between class III HOMEODOMAIN LEUCINE-ZIPPER (HD-ZIP III) and KANADI (KAN) transcription factors, resulting in polar YABBY expression, control abaxial-adaxial lateral organ polarity. In Arabidopsis, members of *KAN* and *YABBY* gene families promote abaxial cell fate (Sawa et al. 1999, Siegfried et al. 1999, Eshed et al. 1999, Eshed et al. 2001), whereas members of the HD-ZIP III gene family, such as *PHABULOSA (PHB), PHAVOLUTA (PHV), CORONA (CNA)* and *REVOLUTA (REV)*, promote adaxial cell fate (McConnell and Barton 1998, McConnell et al. 2001, Emery et al. 2003, Kelley et al. 2009). Loss-of-function alleles of HD-ZIP III (*PHB, PHV*) result in radial abaxialized cotyledons (Emery et al. 2003), and gain-of-function alleles in radial adaxialized leaves (McConnell and Barton 1998, McConnell et al. 2001). In contrast, the situation for *KAN* is the opposite: gain-of-function alleles lead to radial abaxialization of organs (Eshed et al. 2001, Kerstetter et al. 2001). Hence, the conversion to all adaxial or all abaxial fates leads to a loss of lamina expansion because the juxtaposition of these two domains is of crucial importance for lamina development. Disruption of the abaxial-adaxial polarity can lead to ectopic outgrowth ((Eshed et al. 2001, Kerstetter et al. 2001), see section 1.3.2). The restriction of the TFs to their domains is mediated by micro RNA (miRNA) activity (such as miRNA 165/166) (Reinhart et al. 2002, Rhoades et al. 2002, Tang et al. 2003, Juarez et al. 2004, Zhong and Ye 2007).

In Arabidopsis, the KANADI TF ATS is restricted to ovule integuments. *ATS* is expressed at the boundary of the two integuments during integument initiation (Figure 1-3, F + I), and expression restricts to the abaxial layer of the inner integument later during integument growth (McAbee et al. 2006). Functional *ATS* is critical for proper ovule development by maintaining the boundary between the two integuments, for promoting laminar growth of the inner integument (McAbee et al. 2006), and acts in concert with *PHB/PHV/CNA* in order to regulate integument morphogenesis (Kelley et al. 2009). Loss-of-function leads to inherent fusion of the outer and the inner integument, and thus, to aberrant seed coat formation (Leon-Kloosterziel et al. 1994, McAbee et al. 2006). In contrast, loss of *KAN1* and *KAN2* leads to the disruption of the outer integument (Eshed et al. 2001, McAbee et al. 2006). These genes act redundantly in the outer

integument but, in contrast to *ATS*, are not only involved in integument development (Leon-Kloosterziel et al. 1994, Eshed et al. 2001, McAbee et al. 2006). KAN control auxin signaling in concert with AUXIN RESPONSE FACTOR (ARF) proteins (Pekker et al. 2005). Especially ETTIN (ETT/ARF3) plays a pivotal role in ovule development (Sessions et al. 1997, Kelley et al. 2012). ETT forms a functional complex with ATS, which accumulates in the abaxial layer of the inner integument and modifies auxin action by negatively regulating PIN1 expression (Kelley et al. 2012). Moreover, evidence was provided that ETT forms a similar complex with other KAN transcription factors (Kelley et al. 2012).

Another important player in outer integument development is the YABBY TF INNER NO OUTER (INO). ATS and REV together restrict *INO* expression to the abaxial layer of the outer integument and thereby outer integument growth (Kelley et al. 2009). Loss-of-*INO*-function mutants depict outer integument initiation but no growth, and therefore lacking ovule curvature (Baker et al. 1997, Villanueva et al. 1999). Loss of the outer integument resulting in loss of curvature suggests that the outer integument itself imposes curvature resulting in the final amphitropous configuration.

1.2 Protein kinases in plant development and physiology

Phosphorylation and dephosphorylation of proteins play important roles in all aspects of the life cycle of plants. Thereby, protein kinases (PK) accomplish the process of protein phosphorylation whereas protein phosphatases catalyze protein dephosphorylation. Phosphorylation and dephosphorylation represent quick and reversible posttranslational protein modifications leading to conformational changes, translocation and/or changes in substrate activity. Protein phosphorylation is highly specific, strictly controlled, and enables regulation, amplification and interconnection of molecular signals (Pawson and Scott 2005). If the substrate of a protein kinase itself is a protein kinase, the initial phosphorylation signal can lead to the activation or inactivation of many effector proteins, and hence, activation of a complete signaling cascade can occur (Pawson and Scott 2005). Therefore, PKs are crucial for plant development and adaption to changing environmental conditions. In Arabidopsis, more than 1000 genes encode protein kinases (kinome), which comprises 4% of all protein-encoding genes (Zulawski et al. 2014), whereas the human kinome only represents 2% of the protein-encoding genes (Manning et al. 2002). Kinases have been subdivided in several major phylogenetic groups. The receptor-like

kinases (RLK), including the large family of transmembrane leucine-rich-repeat receptor-like kinases (LRR-RLK), and the membrane-associated receptor-like cytoplasmic kinases (RLCK), represent about 60% of all kinases (Zulawski et al. 2014, Zulawski and Schulze 2015). This high abundance of RLKs is a unique feature for the plant kingdom. In addition, the following plant kinase families can be distinguished: CMGC kinases, named after their members cyclin-dependent kinases (CDK) and mitogen-activated protein kinases (MAPK); Ca^{2+}/Calmodulin (CaM)-dependent kinases (CaMK); STE kinases (homologs of *S. cerevisiae* sterile kinase); and AGC kinases, named after the cAMP-dependent protein kinase A, cGMP-dependent protein kinase G and the phospholipid-dependent protein kinase C families (PKA, PKG, PKC) (Champion et al. 2004, Dissmeyer and Schnittger 2011, Zulawski and Schulze 2015). Additionally, other kinases are present, which do not fall into one of the above-mentioned families. For instance, AURORA kinases that are involved in the regulation of asymmetric cell divisions via phosphorylation of histone 3 during mitosis (Demidov et al. 2009, Kawabe et al. 2005, Kurihara et al. 2006, Van Damme et al. 2011), and the TARGET OF RAPAMYCIN (TOR) kinase, which represents an essential regulator of nutritional, stress-related and developmental pathways (Menand et al. 2002, Ren et al. 2012).

1.2.1 AGC kinases and plant development

Plants possess the same basic AGC kinase subfamilies (PDK1, S6K, and NDR) as other eukaryotes but they do not encode for the typical AGC kinases, such as PKA and PKC, involved in the control of cell expansion, proliferation and polarity in fungi and animals. The Arabidopsis genome encodes 39 AGC kinases, 23 of which belong to the plant specific AGCVIII subfamily (Figure 1-4). Several of those are involved in hormone signaling. PID, D6PK, WAG1, WAG2, and the blue light receptors PHOTOTROPIN1 (PHOT 1) and PHOT2 are involved in auxin signaling (Santner and Watson 2006, Cho et al. 2007, Zhang et al. 2009, Dhonukshe et al. 2010, Willige et al. 2013, Zourelidou et al. 2014, Weller et al. 2017). WAG2 is also involved in gibberellic acid (GA) signaling (Willige et al. 2012), and S6K plays a role in abscisic acid (ABA) and auxin signaling (Mahfouz et al. 2006, Turck et al. 2004). Furthermore, OXIDATIVE SIGNAL INDUCIBLE 1 (OXI1) and AGC2-2/OXI2 were shown to have functions in biotic and abiotic stresses downstream of 3-PHOSPHOINOSITIDE-DEPENDENT KINASE 1 (PDK1) (Anthony et al. 2006, Camehl et al. 2011, Howden et al. 2011). Enugutti et al. (2012) showed that the AGCVIII kinase UNICORN (UCN) suppresses ectopic growth in Arabidopsis ovule integuments by directly repressing the KANADI transcription factor ATS through phosphorylation. In general, AGC kinases become activated by phosphorylation of the T-loop within the activation segment. In mammalian systems, PDK1 acts as the master regulator of

AGC kinase activity by activating various AGC kinases through phosphorylation of their T-loops. Other AGC kinases, including PDK1, are capable of auto-activation through auto-phosphorylation (Rademacher and Offringa 2012). Two Arabidopsis genes encoding for PDK1 (PDK1.1 and PDK1.2) have been identified. Although they were shown to be involved in the in vitro activation of a minimum of 16 AGC kinases, biological relevance of PDK1-mediated activation could not be demonstrated (Bögre et al. 2003, Anthony et al. 2004, Zegzouti et al. 2006a, Zegzouti et al. 2006b)

1.2.2 PDK1 – master of the AGCs?

PDK1 genes are present throughout eukaryotes (Zegzouti et al. 2006a, Zegzouti et al. 2006b,

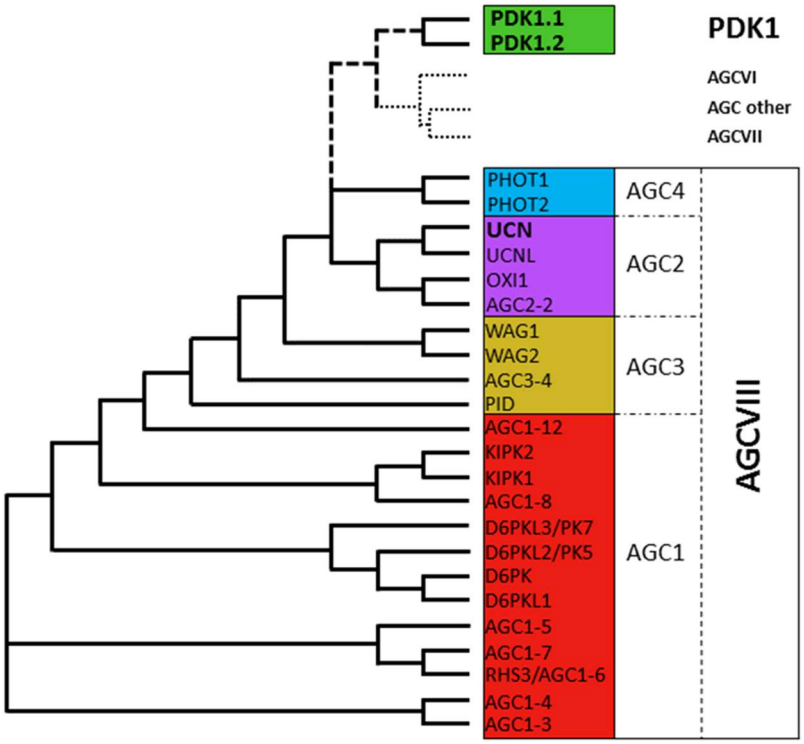

Figure 1-4 Phylogenetic tree of the Arabidopsis AGC kinase family.

The AGCVI subfamily contains the two S6 KINASES (S6K1 and S6K2), the AGCVII subfamily has eight members related to the nuclear Dbf2-related kinase (NDR1 – NDR8), and the AGC other group contains four members, which are named after one member INCOMPLETE ROOT HAIR ELONGATION (IRE, IRE-H1, IRE3, and IRE4). The two PDK1s are grouped in the independent PDK1 subfamily. Consisting of 23 kinases, the AGCVIII subfamily forms the plant specific major subfamily within the AGC family. Adapted from Bögre et al. (2003).

Dittrich and Devarenne 2012). Reduced PDK1 activity leads to severe developmental defects in animal organisms (Mora et al. 2004), and knockout of *PDK1* causes embryo-lethality in mice (Lawlor et al. 2002), and double knockdown of both *PDK1* genes in *Solanum lycopersicum* (tomato) is lethal as well (Devarenne et al. 2006). *Physcomitrella patens PDK1* knockout elicits strongly impaired growth and severely decreased resistance to abiotic stress (Dittrich and Devarenne 2012). Moreover, *ospdk1* mutants in rice (*Oryza sativa*) display a moderate dwarf phenotype (half-size of WT), and overexpression leads to increased disease resistance (Matsui et al. 2010).

Interestingly, Arabidopsis double knockout plants (*pdk1.1 pdk1.2*) depict only very mild phenotypes regarding plant height and silique length but are strongly impaired in *Piriformaspora indica*-induced growth promotion (Camehl et al. 2011). As mentioned above, PDK1 acts as the master kinase of AGC kinase signaling in mammals. The two Arabidopsis PDK1s were shown to activate various AGC kinases through the phosphorylation of the T-loop of the substrates (Bögre et al. 2003, Anthony et al. 2004, Zegzouti et al. 2006a, Zegzouti et al. 2006b) but for the others the upstream regulators remain unknown. Several AGC kinases comprise a short PDK1-interacting fragment (PIF motif, FxxF) at their C-terminus, which is thought to be responsible for the interaction between PDK1 and its target kinases. In addition, another highly conserved motif (Ade) was identified (Kannan et al. 2007), and shown to mediate interaction between PDK1 and AGC kinases (Romano et al. 2009), which is highly conserved among animal AGC kinases but not present in AGCVIII kinases of plants (Zhang and McCormick 2009). In vitro studies suggest that plant PDK1s interact in a quite promiscuous fashion with AGCVIII kinases, which leads to a significant increase of auto- and transphosphorylation of several AGCVIII kinases (Anthony et al. 2006, Devarenne et al. 2006, Zegzouti et al. 2006a, Zegzouti et al. 2006b). PDK1 phosphorylates a conserved threonine residue within the T-loop of animal AGC kinases (Romanelli et al. 2002). AGCVIII kinases possess a conserved serine residue at the same position, which represents a phosphorylation target of PDK1 (Anthony et al. 2004, Devarenne et al. 2006, Zegzouti et al. 2006a). These observations suggest an evolutionary conserved PDK1-mediated mechanism of AGC kinase regulation. Despite the in vitro phosphorylation characteristics, it remains unknown if PDK1 is the master regulator of AGCVIII kinase for various reasons. First, the activity of many AGCVIII kinases is increased by PDK1 in vitro but does not depend on the presence of PDK1 (Anthony et al. 2004, Devarenne et al. 2006, Zegzouti et al. 2006a). The second point is that neither spatiotemporal expression patterns by in situ hybridization or promoter-reporter constructs nor localization studies of PDK1 have been carried out so far. Additionally, the absence of a severe *pdk1.1 pdk1.2* developmental phenotype in Arabidopsis makes it difficult to debate about PDK1's role as a master regulator of AGCVIII kinases. It was speculated that there might be a third kinase with overlapping PDK1 functions, which shares only little sequence similarity with PDK1, and has therefore not been identified yet (Zhang and McCormick 2009, Zulawski et al. 2014). Other upstream regulators of AGCVIII kinases have become subjects of the discussion, such as the secondary messengers Ca^{2+}, cAMP, cGMP, and phospholipids (Zhang and McCormick 2009). Benjamins et al. (2001) showed that PID BINDING PROTEIN 1 (PBP1) and TOUCH3 contain EF-hands and interact with PID in a Ca^{2+}-dependent manner. Ca^{2+} and a calmodulin inhibitor repress PID activity (Benjamins et al. 2003, Zegzouti et al.

2006a). Although AGCVIII kinases do not contain recognizable lipid binding domains (van Leeuwen et al. 2004), PID was shown to bind several phospholipids in vitro (Zegzouti et al. 2006b). Furthermore, OXI1 activity increases upon phosphatidic acid treatment in a PDK1-dependent manner (Anthony et al. 2006). Besides others, these findings open a new sight on PDK1-dependent and -independent AGCVIII kinase regulation.

1.2.3 UNICORN – a suppressor of ectopic growth

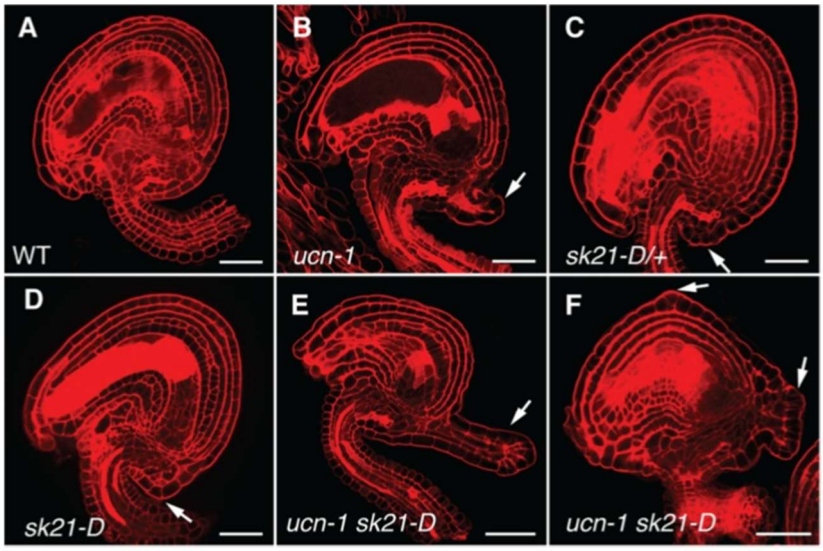

Figure 1-5 Confocal micrographs of mPS-PI stained ovules depicting protrusion formation.

(A) L*er* WT, and (B – F) several ovule mutants are shown. Please note protrusion formation in dominant *sk21-D* line (C and D); and enhanced phenotype in *ucn-1 sk21-D* double mutants (E) strongly enlarged and (F) multiple protrusions (compare with B and D). Arrows indicate protrusions. Scale bars: 20 µm. Figure from Enugutti and Schneitz (2013).

Originally described by Schneitz et al. (1997), *ucn* mutants show aberrant cell divisions and ectopic growth in ovule integuments (Figure 1 3), stamens, petals and cotyledons but never on sepals or carpels (Enugutti et al. 2012). The earliest ectopic outgrowths were observed in stages 2-IV/V but usually the protrusions become obvious in later developmental stages (from early stage 3). Cells of the abaxial inner or the adaxial outer integument dividing periclinally and/or obliquely instead of strictly anticlinally cause the initiation of the outgrowth. These aberrant divisions lead to the introduction of additional cell layers, which will be surrounded by the outer layers, i.e. the two layers of the outer integument or only the outermost abaxial layer (Enugutti et al. 2012). In *ino-2 ucn-1* double mutants, it was shown that the presence of an outer integument is not necessary for the formation of aberrant divisions in the inner integument. The authors showed that the cells contributing to the outgrowth exhibit at least partial integument identity rather than callus (Enugutti et al. 2012). The *UCN* gene encodes an active AGCVIII kinase that facilitates ectopic growth suppression in integuments by directly repressing the KANADI TF ATS

(Enugutti et al. 2012). Overexpression of *ATS* within its own expression domain in the dominant activation tagging line *sk21-D* (Gao et al. 2010) causes *ucn*-related protrusion arising from the integuments, and in *ucn-1 sk21-D* lines the protrusion are strongly enlarged (Figure 1-5). This suggests a model, in which the levels of active UCN and ATS relative to each other are of critical relevance in the process of ectopic growth suppression in integuments (Enugutti and Schneitz 2013).

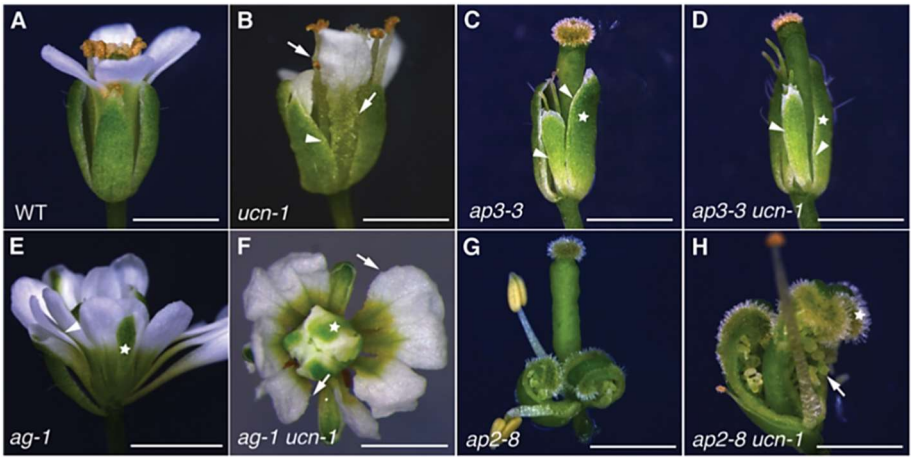

Figure 1-6 Floral phenotypes of *ap3 ucn*, *ag ucn* and *ap2 ucn* double mutants.

Light micrographs of (A) L*er* WT, (B) *ucn-1*, (C) *ap3-3*, (D) *ap3-3 ucn-1* (please note absence of protrusions on sepals), (E) *ag-1*, (F) *ag-1 ucn-1* (please note presence of petal protrusions in second- and third-whorl (arrows)), (G) *ap2-8*, and (H) *ap2-8 ucn-1* (please note protrusions on first-whorl ovules (arrow)). Scale bars: 0.5 mm. Figure from Enugutti and Schneitz (2013).

Several double mutants between *ucn-1* and floral homeotic mutants (Figure 1-6) such as *ucn-1 agamous-1* (*ag-1)*, *ucn-1 apetala2-8* (*ap2-8*) and *ucn-1 apetala3-3* (*ap-3-3*) displayed that *UCN* acts in an organ- and not in a whorl-specific fashion (Enugutti and Schneitz 2013). Furthermore, the authors showed that *ucn-1* protrusions arise in an auxin- and cytokinin-independent manner, and that *UCN* acts autonomously with respect to *ETT* and *ARF4* (Enugutti and Schneitz 2013) suggesting that *UCN* is independent of the ATS/ETT protein complex important for integument initiation. Upstream regulators and downstream targets of UCN, besides ATS, remain unknown. UCN's nature as an AGCVIII kinase raises the question whether PDK1 is involved in the regulation of *UCN* signaling during floral organ and ovule development.

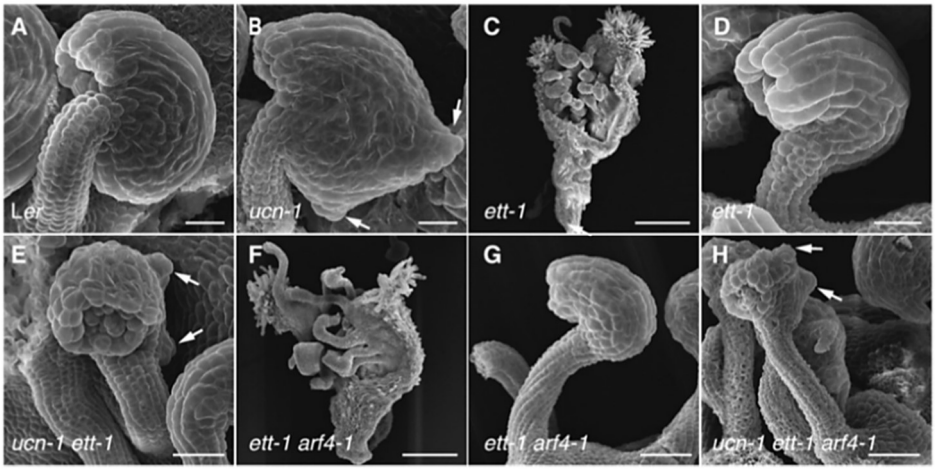

Figure 1-7 *ucn ett* and *ucn ett arf4* ovules depict additive phenotypes.

Scanning electron micrographs of (A, B, D, E, G, H) stage 4 ovules, and of (C, F) flower stage 14 gynoecia. (A) L*er* WT, (B) *ucn-1*, (C) *ett-1* gynoecium, (D) *ett-1* ovule, (E) *ucn-1 ett-1* ovule, (F) *ett-1 arf4-1* gynoecium, (G) *ett-1 arf4-1* ovule, and (H) *ucn-1 ett-1 arf4-1* ovule. Please note the additive phenotypes in E and H (compare with B, D and B, G. Arrows indicate protrusions. Scale bars: 20 µm. Figure from Enugutti and Schneitz (2013).

1.3 Tumorigenesis in animals and plants

Commonly, a tumor is defined as a neoplastic outgrowth, in which the tumorous cells are not in coordination with the surrounding 'normal' cells anymore caused by ectopic cell proliferation. This definition pertains for animals (Weinberg 2014) as well as for plants (Doonan and Sablowski 2010). Animal tumors can be subdivided into benign and malignant tumors. Benign tumors, such as lipomas or adenomas for instance, are neoplasms spatially restricted in growth that usually grow slowly, display distinct boundaries, and contain differentiated cells. They are non-invasive and do not develop metastases. By contrast, malignant tumors (cancers), for example testicular or mammary carcinoma, consist of diversely or poorly differentiated cells combined with high levels of genomic instability, grow invasively and uncontrollably, and develop metastases at a certain point of time (Weinberg 2014). Based on this definition, all observed plant tumors so far are of benign origin (Ahuja 1965, Braun 1972, Braun 1975, Dodueva et al. 2007, Doonan and Sablowski 2010). The absence of metastatic spread like in animal cancers is explained by the presence of rigid cell walls that surround and fix plant cells (Doonan and Sablowski 2010).

In animals, many tumor suppressor genes have been identified in the last decades of cancer research. Amongst many others, AGC kinase family members playing pivotal roles in the regulation of proliferation and expansion were shown to be involved in tumorigenesis and cancerogenesis (Pearce et al. 2010). For instance, the AGC kinase Warts/LATS that represents a core component of Hippo signaling necessary for tumor suppression and organ size regulation (Halder and Johnson

2011). Mutations in *Warts/LATS* lead to tumorigenesis in mouse and Drosophila (Justice et al. 1995, Xu et al. 1995, St John et al. 1999). As well as loss-of-function, increased activity of AGC kinases such as Akt/PKB have been demonstrated to be involved in cancer in humans (Vivanco and Sawyers 2002, Carpten et al. 2007). Beyond that, the central regulator of animal AGC kinases, PDK1, is associated with a variety of human cancers such as melanomas, breast, prostate, and gastric cancer (Gagliardi et al. 2017). For detailed information on the role of PDK1 in human cancer, see section 1.3.4.

1.3.1 Pathogen-induced tumors

Most tumor formation in plants is caused by a variety of pathogens, i.e. bacteria, fungi or viruses. Several bacteria were shown to cause ectopic outgrowth on their respective host plants including the genus *Agrobacterium* (Lippincott and Lippincott 1975, Gelvin 2003), *Pantoea agglomerata* pv. *gypsophilae* (Chalupowicz et al. 2006), *Pseudomonas savastanoi* (Wilson and Magie 1964, Wilson 1965, Glickmann et al. 1998, Temsah et al. 2010), and *Rhodococcus fascians* (Vandeputte et al. 2005). These bacteria lead to the formation of gall tumors with variable sizes. In order to implement the tumor-inducing molecular mechanisms, all tumor-inducing bacteria have achieved the ability, which is determinate on either their plasmids (e.g, Ti-plasmids of *Agrobacterium tumefaciens*) or their chromosomal genes (Morris 1986), to control cytokinin and auxin synthesis in the host plant. The best-studied tumor-inducing bacterium is *A. tumefaciens* due to its utilization in the generation of genetically modified plants (Bechtold et al. 1993, Clough and Bent 1998).

Few plant viruses are also capable of tumor induction. The *Geminiviridae* family (Nagar et al. 1995), and *Phytoreoviruses* of the *Reoviridae* family (Streissle and Maramorosch 1963, Kudo et al. 1991) represent two examples of tumor-inducing plant viruses. *Geminiviruses* interfere directly with the central cell cycle control machinery (Hanley-Bowdoin et al. 2004, Desvoyes et al. 2006, Ascencio-Ibáñez et al. 2008, Doonan and Sablowski 2010), which is interesting regarding the fact that aberrant activity of central cell cycle control genes does not cause tumor formation in plants (Beemster et al. 2003, Doonan and Sablowski 2010, Harashima and Schnittger 2010).

In addition, some fungi have the ability to cause tumor formation on their host plants. For example *Ustilago maydis* induces tumors on maize plants by fungal protein transfer to (Brefort et al. 2009, Skibbe et al. 2010), and induction of auxin synthesis and expression of auxin-responsive

genes in the host cells (Doehlemann et al. 2008). Other examples for tumor-inducing fungi are *Taphrina deformans* that leads to tumor formation on peach leaves by increasing cytokinin and auxin levels (Sziraki et al. 1975, Tavares et al. 2004), an *Dibotryon morbosum* (*Apiosporina morbosa*), which causes black knot galls on plants of the *Rosaceae* family (Fernando et al. 2005).

Furthermore, plant tumors can be induced by root-knot nematodes, cyst nematodes (Bird and Koltai 2000, De Meutter et al. 2003), protists such as *Plasmodiophora brassicae* (Devos et al. 2005), and several insects such as gall wasps, aphids and flies (Armstrong 1995).

1.3.2 Genetic tumors

Genetic alterations can cause spontaneous tumor development without presence of exogenous agents or pathogens. Knowledge gained in animal tumor formation, suggests that genetic lesions in genes of core cell cycle regulation result in overproliferation and tumorigenesis in plants as well. Various plant tumors caused by several agents exhibit aberrant behavior of genes involved in different steps of cell cycle control (Frank et al. 2002, Harrar et al. 2003, Lee et al. 2004). Interestingly, alterations in many core cell cycle genes does not lead to neoplasm development (Beemster et al. 2003, Doonan and Sablowski 2010, Harashima and Schnittger 2010). For instance, null-alleles of *RETINOBLASTOMA-RELATED* (*RBR*), the single Arabidopsis ortholog of the outstanding human tumor suppressor *Rb,* do not cause tumor formation (Ebel et al. 2004, Wachsman et al. 2011). In contrast to animals, plants seem to be quite resistive to tumor formation but some genetic examples for tumorigenesis in plants are known, which involve complex genetics. Spontaneous genetic tumors appear in interspecies hybrids in particular (Ahuja 1998). Although some examples including tumor formation in tobacco flowers (Kostoff 1939, Sharp and Gunckel 1969), Datura ovules (Blakeslee and Satina 1947), and tomato leaves (Martin 1966) have been demonstrated quite long time ago, the underlying genetic mechanisms remain mostly unknown.

Single-locus lesions can cause the formation of tumorous structures in plants (Nuttall and Lyall 1964). In the last decades, progress on the identification of single-loci has been made, and a few examples are presented here. Dominant neomorphic alleles of the maize homeobox gene *Knotted-1* (*Kn-1*) lead to ectopic *Kn-1* expression resulting in leaf 'knots' (Freeling and Hake 1985, Smith et al. 1992), and over-dominant allele compilations of the *OUTGROWTH-ASSOCIATED KINASE* (*OAK*) locus cause ectopic outgrowth on Arabidopsis leaf petioles (Smith et al. 2011). Moreover, very-long-chain fatty acids (VLCFAs) were shown to play a critical role in plant growth

through the investigation of the pleiotropic *gurke* (*gk*)/*pepino* (*pep*)/*pasticcino* (*pas*) mutants. These mutants show ectopic cell proliferation, and the respective genes are involved in VLCFA biosynthesis (Torres-Ruiz et al. 1996, Faure et al. 1998, Haberer et al. 2002, Baud et al. 2004, Roudier et al. 2010). Furthermore, mutants of the genes *TUMOROUS SHOOT DEVELOPMENT1/KORRIGAN* (*TSD1/KOR*) and *TSD2/QUASIMODO2* (*QUA2*), which are involved in pectin and cellulose biosynthesis, show callus formation at the apex (Frank et al. 2002). These findings suggest a crucial role of the cell wall in the control of cellular growth (Mouille et al. 2007, Krupková et al. 2007, Krupková and Schmülling 2009). The maintenance of abaxial-adaxial polarity in lateral organs is of crucial importance to restrict growth (Eshed et al. 2001, Eshed et al. 2004, Pekker et al. 2005, Nakata and Okada 2013). The above-described *ett arf4* double mutant as well as the *kan1 kan2* double mutant show aberrant abaxial outgrowth on leaves (Eshed et al. 2001, Pekker et al. 2005), proposing an important role in abaxial fate determination for the auxin response factor family members ETT and ARF4 (Ulmasov et al. 1999, Remington et al. 2004).

Recently, the above-described AGCVIII kinase UCN was shown to act as an Arabidopsis tumor suppressor gene in ovules by repressing the KANADI TF ATS (Enugutti et al. 2012, Enugutti and Schneitz 2013). Other components of UCN-mediated control of division plane orientation and planar growth remain unexposed.

1.3.3 (Phyto-) hormones in tumorigenesis

Hormones in animals as well as phytohormones in plants play pivotal roles in growth regulation, development and tumorigenesis. For example, altered estrogen and progestogen levels are related to the development of breast cancer as they act with and through proto-oncogenes and growth factors to alter normal breast cell proliferation (MacMahon et al. 1973, Pike et al. 1993), and hypothalamic hormones are involved in the malignant growth formation in many different human organs, e.g. prostatic, ovarian, breast, and pancreatic cancers (Schally et al. 2001). In plants, altered cytokinin and auxin homeostasis occasionally relate to dedifferentiation and tumor formation (Sziraki et al. 1975, Morris 1986, Ahuja 1998, Tavares et al. 2004, Dodueva et al. 2007, Doonan and Sablowski 2010). In addition, phytohormones control various cell cycle regulators. For example, some cyclins and cyclin-dependent kinases were found to be upregulated in response to auxin or cytokinin (Chung and Parish 1995, Riou-Khamlichi et al. 1999, Roudier et al. 2003, Sieberer et al. 2003). Taken together, animal and plant hormones have the ability to

induce or enhance tumor formation and growth by interfering with the cell cycle control machinery.

1.3.4 AGC kinases in tumorigenesis

As described above, several animal AGC kinases, such as Warts/LATS (Justice et al. 1995, Xu et al. 1995, St John et al. 1999, Halder and Johnson 2011) and Akt/PKB (Vivanco and Sawyers 2002, Carpten et al. 2007) have been described to be involved in tumorigenesis. Among the human AGC kinases, one of them plays the central role in tumor formation and proliferation in various tissues: PDK1. This so-called master regulator of AGC kinase signaling is overexpressed in many different tumors (Gagliardi et al. 2017). Most forms of mammary carcinoma show *PDK1* overexpression caused by increased copy number, which is often associated with other genetic alterations in *Akt* signaling (Maurer et al. 2009). In castration-resistant prostate cancer and lymph node metastases, the *PDK1* containing locus is frequently amplified (Choucair et al. 2012), and in esophageal squamous cell carcinoma cells more PDK1 is abundant compared to non-cancerous adjacent cells and higher levels of PDK1 are associated with increasaed severity of this cancer type and poor prognosis (Yang et al. 2014). Furthermore, *PDK1* overexpression is related to melanoma (Scortegagna et al. 2014), acute myeloid leukemia (Zabkiewicz et al. 2014), hepatocellular carcinoma (Wang et al. 2016), and to gastric cancer, in which the level of PDK1 abundance negatively correlates with survival rates (Bai et al. 2016). In plants, PDK1 has not yet been associated with tumor formation. In general, only UCN as an AGC kinase within the plant kingdom was shown to be involved in tumorous outgrowth suppression in a phytohormone-independent manner so far (Enugutti et al. 2012).

1.4 Objectives

3-Phosphoinositide-dependent protein kinases (PDK1s) play pivotal roles in all eukaryotic kingdoms of life. In humans, *PDK1* is crucial in many developmental and physiological processes including tumorigenesis and cancer. In contrast to mammals, the functions of plant PDK1 proteins are poorly understood. In this study, I wanted to examine the role of the two Arabidopsis *PDK1* genes in general and their specific roles with respect to the UCN signaling pathway in the control of planar growth.

In addition, I was interested to elucidate the relationship between ATS, which was shown to be a component of *UCN* signaling in integuments, and PDK1.

My data imply that PDK1 is able to activate UCN and that the activated UCN directly represses PDK1 in order to maintain the cell division planes in petals and ovules in an anticlinal orientation. Both, PDK1 and ATS need to be present for protrusion formation in *ucn-1* ovules.

2 MATERIAL AND METHODS

2.1 Plant work, Plant Genetics and Plant Transformation

Arabidopsis thaliana (L.) Heynh. var. Columbia (Col-0) and var. Landsberg (*erecta* mutant) (L*er*) were used as wild type strains. Plants were grown as described earlier (Fulton et al. 2009). The *ucn-1* mutant (in L*er*) was described previously (Enugutti et al. 2012), and *pdk-1* T-DNA lines were described before (Camehl et al. 2011). T-DNA insertion lines were received from the NASC (*pdk1.1-1* SALK_053385, *pdk1.1-2* SALK_113251, *pdk1.2-2* SAIL_62_G04, *pdk1.2-3* SAIL_450_B01). Wild type L*er* and Col-0 and *pdk1.1 pdk1.2* mutant plants were transformed with different constructs using Agrobacterium strain GV3101/pMP90 (Deak et al. 1986, Sambrook et al. 1989) and the floral dip method (Clough and Bent 1998). Transgenic T1 plants were selected on Hygromycin (25 µg/ml) plates, and around 10 dag, viable seedlings were transferred to soil for further inspection.

2.2 Recombinant DNA work

For DNA and RNA work standard molecular biology techniques were used. PCR-fragments used for cloning were obtained using Phusion or Q5 high-fidelity DNA polymerase (both New England Biolabs, Frankfurt, Germany). All PCR-based constructs were sequenced (Eurofins Genomics, Ebersberg, Germany). The Gateway-based (Invitrogen) pDONR207 was used as entry vector, and destination vectors pMDC43 and pMDC83 (Curtis and Grossniklaus 2003) were used as binary vectors. Detailed information for all oligonucleotides used in this study is given in table 7-1 in the supplement.

A PCR standard protocol:

1. 95 – 98°C → 5 min
2. 95 – 98°C → 20 s
3. 55 – 60°C → 20 s
4. 72°C → (Phusion and Q5 polymerase 30 s/kb; Taq 60 s/kb)
5. 72°C → 5 min
6. 16°C → pause. Steps 2 – 4 were repeated for 30 – 38 cycles.

2.3 Quantitative real-time PCR

Tissue for quantitative real-time PCR was harvested from 30-day old plants grown under long day conditions. Tissue was harvested into Eppendorf tubes, snap frozen in liquid nitrogen, and stored at -80°C. With minor changes, RNA extraction, DNase treatment using rDNase (Macherey-Nagel, Düren, Germany) and quality control were performed according to the manufacturer's instruction (Macherey-Nagel, Düren, Germany). First-strand cDNA was synthesized from 0.5 - 1.0 µg of total RNA via reverse transcription, using the First Strand cDNA Synthesis Kit (ThermoFisher, Schwerte, Germany). Quantitative real-time PCR was performed in the 2 step + MeltCurve programme on a CFX 96 Touch™ Real-Time PCR detection system (Bio-Rad Laboratories GmbH, Munich, Germany) using the GoTaq Real-Time qPCR kit (Promega, Mannheim, Germany), and analysis was done essentially as described (Enugutti et al. 2012). Using the ΔΔ-Ct method, *PDK1.1* and *PDK1.2* gene expression levels were normalized against At4g33380, At2g28390, and At5g46630 expression. Primer pairs are given in table S1.

2.4 Reporter Constructs

For plasmid pPDK1.2::gPDK1.2:EGFP pMDC83, 4.253 kb of *gPDK1.2* sequence was amplified from Col-0 genomic DNA including promoter sequence spanning genomic DNA up to the 3' end of the adjacent gene (1.245 kb) and 3'UTR of *PDK1.2* and cloned into pDONR207. pMDC83 (35S promoter was removed) was used as destinantion vector. For overexpression constructs, *gPDK1.1* or *gPDK1.2* were amplified from Col-0 genomic DNA and cloned into pDONR207. As destination vectors, pMDC43 or pMDC83 (35S promoter was replaced by either pUBQ10 or p16) were used, respectively. Reporter constructs were cloned by lab technician Regina Hüttl.

2.5 CRISPR/Cas9 Constructs

Therefore, I made use of the system developed by Wang et al. (2015), in which an egg cell specific promoter (*pEC1.2*) controls *Cas9* expression. I designed a single guide RNA (sgRNA) binding to the region +346 to +365 of the *UCN* coding sequence. The destination vector pHEE401 containing this sgRNA under control of the *U6-26* promoter and the plant optimized *Cas9* coding sequence under control of *pEC1.2* was transformed into L*er* and Col-0 WT plants. I thank Qi-Jun

Chen (China Agricultural University, Beijing) and Stefanie Sprunck (University of Regensburg, Germany) for providing the CRISPR plasmid pHEE401 and pCBC-DT1T2.

2.6 Generation, Expression and Purification of Recombinant Proteins

UCN and PDK1 coding sequences were amplified from floral cDNA (L*er*) and cloned into pGEX-6P-1 (UCN versions; GE Healthcare, Munich, Germany), pMal-c2x (PDK1 versions; New England Biolabs, Frankfurt, Germany), or pET32a (ATS; Novagen, now Merck, Darmstadt, Germany). The clones were expressed in the *E. coli* strain BL21 (DE3) pLysS. Expression from the pGEX vector leads to proteins fused to a N-terminal Glutathione Transferase (GST) protein, expression from pMal leads to proteins fused to a N-terminal Maltose Binding Protein (MBP). For protein expression and purification, bacterial cultures were grown to OD 0.6-0.8 at 37°C. Then, the bacteria were induced with 0.8 mM isopropyl-beta-thio galactopyranoside (IPTG) for UCN and 1.5 mM IPTG for PDK1 and grown at 30°C for 4 h. Subsequently, the recombinant proteins were purified from the bacteria by batch purification under native conditions using the Glutathione Sepharose 4 Fast Flow (GE Healthcare) for GST fusion proteins and Amylose resin (New England Biolabs) for MBP fusion proteins according to the manufacturer's instructions. As elution buffers 1xPBS supplemented with 10 mM reduced glutathione or 10 mM maltose was used, respectively. For PDK1, four different protein versions were expressed and purified (PDK1.1 WT, $PDK1.1_{KD}$ (kinase deficient version containing a K73A mutation), PDK1.2 WT and $PDK1.2_{KD}$ (kinase deficient version containing a K74A mutation). For UCN, five different protein versions were expressed and purified (UCN WT, UCN_{G165S} (ucn-1 mutation, kinase deficient), UCN_{KD} (kinase deficient version containing a K55E mutation), $UCN_{\Delta PIF}$ (kinase active version lacking the PIF motif at the C-terminus), and $UCN_{KD/\Delta PIF}$ (kinase deficient version lacking the PIF motif at the C-terminus). For ATS, WT versions and single, double and triple mutants for S13A, S92A, and S211A were used. For MST measurements, the purified proteins were labeled with NT-647 and subsequent MST measurements were performed according to the manufacturer's instructions (NanoTemper GmbH, Munich, Germany).

2.7 In vitro kinase assay

For kinase assays, the proteins were purified as described above and concentrations were estimated on a 12% SDS PAGE using BSA as standard protein. Assays were performed with approximately 500 ng of respective protein(s) and incubated in HMK buffer (10 mM HEPES, 10 mM $MgCl_2$, 10 µM ATP and 2 µCi of either γ-^{32}P-ATP or γ-^{33}P-ATP (Hartmann Analytik, Braunschweig, Germany)) at RT for 1 h. Reactions were stopped by adding 4 µL 6xLaemmli buffer and boiling at 95°C for 5 min. In order to separate the proteins, 12% SDS PAGE was performed. Subsequently, the gels were stained with Coomassie Brilliant Blue G250, destained in 10% acetic acid and dried. Phosphorimager plates were exposed at RT over night and signals were detected using a Fuji BAS Phosphorimager (Fujifilm, Düsseldorf, Germany).

2.8 Yeast Two-Hybrid assay

For yeast two-hybrid assays, the above-mentioned four PDK1 and five UCN versions were used. The coding sequences of these versions were cloned into pGBKT7 and pGADT7 vectors, respectively (Clontech Laboratories/Takara Bio, Saint-Germain-en-Laye, France). Plasmids were transformed into yeast strain AH109 and transformants were selected on SD_{-LW} medium (SD medium without Leu and Trp). Three independent colonies of each combination were resuspended each in 500 µL ddH_2O, diluted 1:100 and 10µL of the dilutions were spotted on SD_{-LWHA} (SD medium without Leu, Trp, His and Adenine) supplemented with 5 mM 3-AT and grown at 30°C for 3 days.

2.9 BiFC assay

For Bimolecular Fluorescence Complementation (BiFC), the above-mentioned four PDK1 and five UCN versions were cloned into pSPYCE-35S and pSPYNE-35S vectors, respectively (Walter et al. 2004). Plasmids were transformed into Col-0 mesophyll protoplasts as published (Yoo et al. 2007). Protoplasts were incubated gently shaking at 21°C in the dark for 10 – 15 h and subsequently imaged using a FV1000 confocal microscope (Olympus, Hamburg, Germany) with excitation at 515 nm and detection at 521 – 559 nm for YFP fluorescence. At least 800 viable protoplasts per combination were analyzed using a FV1000 confocal microscope.

2.10 In Situ Hybridization and Microscopy

Whole mount in situ hybridization of ovules was performed according to Bleckmann and Dresselhaus (2016). Digoxigenin-labeled probe generation has been described earlier (Sieber et al. 2004). For microscopic analysis of in situ hybridizations, an Olympus BX61 upright microscope with DIC optics was used. Whole mount in situ hybridization was performed by lab technician Katrin Wassmer.

Confocal laser scanning microscopy using modified pseudo-Schiff propidium iodide (mPS-PI) staining or detection of EGFP was performed as described earlier (Vaddepalli et al. 2014). mPS-PI staining was performed according to Truernit et al. (2008). Whole flowers and silique micrographs were obtained using an Olympus SZX12 stereomicroscope equipped with a XC CCD camera and Cell Sense Dimension software.

2.11 Growth media, growth conditions and frequently used buffers

Ingredients are dissolved in deionized H_2O, and all media need to be autoclaved.

Lysogeny broth (LB) medium (for standard molecular biology/cloning):

1% tryptone, 0.5% yeast extract, 10% NaCl, (0.9% bacto agar)

Terrific broth (TB) medium (for protein expression in *E.coli*):

1.2% tryptone, 2.4% yeast extract, 0.5% glycerol

Dissolve in deionized water and autoclave. Add 1/10 of the final volume of 10x TB phosphate buffer (0.17 M KH_2PO_4, 0.72 M K_2HPO_4).

½ Murashige-Skoog medium (for plant tissue culture):

0.22% MS medium powder, (1% sucrose), 0.9% Agar (plant cell culture tested)

YPD medium (yeast rich medium):

2% tryptone, 1% yeast extract, (2.4% bacto agar), 2% glucose

SD-LW:

0.67% yeast nitrogen base (double drop-out; SD lacking leucine and tryptophan), 2% glucose, (2% bacto agar)

SD-LWH:

0.67% yeast nitrogen base (triple drop-out; SD lacking leucine, tryptophan and histidine), 2% glucose , (2% bacto agar)

SD media might be supplemented with 5 – 10 mM 3-AT.

YEB medium (*A. tumefaciens* liquid culture for plant transformation):

0.5% beef extract, 0.1 % yeast extract, 0.5% tryptone, 0.5% sucrose, 0.5 g/L $MgCl_2$

SOC medium (for regeneration of *E.coli* after transformation):

0.5% yeast extract, 2% tryptone, 10 mM NaCl, 2.5 mM KCl, 20 mM glucose, supplemented with 20 mM Mg^{2+} (10 mM $MgCl_2$; 10 mM $MgSO_4$) after autoclaving.

10x PBS:

30 mM NaH_2PO_4, 70 mM Na_2HPO_4, 1.3 M NaCl

5x TBE:

450 mM Tris Base, 400 mM boric acid, 10 mM EDTA pH 8, pH should be 8.3

Growth conditions were as follows: *E.coli* for standard molecular biology was grown at 37°C over night. *E.coli* BL21(DE3) for protein expression and purification was grown at 37°C until they reached OD_{600} = 0.5 – 0.6. Subsequently, IPTG was added to a final concentration of 0.8 mM (for GST-UCN version), 1.5 mM (for MBP-PDK1 versions) and 1 mM (for Trx-6xHis-ATS) and the cells were incubated at 30°C for another 4 h. Yeast AH109 was grown at 30°C for 2 – 3 d. Seedlings were grown on ½ MS with or without 1% sucrose at 22°C and continuous light for 8 – 12 d.

Antibiotics for bacterial selection were used at final concentrations as follows: Kanamycin 50 µg/mL; Ampicillin 100 µg/mL; Spectinomycin 100 µg/mL; Gentamycin 25 µg/mL; Tetracyclin 12.5 µg/mL; and Rifampicin 10 µg/mL.

2.12 Bioinformatics

Bioinformatic analysis was mainly performed using geneious software. Alignments were generated with geneious software using a ClustalW algorithm with BLOSUM62 matrix. Sequencing results were analyzed in geneious software using the map to reference tool with geneious mapper and highest sensitivity.

3 RESULTS

3.1 Characterization of the Arabidopsis AGC kinases PDK1.1 and PDK1.2

3.1.1 Structure-function properties of PDK1 and conservation between the two Arabidopsis PDK1 and PDK1 proteins of other plant species

In order to evaluate the importance of 3-phosphoinositide-dependent protein kinases (PDK1), I have performed in silico analyses regarding structural and functional properties and conservation within the plant kingdom. PDK1 shows unique structural and functional properties within the AGC kinase family. This kinase is the only plant AGC kinase containing a lipid-binding domain, the Pleckstrin Homology (PH) domain. This domain facilitates the interaction of PDK1 with phospholipids such as phosphatidic acid in order to transduce signals from outside the cell usually via other AGC kinases to adapt the expression patterns and/or levels of target genes or modify enzymatic activity in order to respond to intrinsic or environmental changes. Besides the presence of the PH domain and the PIF binding pocket, which enables PDK1 to interact with downstream AGC kinases containing a PDK1 interacting fragment (PIF), the structural properties resemble standard kinase structure including an activation segment starting with the Magnesium-binding loop DFG and containing a conserved T-residue in the so-called T-loop.

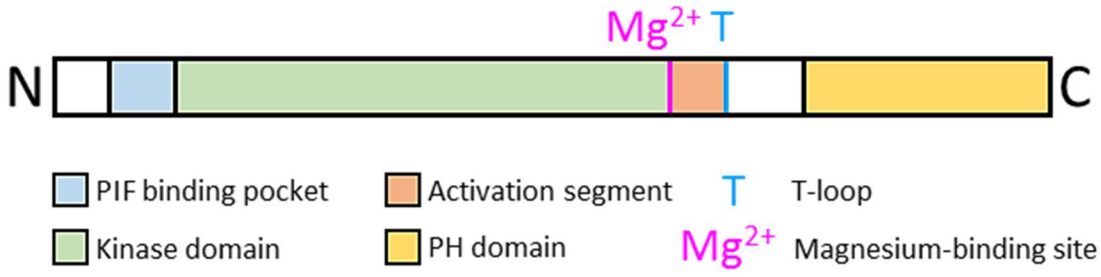

Figure 3-1 Schematic depiction of PDK1 domain structure.
The Pleckstrin Homology (PH) domain facilitates the interaction with phospholipids such as phosphatidic acid, the T-loop of the activation segment needs to be autophosphorylated to activate the kinase, and the PIF binding pocket ensures the interaction with the substrates of the AGC kinase family.

Since PDK1s are protein kinases of fundamental importance in the life cycle of many eukaryotic organisms, I have analyzed the sequences of 29 flowering plant species using ClustalW algorithm and BLOSUM62 (BLSM62) matrix (-1; for detailed protein sequences see Figure 7-1 in

the supplement). The black bars show highly conserved regions, which are depicted in the identity bar in green (identical) or ocher (highly similar). Here, I found that PDK1 protein sequences of very distinct angiosperm species such as Brassicaceae family members (No. 1 – 10), trees (No. 15, 19, and 23) or important crop plants (No. 26 – 29) show high conservation of more than 75% at the protein sequence level. Excluding *Ricinus communis* and *Vitis vinifera*, the gap of 23 amino acids (AA) at positions 27 to 49 narrows down and results in even higher conservation of the remaining 27 kinases. Two regions, the first one of eleven AA (363 – 373) and the second one of 19 AA at positions 387 – 405 show moderate to little conservation and are therefore variable. Pairwise identity between all 29 analyzed kinases is 82.6 % and pairwise positive are 87 % according to the used BLSM62 matrix. The *in silico* analysis shows high overall conservation of the unique lipid binding AGC kinase among flowering plants leading to the assumption that PDK1 is a kinase of crucial importance as it has been shown for the animal PDK1s (Lawlor et al. 2002, Mora et al. 2004).

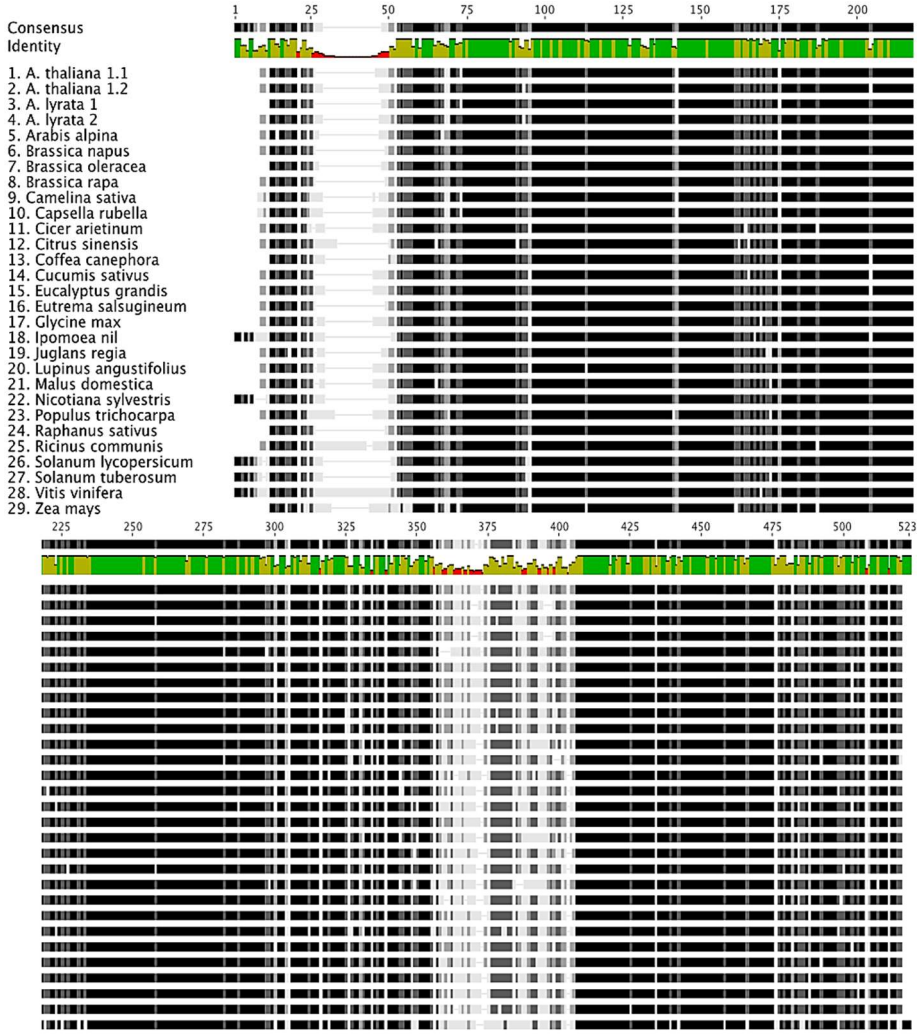

Figure 3-2 Alignment of PDK1 protein sequences of different plant species. Black bars indicate identity or high similarity, grey bars similarity, and light grey bars little similarity. Lines show gaps. Alignment was performed in Geneious software using ClustalW algorithm with BLSM62 matrix. Detailed sequence information is shown in Figure 7-1 in the supplement.

3.1.2 PDK1 expression analysis

In order to examine if the Arabidopsis *PDK1* genes have specific expression properties during plant development or physiological changes in the environment, expression levels of *PDK1.1* and *PDK1.2* were analyzed using AtGenExpress (Kilian et al. 2007). This analysis reveals constant expression throughout plant development with an exception during stamen and pollen development, in which especially *PDK1.2* is strongly upregulated (Figure 3-3). Furthermore, the expression levels of both the *PDK1* genes are quite constant in all applied treatments (light, pathogen, hormone and abiotic stress). Thus, *PDK1* seems not to be specifically involved in particular processes but throughout plant development indicating a role for *PDK1* in many aspects of the Arabidopsis life cycle. In addition to the above mentioned in silico analysis, I performed quantitative Real-Time PCR (qPCR) experiments of stage 9 – 13 flowers, and in situ hybridizations were performed by lab technician Katrin Wassmer (see section 3.2.1.2, Figure 3-9). In these experiments, no significant difference between the two *PDK1* genes as well as the tested tissues could be demonstrated supporting the results from AtGenExpress.

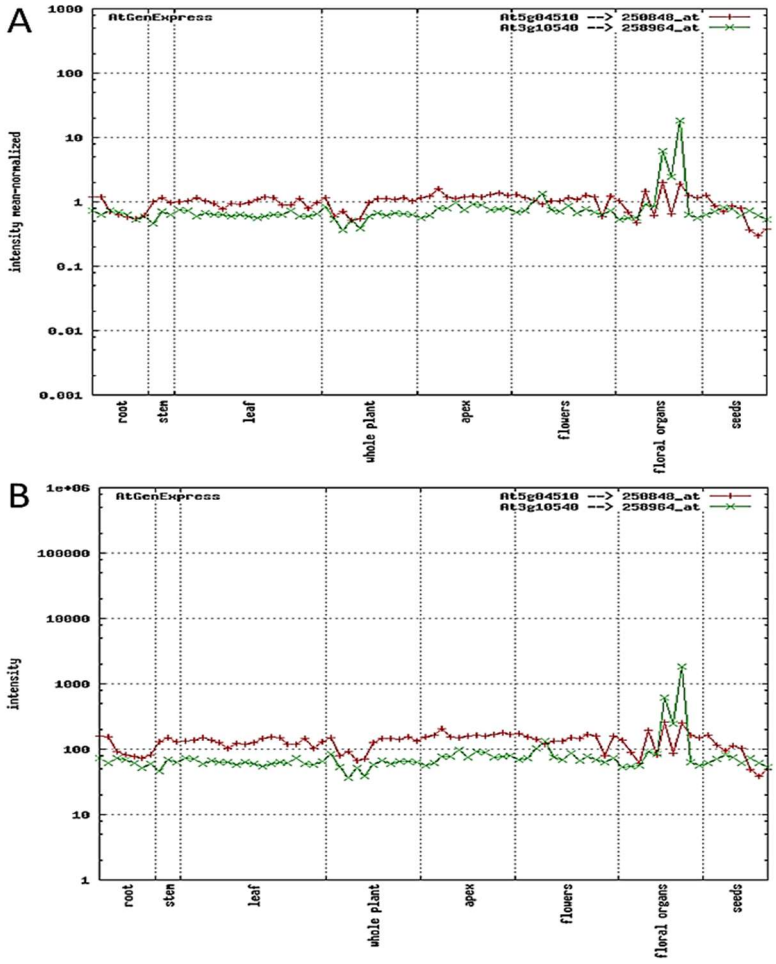

Figure 3-3 Mean-normalized and absolute expression levels of *PDK1.1* (*At5g04510*) and *PDK1.2* (*At3g10540*).
The expression levels of *PDK1.1* (red) and *PDK1.2* (green) according to AtGenExpress (Kilian et al. 2007) are shown. (A) Mean-normalized and (B) absolute expression levels. Both PDK1s are expressed in all developmental stages as well as in all other tested conditions (data of light, hormonal, pathogen, and abiotic stress treatments are not shown. Both the *PDK1* genes are expressed at constant levels except for stamen and pollen development, in which especially *PDK1.2* is strongly upregulated.

3.1.3 *pdk1* double knockout plants show a surprisingly mild phenotype

Figure 3-4 Phenotypic characterization of *pdk1* T-DNA lines.
Floral shapes and silique sizes of (A) Col-0 WT, (B) *pdk1.1*, (C) *pdk1.2*, and (D) *pdk1.1 pdk1.2* T-DNA lines are shown. Please note that flowers do not show an obvious phenotype. Siliques of the double insertion lines (DILs) are shorter, slightly thicker and contain less ovules compared to WT and single insertion lines. (E) 35 days old plants of *pdk1.1-1 pdk1.2-2*, *pdk1.1-2 pdk1.2-3* and Col-0 WT (from left to right). DILs exhibit reduced height, single insertion lines (supplemental Figure 7-2) are indistinguishable from WT. (F) Gene structure of *PDK1.1* and *PDK1.2* including T-DNA insertion sites. Grey boxes represent UTRs, black boxes exons, lines introns, and light grey arrowheads indicate primer pairs to determine transcripts in Col-0 and T-DNA lines. Scale bars (flowers) 1mm; (siliques) 2 mm; (E) 10 cm.

In order to examine the phenotypic characteristics of *pdk1* knockout lines, I received two independent T-DNA lines for each of the *PDK1* genes from the Nottingham Arabidopsis Stock Centre (NASC). For *PDK1.1*, I named these lines *pdk1.1-1* (SALK_053385) and *pdk1.1-2* (SALK_113251), and for *PDK1.2* I called them *pdk1.2-2* (SAIL_62_G04) and *pdk1.2-3* (SAIL_450_B01). Insertion sites were analyzed by sequencing. SALK_053385 T-DNA is located 305 bp upstream of the first ATG within the 5' untranslated region (5' UTR), SALK_113251 is integrated within the tenth exon 2255 bp downstream of the first ATG of *PDK1.1*. These lines do not exhibit *PDK1.1* expression by RT-PCR (supplemental Figure 7-2). SAIL_62_G04 was detected within the

fourth exon 858 bp downstream of the first ATG, and SAIL_450_B01 is situated within the sixth intron at position +1311 of the genomic DNA. RT-PCR revealed no transcript in both the *pdk1.2* T-DNA lines (supplemental Figure 7-2). These results corroborate the ones obtained by Camehl et al. (2011), who analyzed two of them before (SALK_113251 and SAIL_450_B01). I have performed subsequent analysis of their phenotypic characteristics in all four above mentioned T-DNA lines and in two independent double insertion lines (*pdk1.1-1 pdk1.2-2* and *pdk1.1-2 pdk1.2-3*, 'DILs'). As shown in Figure 3-4, the single *pdk1* lines do not exhibit any phenotype (A, B) but both DILs differ from the WT slightly in plant height and silique size as well as in number of ovules per silique. Interestingly, the DIL phenotype is not very severe compared to other species, in which a *PDK1* knockout leads often to (embryo) lethality. It was speculated that there might be a third kinase in Arabidopsis with overlapping PDK1 function. Zulawski and colleagues claimed that they found in in silico analyses a third *PDK1* gene, which they named *PDK1.3* (*At2g20050*) (Zulawski et al. 2014). I have analyzed this gene with respect to the two known *PDK1* genes *PDK1.1* (At5g04510) and *PDK1.2* (At3g10540). In fact, *At2g20050* encodes a PROTEIN PHOSPHATASE 2C (PP2C) containing an additional cyclic nucleotide-binding/kinase domain (Schweighofer et al. 2004, Xue et al. 2008). In my analysis (see supplemental Figure 7-4), I could not reveal any indication that At2g20050 represents a third Arabidopsis 3-phosphoinositide-dependent kinase 1 (PDK1). The protein encoded by *At2g20050* does neither contain a typical Mg^{2+}-binding site (DFD or DFG) nor a T-loop (C**TFVGT**AAY) both crucial for kinase activity. Furthermore, I performed a pairwise alignment using ClustalW algorithm and BLOSUM62 matrix. Whereas the two PDK1 proteins (PDK1.1 and 1.2) exhibit 91.1% identical sites, AT2g20050 shares only 10.4% identity with them (supplemental Figure 7-4). In addition, At2g20050 comprises a sequence length of 1094 AA whereas PDK1.1 and 1.2 are 491 and 486 AA in length, respectively. Therefore, I strongly doubt that the gene product of the locus *At2g20050* represents a protein with PDK1 function.

3.1.4 Subcellular distribution of PDK1:EGFP fusion proteins

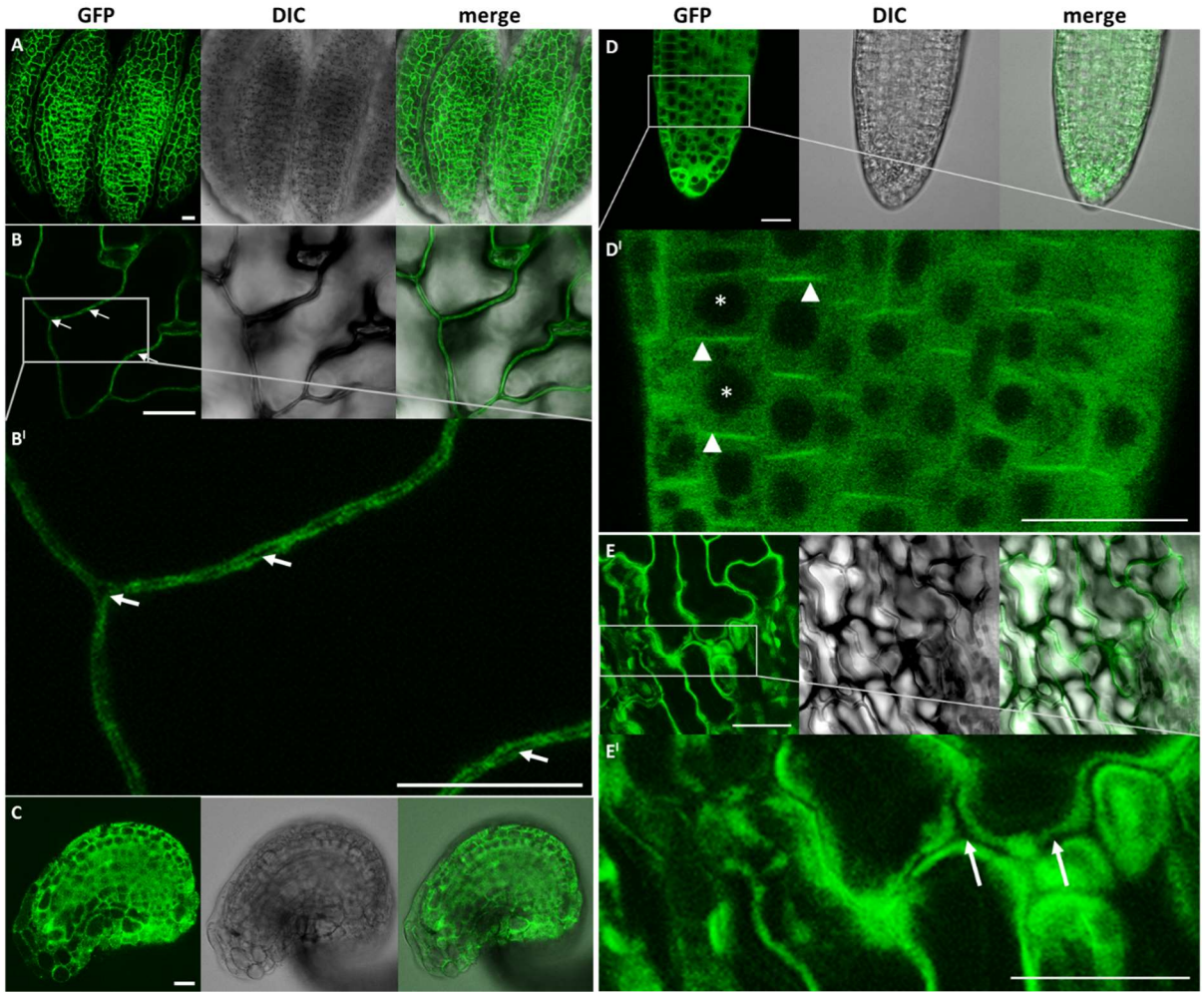

Figure 3-5 Subcellular localization of PDK1.2:EGFP fusion proteins in different tissues.

Confocal micrographs depicting the subcellular distribution of PDK1.2:EGFP fusion proteins under control of the native *PDK1.2* promoter. (A) Anther, (B) cauline leaf, (B') higher magnification of the region in (B), (C) ovule. (D) lateral root, (D') higher magnification of the region in (D), (E) sepal, (E') higher magnification of the region in (E). Arrows indicate the absence of GFP signals at the cell wall, arrowheads indicate plasma membranes, and asterisks indicate absence of GFP signals in the nuclei. Scale bars: 20µm.

As shown in section 3.1.2, both *PDK1* genes are expressed throughout all developmental stages in Arabidopsis. In order to investigate the subcellular localization of PDK1, I first explored the SUBA4 database (Hooper et al. 2014, Hooper et al. 2017). Their predictions localize PDK1.1 to

the nucleus and PDK1.2 to the cytosol. Furthermore, I generated *pPDK1.2::PDK1.2::EGFP* lines and analyzed them using a confocal microscope. All lines, native *pPDK1.2::gPDK1.2:EGFP* and overexpressors (under *pUBQ10* or *p16* promoter), show GFP signal distribution within the cytosol (Figure 3-5 and Figure 3-6). I studied all above-mentioned lines in several different tissues and found subcellular distribution to be almost uniform in all lines and tissues. To examine the localization under more natural conditions, I analyzed four lines expressing *pPDK1.2::PDK1.2:EGFP*. These lines showed rescue of the DIL phenotype making it a functional construct. I observed GFP signals in all four lines and all examined tissues. In Figure 3-5 A, the localization of PDK1.2:EGFP in an anther is shown and localization does not differ from those in cauline leafs (Figure 3-5 B and B^{I}), ovules (Figure 3-5 C), and sepals (Figure 3-5 E and E^{I}). In roots (Figure 3-5 D and D^{I}), PDK1.2:EGFP localizes to the cytosol and most likely to the plasma membrane.

Interestingly, PDK1.1:EGFP in overexpressors (driven by *pUBQ10*) also localizes to the cytosol, not in the nucleus as predicted. In roots, I observed that PDK1.1:EGFP is not localizing to nuclei but to the cytosol, the plasma membrane and probably in the endoplasmic reticulum (ER) (Figure 3-6 C and C^{I}, arrowheads indicate plasma membranes, asterisks indicate nuclei, and magenta arrows might indicate ER). By contrast, ER localization was not observed in native *pPDK1.2::PDK1.2:EGFP* lines. Taken together, both PDK1:EGFP fusion proteins localize equally to the cytosol in all examined tissues, and the data suggest that PDK1:EGFP localizes as well to the plasma membrane. ER localization might be an artifact of overexpression.

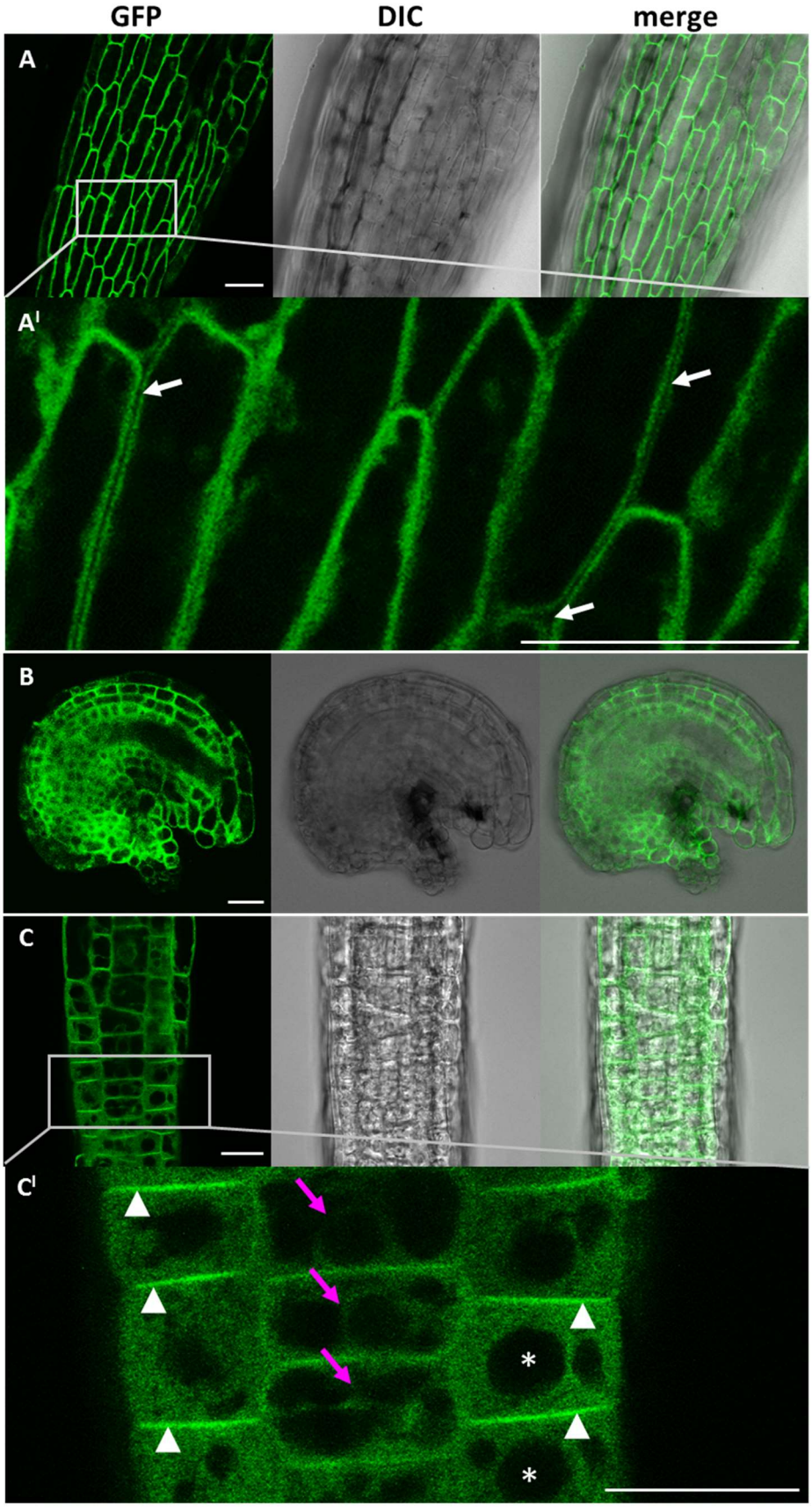

Figure 3-6 Subcellular localization of PDK1:EGFP.

Confocal micrographs depicting subcellular distribution of PDK1:EGFP in overexpression lines. (A) pUBQ10::PDK1.2:EGFP, (B+C) pUBQ10::PDK1.1:EGFP.

(A) Filament, (A^{I}) higher magnification of the region in (A), (B) ovule, (C) transition zone of a root, and (C^{I}) higher magnification of the region in (C). Arrows in (A^{I}) indicate the absence of GFP signal at the cell walls, magenta arrows in (C^{I}) indicate most likely endoplasmic reticulum (ER), arrowheads indicate plasma membranes and asterisks indicate nuclei. Scale bars: 20 µm.

3.2 Mechanism of *UCN*-mediated control of ovule and floral organ development via *PDK1*

PDK1 is known to be a major regulator for AGC kinase signaling in mammals as well as in plants (Pearce et al. 2010). For several AGCVIII kinases of Arabidopsis, PDK1 is the upstream modulator including AGC2-1, which represents one of the closest relatives of UCN. Thus, I tested involvement of *PDK1* in *UCN* signaling.

3.2.1 The knockout of either *PDK1* gene almost completely rescues *ucn-1*

The *ucn-1* mutant exhibits aberrant cell divisions and growth aberrations in several tissues, including petals and ovule integuments. These aberrant cell divisions eventually result in tumor-like structures, the so-called protrusions, which consist of differentiated cells (Enugutti et al. 2012). Wild type integument cells divide in a stereotypic anticlinal fashion but *ucn-1* mutants are impaired in these stereotypic divisions. In order to examine whether or not *PDK1* interacts genetically with *UCN*, I analyzed *ucn-1 pdk1* double mutants in homozygous F3 generation. To eliminate effects deriving from the genetic background, I performed three independent crossings of *ucn-1* (female) and Col-0 (male) and reciprocal.

3.2.1.1 Flower and ovule phenotypes

To investigate the role of *PDK1* in *UCN* signaling, I have analyzed a total number of more than 30,000 ovules of three independent crossings of each combination. For each crossing, three independent F3 plants were analyzed (for raw data see Table 7-2 in the supplement). Surprisingly, the knockout of either *PDK1.1* or *PDK1.2* is sufficient to rescue floral and ovule phenotypes of *ucn-1* (Figure 3-7). The *pdk1.1 ucn-1* lines are able to rescue 80 % of the analyzed ovules; *pdk1.2* restores aberrations in 90 % of the ovules of *pdk1.2 ucn-1* double mutants whereas in *ucn-1* Col-0 outcrosses the proportion of intact ovules only increases by 10 % to 20 % ovules without aberrations. Interestingly, the knockout of both *PDK1* genes in *ucn-1* background does not lead to a higher rescue level compared to *pdk1.2 ucn-1* double mutants (Figure 3-7, E).

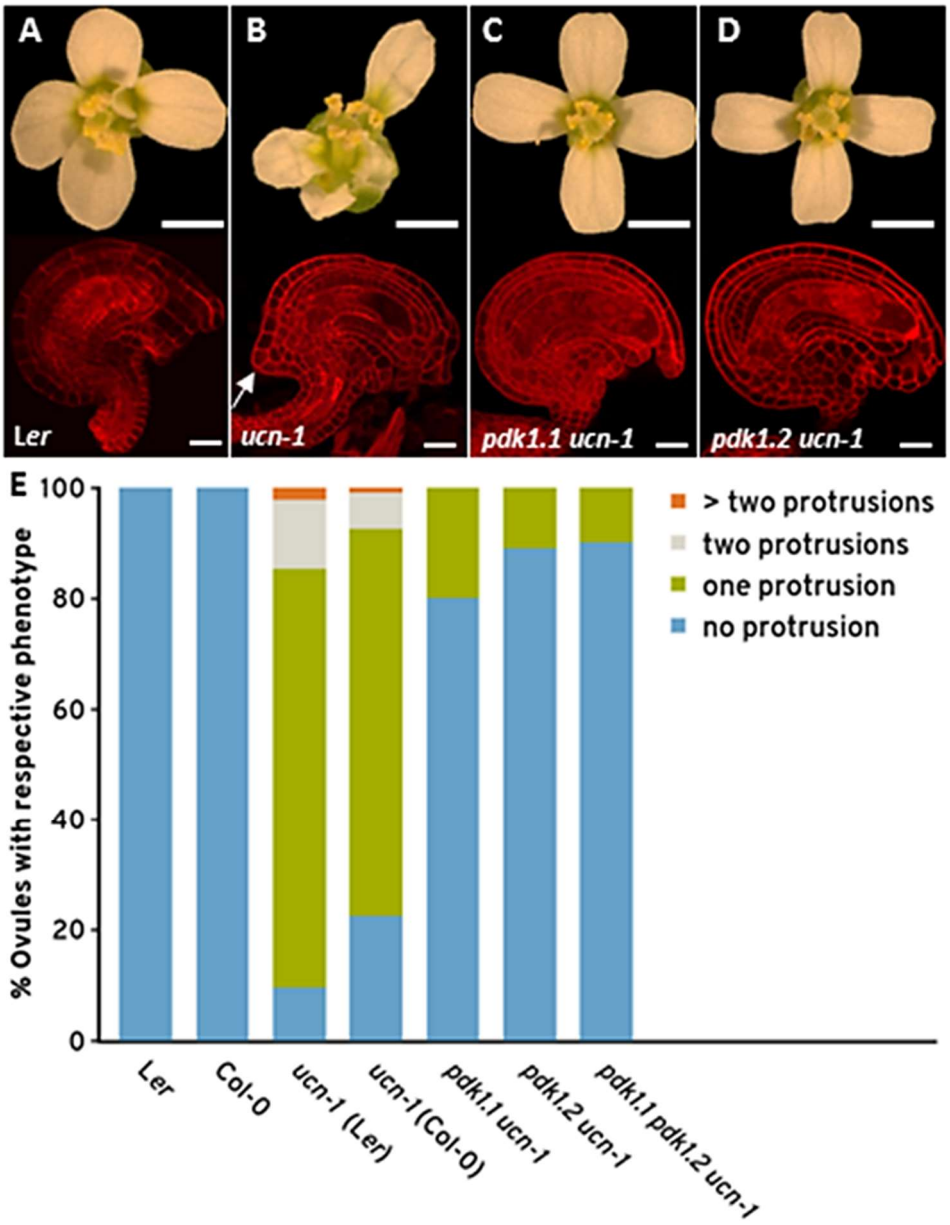

Figure 3-7 Restoration of floral and ovule phenotypes in *pdk1 ucn-1* double mutants.

(A – D) Upper panel: Floral phenotypes, lower panel: confocal micrographs of mPS-PI stained ovules. (A) L*er*, (B) *ucn-1*, (C) *pdk1.1-1 ucn-1* and (D) *pdk1.2-2 ucn-1*. (E) Percentage of respective ovule phenotypes of L*er*, *ucn-1*, Col-0, *ucn-1* outcrossed to L*er* and Col-0 (F3 plants homozygous for *ucn-1*) and homozygous double mutants (*pdk1.1 ucn-1* and *pdk1.2 ucn-1*). Knockout of *pdk1.1* and *pdk1.2* restore *ucn-1* phenotype to 80 % and 90 % of the WT level, respectively. Arrow indicates protrusion in *ucn-1* ovule. Scale bars (upper panel): 1 mm, (lower panel): 20 µm. Sample size were as given in Table 7-2 (see supplement).

Here, I show that knockout of only one of the two *PDK1* genes is sufficient to prevent the occurrence of tumor-like outgrowths from the ovule integuments (80 – 90 % rescue), and to restore the floral shape to WT. *pdk1* does not only inhibit the outgrowth of the typical *ucn-1* protrusions but also restores the stereotypic anticlinal division plane within the integuments (Figure 3-7). The result further suggests that *UCN* represses *PDK1* in the control of integument growth and floral organ development.

3.2.1.2 PDK1 expression is not altered in *ucn-1* mutants

The above-mentioned rescue of *ucn-1* phenotypes by *pdk1* raised the question how *PDK1* is downregulated in the control of planar growth. A previous study indicated that *PDK1.2* transcript levels are increased in inflorescences and stems of *ucn-1* compared to L*er* (Kirchhelle 2012). In order to exclude that the increment in inflorescences is due to stem contamination, I performed new qPCR experiments together with Annemarie Krauss (internship student) using only flowers without pedicel and stem. Thereby I realized that the forward primer for *PDK1.2* used in Kirchhelle (2012) binds upon a SNP between L*er* and Col-0. It seems that she designed the primers according to Col-0 sequence, which leads to a mismatch binding in L*er.* Hence, I designed a new primer according to L*er* sequence in order to exclude adulteration of transcript levels due to mismatch binding. The results of the new qPCR experiments show that transcript levels are not significantly altered, neither for any *PDK1* nor for the two tested tissues (Figure 3-8). This indicates that *UCN* does not influence the expression levels of the *PDK1* genes.

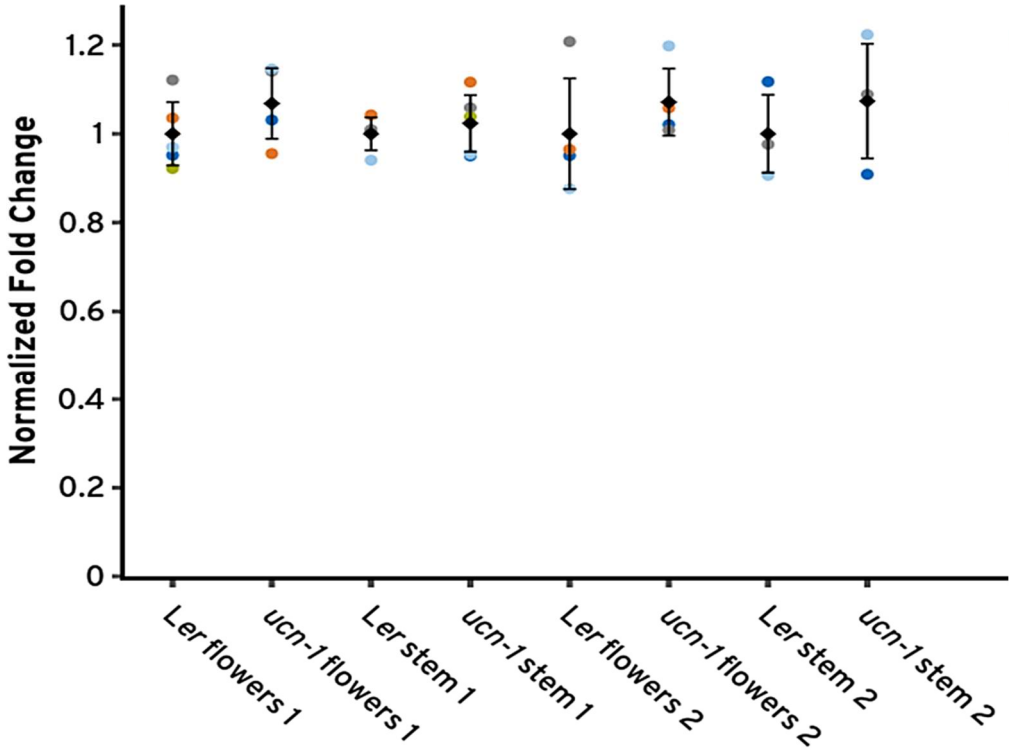

Figure 3-8 *PDK1.1* and *PDK1.2* expression levels in flowers and stems of L*er* and *ucn-1.*

Expression is depicted as relative expression normalized against references gene *At5g25760 (UBC21), At2g28390*, and *At4g33380*. *PDK1.1* expression levels are named '1', and *PDK1.2* expression levels are named '2'. Expression levels are depicted as relative to L*er* expression (=1). Please note no significant differences between L*er* and *ucn-1*. p-values (*Ler* vs. *ucn-1*) are as follows: *PDK1.1* flowers p=0.28; *PDK1.1* stem p=0.56; *PDK1.2* flowers p=0.44; *PDK1.2 stem* p=0.55. n = 5.

Moreover, I investigated expression patterns of both *PDK1* genes in *ucn-1* mutant ovules compared to L*er*. Interestingly, the localization of both *PDK1* mRNAs did not show any alterations in *ucn-1* mutants compared to L*er* WT. Whole mount in situ hybridizations using antisense probe against *PDK1.1* and *PDK1.2* mRNA, respectively, revealed that there was no obvious change in the expression patterns of *PDK1* genes during different stages of ovule development of *ucn-1* and L*er* are equal. Sense probe controls do not exhibit any signals. Exclusively the nucellus in early developmental stages exhibits no signals (Figure 3-9). Lab technician Katrin Wassmer performed in situ hybridization experiments.

Taken together, the genetic results indicate that *UCN* represses *PDK1*. Enhanced PDK1 activity is responsible for aberrant cell divisions and abnormal development of ovule integuments and abnormal floral organ shape in *ucn-1* mutants. Thus, the results emphasize the significance of correct negative regulation of *PDK1*.

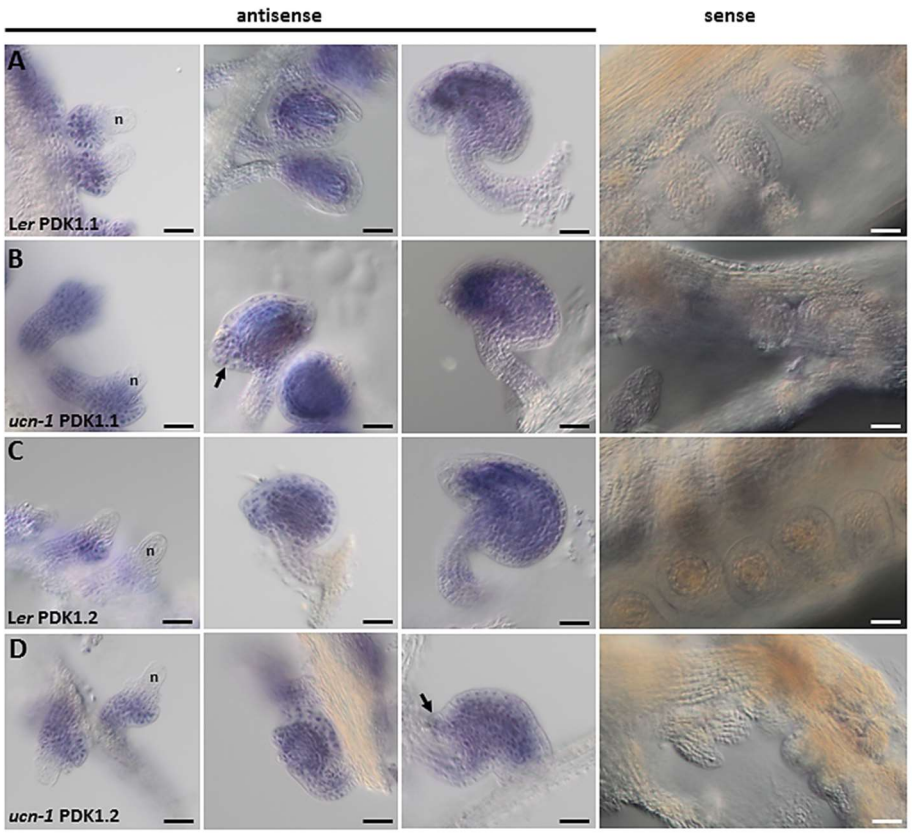

Figure 3-9 Whole mount in situ hybridizations. Stages of ovule organogenesis (anti-sense, from left to right): 2-V, 3-I to 3-II, and 3-VI; stages according to Schneitz et al. (1995).

Distribution of *PDK1.1* mRNA in (A) L*er* and (B) *ucn-1* ovules, and distribution of *PDK1.2* mRNA in (C) L*er* and (D) *ucn-1* ovules of three different developmental stages. The right panel shows sense probe control lacking any signals. Please note that mRNA distribution of both *PDK1s* is equal between L*er* and *ucn-1*, and present throughout ovule development except in nucelli (n) in early developmental stages. Arrows indicate typical *ucn-1* protrusions, in which *PDK1* mRNA is present. Scale bars: 25 µm.

3.2.2 *PDK1* overexpression leads to a *ucn-1*-like phenotype

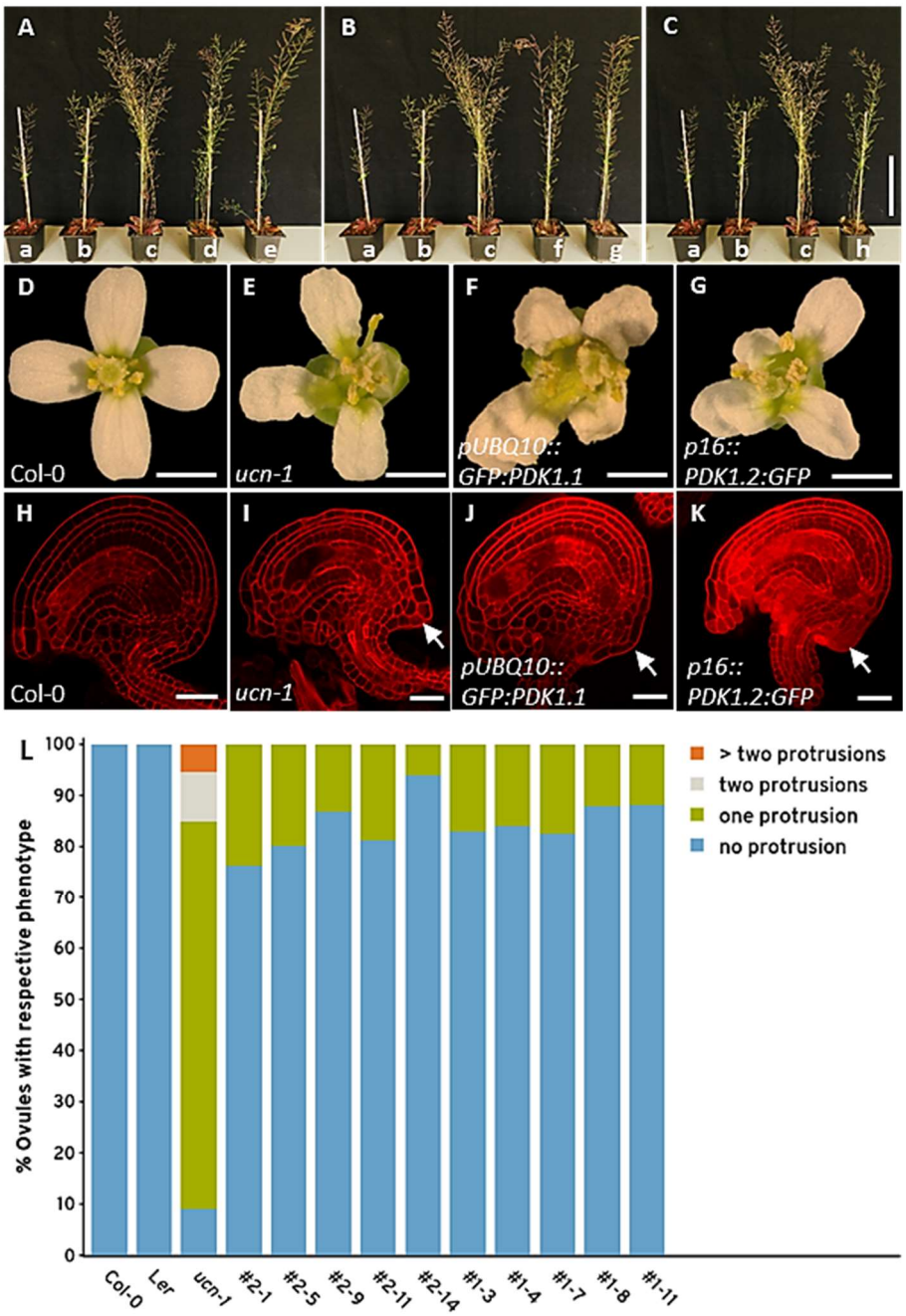

Figure 3-10 Morphological phenotypes of *PDK1* over-expressors.

(A-C) Overexpression of either *PDK1* rescues the double KO phenotype. (a, b) *pdk1* double mutants, (c) Col-0 WT, (d) *p16::gPDK1.1:EGFP,* (e) *p16::gPDK1.2 :EGFP,* (f) *pUBQ10::EGFP: gPDK1.1*, (g) *pUBQ10::EGFP :gPDK1.2,* and (h) *pPDK1.2::gPDK1.2:EGFP.* All constructs restore plant height (and silique length (not shown). (D-G) Stereo micrographs of flowers, and (H-I) confocal micrographs of mPS-PI stained ovules of (D, H) Col-0, (E, I) *ucn-1*, (F, J) $PDK1.1_{OX}$, and (G, K) $PDK1.2_{OX}$. *PDK1* overexpression lines show a milder *ucn-1*-like phenotype in flowers and ovules. (L) Percentage of respective ovule phenotypes in WT, *ucn-1*, and 10 independent overexpressors (#2-1 to #2-14 overexpressing *PDK1.2*, and #1-3 to #1-11 overexpressing *PDK1.1*). Sample sizes were as given in Table 3-1. Arrows in (I-K) indicate protrusions. Scale bars: (A-C) 10 cm; (D-G) 1 mm; (H-K) 20 µm.

If *UCN* represses *PDK1* overexpression of *PDK1* in WT should result in a *ucn* phenocopy. In order to test this prediction, I designed several constructs harboring genomic *PDK1.1* or *PDK1.2 (gPDK1.1/gPDK1.2)* sequence, respectively, under control of either *p16*, *UBQ10* or endogenous *PDK1.2* promoter and fused to *EGFP* (N- or C-terminal). For *pPDK1.2*, I used 1039 bp upstream of *PDK1.2* including 3'UTR of the adjacent gene (AT3G10530). Regina Hüttl (lab technician) cloned

these constructs and I transformed them into WT and into DILs to investigate functionality of the constructs. In comparison to Col-0 WT, plant height and silique length are reduced in *pdk1.1 pdk1.2* double KO lines. Introduction of either *PDK1* gene fused to *EGFP* restores these development restraints to WT levels. As shown in Figure 3-10 (A-C), all constructs restore developmental defects of DILs to WT situation. Furthermore, overexpression leads to a milder *ucn-1*-like floral and ovule phenotypes. I analyzed in total 3056 ovules of five independent lines for each *PDK1*, and compared them with 174 Col-0, 193 L*er* and 296 *ucn-1* ovules (see Table 3-1). Severity of the observed ovule phenotypes ranges from 6.1% (Line #2-14) to 23.6% (Line #2-1) of ovules show a single protrusion. Additionally, PDK1 overexpression lines depict polarity defects in root hairs (supplementary Figure 7-3). Root hairs show branching and ballooning. This finding indicates that PDK1 is involved in cell polarity.

Unlike *ucn-1* mutants, $PDK1_{OX}$ lines do not show more than one protrusion in any case, and I did not observe any statistical difference between those lines overexpressing *PDK1.1* and those overexpressing *PDK1.2* (see Figure 3-10 L).

Table 3-1 Ovule phenotypes of *PDK1* overexpressors compared to Col-0, L*er* and *ucn-1* mutant. Absolute numbers and percentages of respective ovule phenotype are given. #2-1 to #2-14 represent five independent transgenic lines overexpressing *PDK1.2:EGFP*. #1-3 to #1-11 represent five independent transgenic lines overexpressing *PDK1.1:EGFP.*

	#2-1	#2-5	#2-9	#2-11	#2-14	#1-3	#1-4	#1-7	#1-8	#1-11	Col-0	Ler	ucn-1
N	313	282	325	326	296	287	255	328	314	330	174	193	296
no protrusion	239	226	282	265	278	238	214	271	276	291	174	193	27
one protrusion	74	56	43	61	18	49	41	57	38	39	0	0	224
two protrsusions	0	0	0	0	0	0	0	0	0	0	0	0	29
>two protrusions	0	0	0	0	0	0	0	0	0	0	0	0	16
% no protr.	76.4	80.1	86.8	81.3	93.9	82.9	83.9	82.6	87.9	88.2	100.0	100.0	9.1
% one protr.	23.6	19.9	13.2	18.7	6.1	17.1	16.1	17.4	12.1	11.8	0.0	0.0	75.7
% two protr.	0.0	0.0	0.0	0.0	0.0	0.0	0.0	0.0	0.0	0.0	0.0	0.0	9.8
% >two protr.	0.0	0.0	0.0	0.0	0.0	0.0	0.0	0.0	0.0	0.0	0.0	0.0	5.4

In addition, I determined the expression levels of the above-mentioned ten independent *PDK1:EGFP* overexpression lines. The expression levels correspond to severity of the ovule phenotypes, i.e. the higher the expression level of either *PDK1* the more ovules with neoplastic integument growth I observed (with an exception for lines #2-9 and #2-11, in which #2-9 shows higher expression levels but less outgrowth; compare Table 3-1, Figure 3-10 and Figure 3-11). It

seems that a certain expression level (about 80-fold) causes the strongest phenotype due to overexpression of *PDK1* because even higher levels of *PDK1* transcript do not lead to stronger phenotypes, i.e. in all lines (#2-1, 2-5, 2-9, 1-3, 1-4 and 1-7), in which the expression level reaches 80-fold the proportion of ovules harboring protrusions is around 20%.

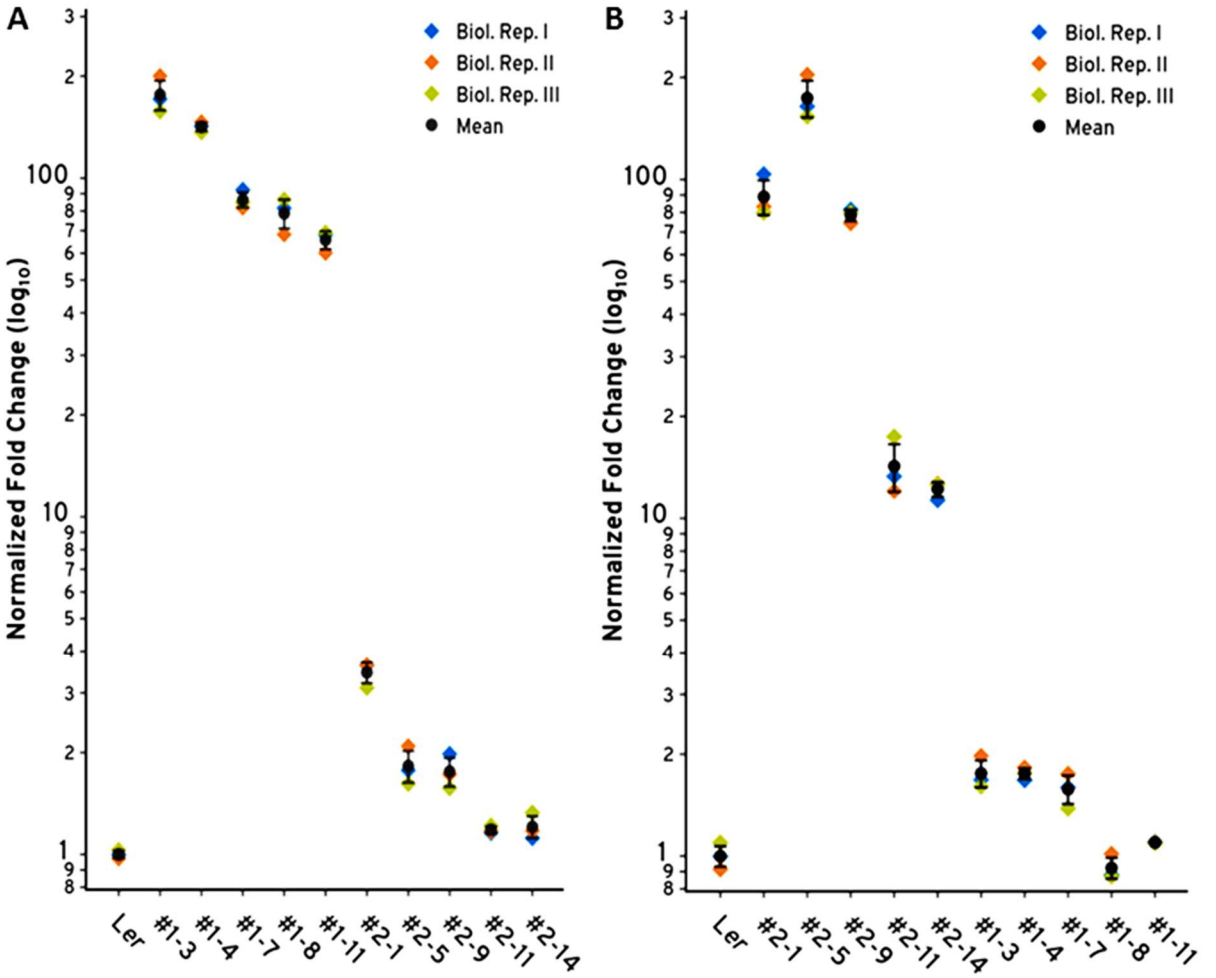

Figure 3-11 *PDK1.1* and *PDK1.2* expression in flowers of overexpression lines.

Expression is depicted as relative expression normalized against reference gene *At5g25760 (UBC21).*(A) *PDK1.1* expression levels relative to L*er* expression (= 1) in five *PDK1.1* (#1-3 to #1-11) and five *PDK1.2* (#2-1 to #2-14) overexpressors. (B) *PDK1.2* expression levels relative to L*er* expression (= 1) in five *PDK1.2* and five *PDK1.1* overexpressors. Note $\log_{10}$ scale on the axis of ordinates (y-axis). N = 3 (biological triplicates).

3.2.3 UCN regulates planar growth in ovule integuments and floral organ development through a direct negative regulation of PDK1

The previous results suggest that UCN represses PDK1 in a posttranscriptional manner. To gain more insights into UCN-mediated PDK1 regulation, I designed independent approaches to examine potential direct PDK1-UCN protein-protein interaction. Therefore, I performed in vitro kinase, yeast two-hybrid (Y2H) and bimolecular fluorescence complementation (BiFC) assays, and microscale thermophoresis (MST) measurements. These studies show that PDK1 and UCN directly interact. Rescue of *ucn* by *pdk1*, the unaltered *PDK1* expression properties in *ucn-1* mutants and the direct protein-protein interaction between PDK1 and UCN suggest that UCN directly represses protein activity of PDK1.

3.2.3.1 PDK1 and UCN interact in MST assays

Microscale thermophoresis (MST) measurements are based on thermophoresis, also termed Ludwig-Soret effect (Ludwig 1856, Soret 1880). Thermophoresis describes the directed movement of molecules along a temperature gradient, in MST along a microscopic temperature gradient (usually 2 – 4 Kelvin). Thermophoresis depends on the size, charge and solvation entropy of the molecules. The thermophoresis of a fluorescently labeled molecule A differs significantly from the thermophoresis of a complex AB. This difference can be used to determine the binding affinity. The principle of MST was described in detail before (Duhr and Braun 2006, Jerabek-Willemsen et al. 2011).

In order to test whether PDK1 and UCN are able to interact in vitro, I employed a MST approach together with Nicole Wenck (Bachelor student). For this purpose, we expressed recombinant proteins in *E.coli* (PDK1 versions N-terminally fused to maltose binding protein (MBP) tags, and UCN N-terminally fused to a glutathione transferase (GST) tag). To measure interactions using MST method, one of the potential interaction partners needs to be fluorescently labeled. Therefore, I labeled MBP, MBP:PDK1.1 and MBP:PDK1.2, respectively, with NT-647-NHS.

To test if MBP can interact with GST in vitro, we labeled MBP and used GST as the ligand. This combination does not show any retardation of movement along the 2 K temperature gradient (Figure 3-12C) meaning that MBP and GST do not interact in MST assays. In preliminary MST approaches, in vitro interaction between MBP:PDK1.1 or MBP:PDK1.2, respectively, and GST:UCN

was shown (Figure 3-12, A and B). Dose response curves of both combinations (PDK1.1$_{labeled}$ + UCN, and PDK1.2$_{labeled}$ + UCN) display the retardation of movement of the labeled partner (PDK1) with increasing concentrations of the ligand (UCN) along the 2 K temperature gradient.

Nicole Wenck showed in MST experiments, in which she labeled either GST or GST:UCN and used MBP or MBP:PDK1 as the ligand, that these combinations all show retardation of movement with increasing ligand concentrations (not shown). These findings indicate that the GST-tag is – despite the instructions of the manufacturer (NanoTemper, Munich) – not useful for MST measurements, and fluorescently labeling of GST-tagged proteins leads to false positive results.

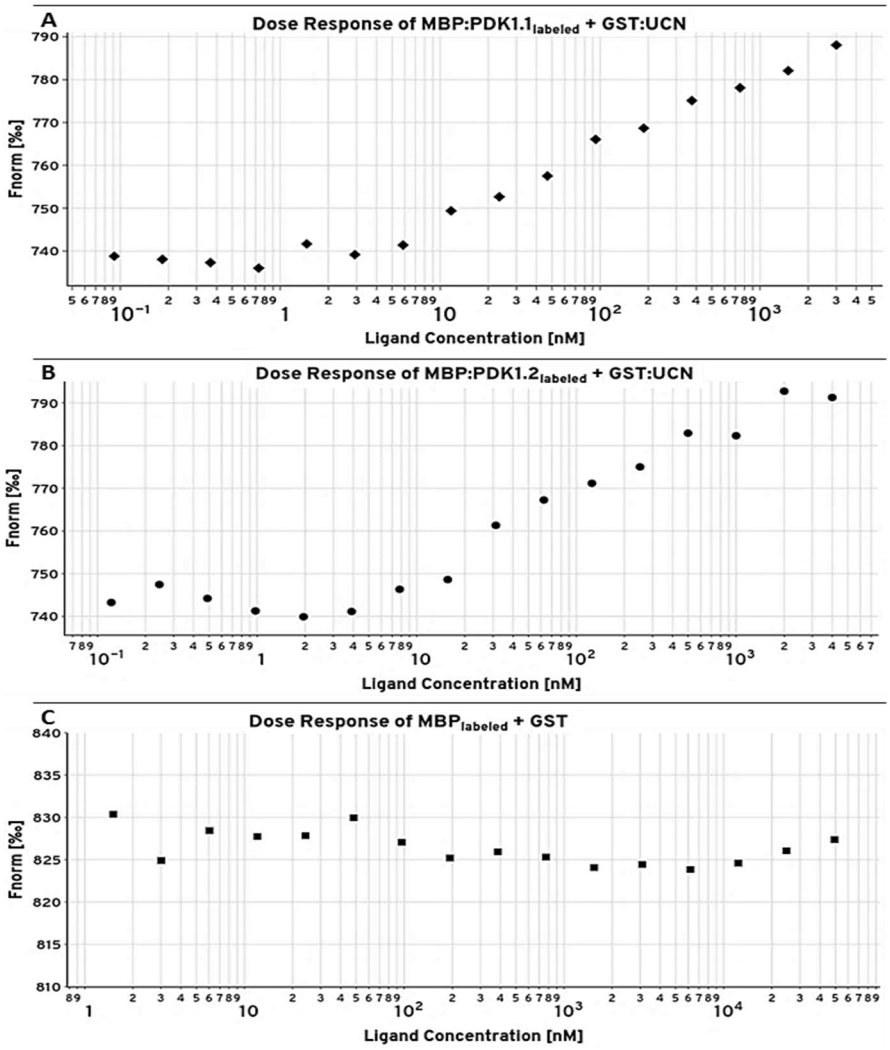

Figure 3-12 Microscale thermophoresis (MST) measurements of MBP: PDK1$_{labeled}$ and GST:UCN.

Dose response curves of MST measurements are depicted. MBP:PDK1.1, MBP:PDK1.2 or MBP were fluorescently labeled with NT-647, respectively. The labeled protein is hold constant, the unlabeled partner (ligand) is applied in a 16 times 1:2 dilution series. (A) Fluorescently labeled MBP:PDK1.1 in combination with GST:UCN. (B) Fluorescently labeled MBP:PDK1.2 in combination with GST:UCN. (C) Control experiment of fluorescently labeled MBP with unlabeled GST. Please note the increase of the normalized fluorescence (Fnorm (‰)) in (A) and (B), whereas Fnorm is constant in the control (C).

3.2.3.2 PDK1 phosphorylates UCN and vice versa

To better characterize PDK1-UCN interaction in vitro, I performed in vitro kinase assays. In a previous study, in her Master's thesis in our lab, Priya Pimprikar showed interaction between recombinant GST:PDK1 and GST:UCN proteins in kinase assays (Pimprikar 2012). GST is prone to dimerize. To exclude false positive interaction due to GST dimerization, I decided to fuse PDK1 to a maltose-binding protein (MBP) tag and repeat the in vitro kinase assays using recombinant GST:UCN and MBP:PDK1. In order to test if kinase activity and/or the presence/absence of the PDK1-interacting fragment (PIF) influence the in vitro interaction behavior, I heterologously expressed five different UCN versions (namely UCN, UCN_{G165S}, UCN_{KD}, $UCN_{\Delta PIF}$, and $UCN_{KD/\Delta PIF}$), and two different versions of each of the PDK1s (PDK1.1, $PDK1.1_{KD}$, PDK1.2, and $PDK1.2_{KD}$) in *E.coli* BL21(DE3)pLysS (see Figure 3-13).

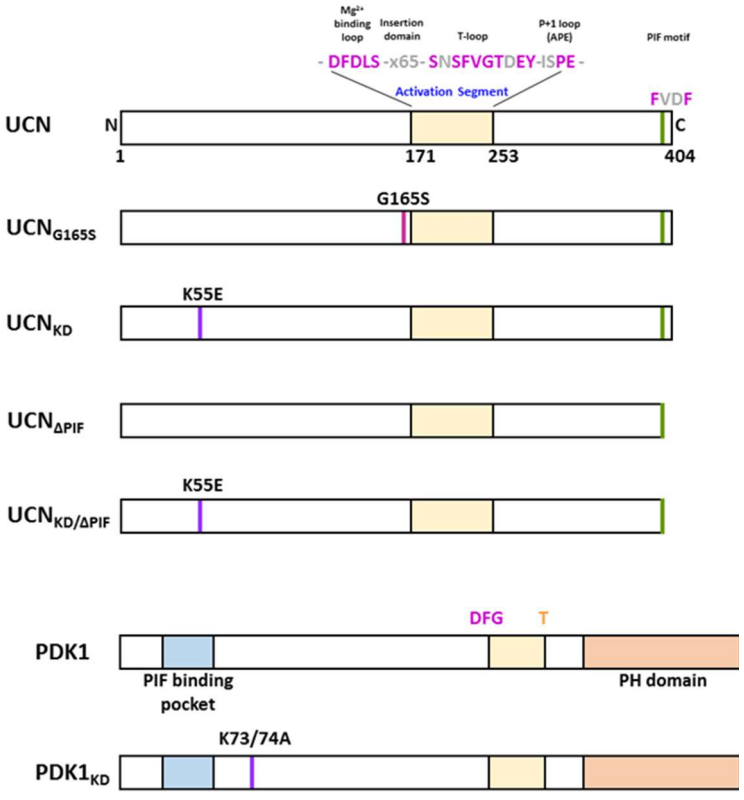

Figure 3-13 Basic structure of UCN and PDK1 proteins.

UCN WT protein consists of 404 AA. The activation segment, which starts with the indicated Mg^{2+}-binding loop followed by an insertion domain of 65 AA, the T-loop necessary for kinase activation and ends at the P+1 loop, is flanked by two kinase subdomains. UCN contains a PIF motif (FVDF) at its C-terminus. *ucn-1* mutation results in a G165S substituted version that lacks kinase activity. The UCN_{KD} (kinase deficient) version contains a K55E substitution, in which the conserved lysine residue is replaced by a glutamate. The $UCN_{\Delta PIF}$ version is lacking only the last four AA resulting in a protein of 400 AA. In KD/ΔPIF version, the latter two versions are combined. For detailed two-dimensional PDK1 structure, see -1. $PDK1_{KD}$ contains a K73A (PDK1.1) or K74A (PDK1.2) substitution, respectively. Substitution of the conserved lysine residue leads to loss of kinase function.

Figure 3-14 shows that purified MBP:PDK1 fusion proteins are able to trans-phosphorylate all purified GST:UCN_x versions. Autophosphorylation activity of MBP:PDK1.1 and MBP:PDK1.2 is shown in the first lanes, and autophosphorylation of GST:UCN is shown in the second lanes of

Figure 3-14, A and B. GST:UCN lacking the PIF motif (GST:UCN$_{\Delta PIF}$) still shows autophosphorylation activity (Figure 3-14 B, lane 8). No other UCN versions (UCN$_{G165S}$, UCN$_{KD}$ and UCN$_{KD/\Delta PIF}$) exhibit any kinase activity (A, lanes 8 and 9; B, lane 9). In combination with either MBP:PDK1.1 or MBP:PDK1.2, all GST:UCN$_x$ versions display signals in the autoradiograms (Figure 3-14 A, B; lanes 3 – 7), which indicates PDK1-mediated transphosphorylation of UCN. To quantify UCN phosphorylation, I have measured the intensities of the autoradiograms and normalized to the intensities on the Coomassie brilliant blue (CBB) SDS polyacrylamide gels using ImageJ2/Fiji (Schneider et al. 2012, Schindelin et al. 2012, Schindelin et al. 2015). The results are depicted in Figure 3-14 C and D. Hence, I can show that PDK1-mediated in vitro phosphorylation is significantly decreased in absence of PIF motif but it is not essential in vitro.

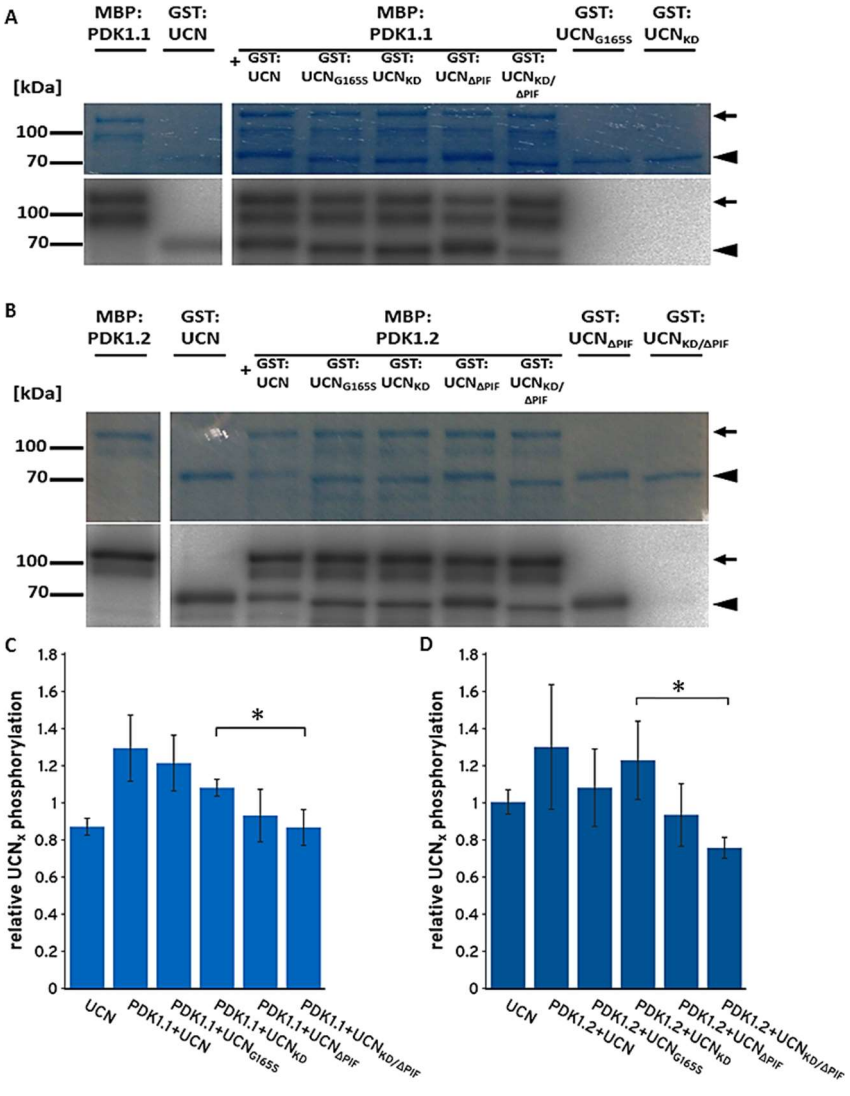

Figure 3-14 In vitro kinase assays of active PDK1.1, PDK1.2 and five different UCN versions.

Coomassie brilliant blue (CBB)-stained gels and autoradiograms for PDK1.1 and PDK1.2, respectively, in combination with different UCN versions are demonstrated. Uppermost band depicts MBP:PKD1 (arrows) and lowermost band depicts GST:UCN$_x$ (arrowheads). (A) Lane 1 shows MBP:PDK1.1 and lane 2 shows GST:UCN autophosphorylation. Lanes 3 – 7 show combinations of MBP:PDK1.1 and the five UCN versions described in Figure 3-13. Please note absence of any signal in lanes 8 and 9 (GST:UCN$_{G165S}$ and GST:UCN$_{KD}$). (B) Lane 1 shows MBP:PDK1.2 and lane 2 shows GST:UCN autophosphorylation. Lanes 3 – 7 show combinations of MBP:PDK1.2 and the five UCN versions described in Please note presence of autophosphorylation in lane 8 (GST:UCN$_{\Delta PIF}$) and absence of any signal in lane 9 (GST:UCN$_{KD/\Delta PIF}$). (C, D) UCN$_x$ phosphorylation intensity relative to CBB input in absence or presence of (C) MBP:PDK1.1 or (D) MBP:PDK1.2 is shown. Please note significant differences of

phosphorylation intensity in a PIF motif dependent manner (asterisks). P-values: (C) p=0.031, (D) p=0.039. Intensities were measured using ImageJ2/Fiji (Schneider et al. 2012, Schindelin et al. 2012, Schindelin et al. 2015). N = 3 (three independent expression-purification replicates and subsequent in vitro kinase assays).

To exclude influence of UCN autophosphorylation, I decided to compare relative UCN_x phosphorylation of GST:UCN_{KD} and GST:$UCN_{KD/\Delta PIF}$. Both PDK1s phosphorylate GST:$UCN_{KD/\Delta PIF}$ significantly less strongly compared to GST:UCN_{KD}. Moreover, PDK1-mediated transphosphorylation of UCN is stronger than UCN autophosphorylation (Figure 3-14 C, D; compare UCN alone with PDK1 + UCN_{KD}).

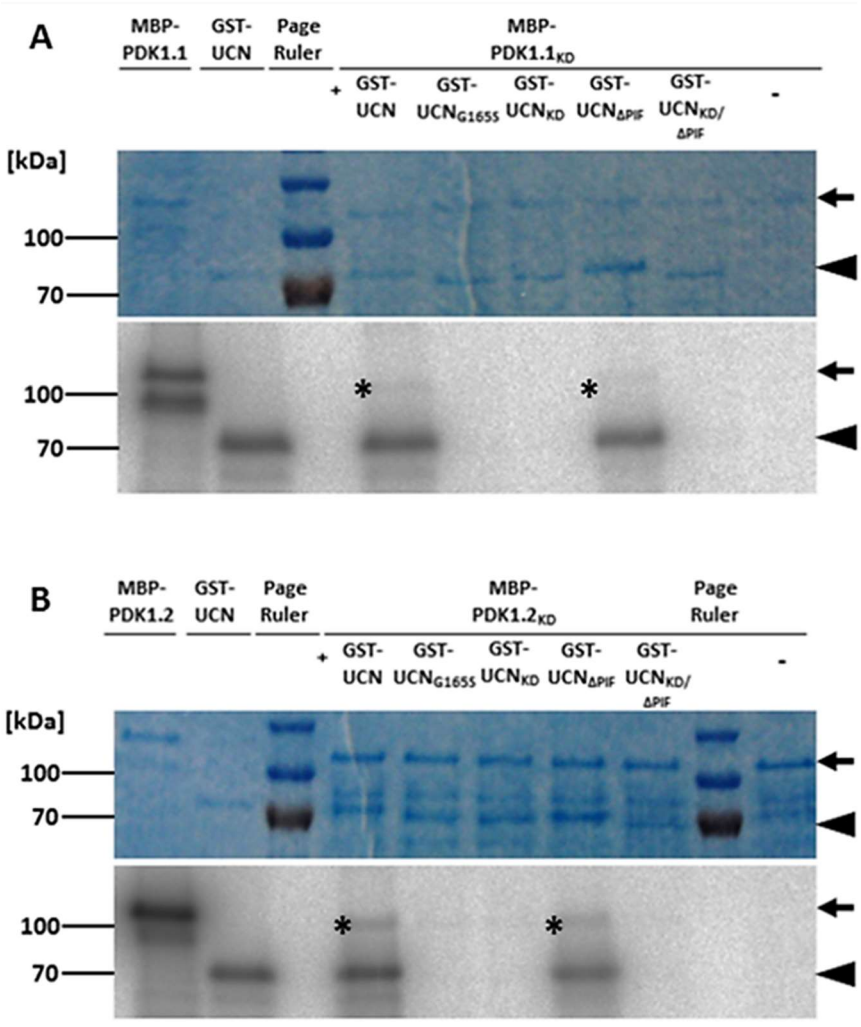

Figure 3-15 In vitro kinase assays of inactive PDK1 and active UCN.

CBB gels and autoradiograms for $PDK1.1^{KD}$ and $PDK1.2^{KD}$, respectively, combined with the five versions of UCN. (A) Lanes 1 and 2 show active PDK1.1 and active UCN, respectively, as controls. Lanes 4 – 8 show inactive PDK1.1 combined with either of the five UCN versions, and lane 9 shows $PDK1.1^{KD}$ without UCN as a control. Please note the UCN-mediated transphospho-rylation (asterisk) of $PDK1.1^{KD}$ in combination with WT UCN and $UCN^{\Delta PIF}$. (B) Lanes 1 and 2 show active PDK1.2 and active UCN, respectively, as controls. Lanes 4 – 8 show inactive PDK1.2 combined with either of the five UCN versions, and lane 9 shows $PDK1.2^{KD}$ without UCN as a control. Please note the UCN-mediated trans-phosphorylation (asterisk) of $PDK1.2^{KD}$ in combination with WT UCN and $UCN^{\Delta PIF}$. Arrows indicate PDK1 and arrowheads indicate UCN. N = 3.

In order to test whether GST:UCN also phosphorylates MBP:PDK1 in vitro, I used the above described kinase deficient versions of PDK1s and analyzed their behavior in kinase assays in absence or presence of the five GST:UCN versions. Figure 3-15 shows that GST:UCN as well as GST:UCN$_{\Delta PIF}$ phosphorylate both inactive MBP:PDK1$_{KD}$ fusion proteins. To summarize, I demonstrate in vitro that the active MBP:PDK1 versions phosphorylate GST:UCN, that active GST:UCN versions phosphorylate kinase deficient versions of MBP:PDK1, and that UCN's PIF motif contributes to this interaction but it is not essential in vitro.

Furthermore, I was interested if the presence of GST:UCN influences MBP:PDK1 activity. Thus, I performed kinase assays using active MBP:PDK1.1 or MBP:PDK1.2, respectively, in combination with increasing amounts of either GST:UCN, GST:UCN$_{G165S}$, or GST:UCN$_{KD}$. As shown in Figure 3-16, the amount of MBP:PDK1.1 (A – C) and MBP:PDK1.2 (D – F) was kept constant (CBB gels, arrows) and GST:UCN was increased from lane 4 to lane 9 (CBB gels, arrowheads). I measured relative MBP:PDK1 phosphorylation intensities as described above. Figure 3-16 reveals that the determined MBP:PDK1 phosphorylation intensities relative to CBB input are constant in combinations with UCN$_{G165S}$ and UCN$_{KD}$ (Figure 3-16, B and C). In combination with active GST:UCN, both MBP:PDK1 phosphorylation intensities show a slight but significant decrease. The higher the GST:UCN level the lower were the measured MBP:PDK1 intensities (Figure 3-17A). The detected decrease in phosphorylation intensity was stronger for PDK1.2 than for PDK1.1.

These results suggest that high levels of active GST:UCN are able to repress PDK1 activity in vitro, whereas the two inactive versions do not significantly alter PDK1 activity.

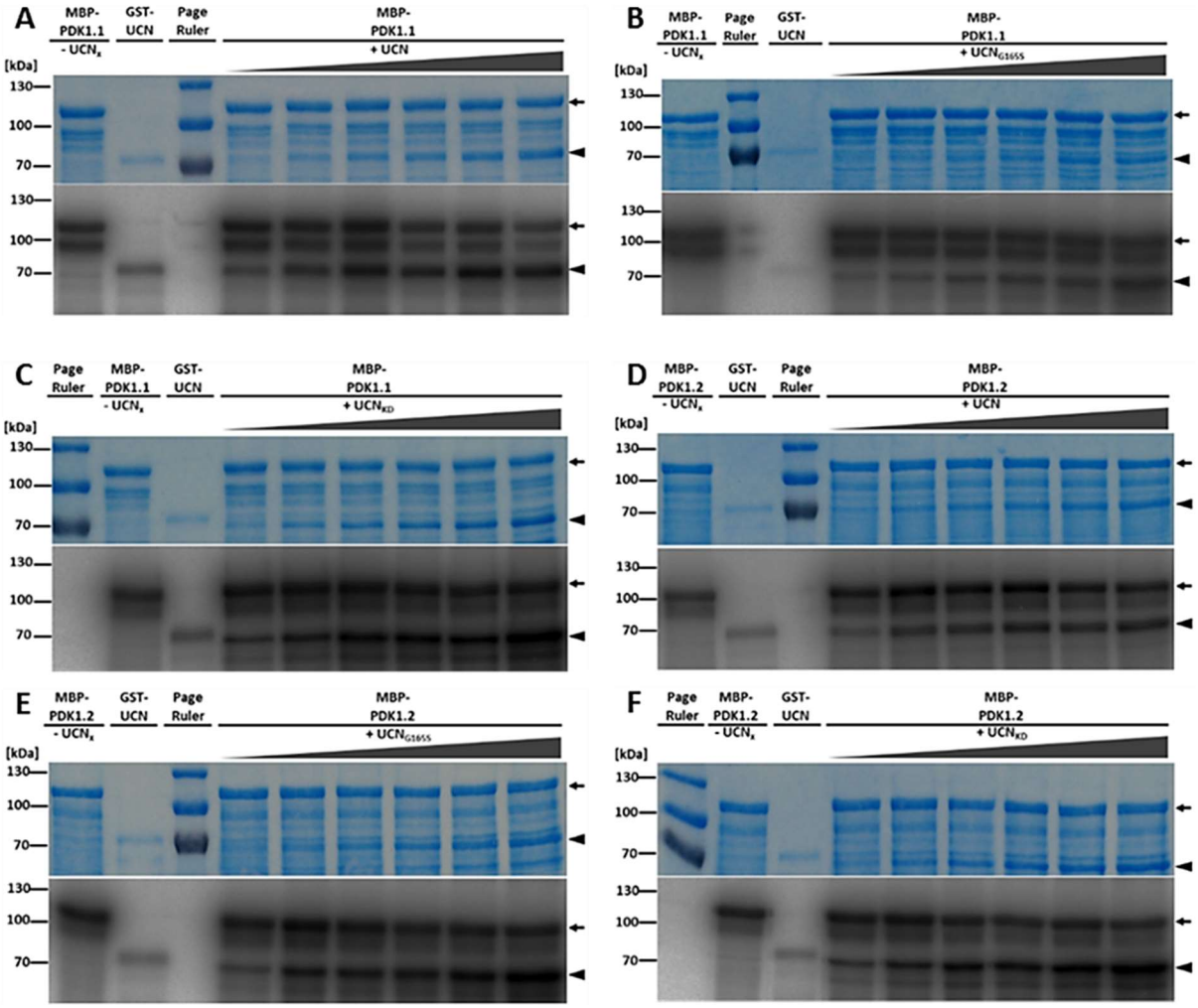

Figure 3-16 Influence of increasing amounts of UCN on PDK1 activity.

CBB gels and autoradiograms for PDK1 and increasing amounts of either UCN, UCN_{G165S} or UCN_{KD}. (A) Constant levels of PDK1.1 with increasing amounts of UCN. (B) Constant levels of PDK1.1 with increasing amounts of UCN_{G165S}. (C) Constant levels of PDK1.1 with increasing amounts of UCN_{KD}. (D) Constant levels of PDK1.2 with increasing amounts of UCN. (E) Constant levels of PDK1.2 with increasing amounts of UCN_{G165S}. (D) Constant levels of PDK1.2 with increasing amounts of UCN_{KD}. Arrows indicate PDK1 and arrowheads indicate UCN_x. The first (A, B, D, E) or the second (C, F) lane shows PDK1 without UCN. The second (A, B, D, E) or the third (C, F) lane shows UCN auto-activity. Lanes 4 – 9 show PDK1 with increasing amounts of UCN_x (with lane 4 containing the lowest, and lane 9 the highest UCN_x amount; indicated by the grey triangles). N = 3.

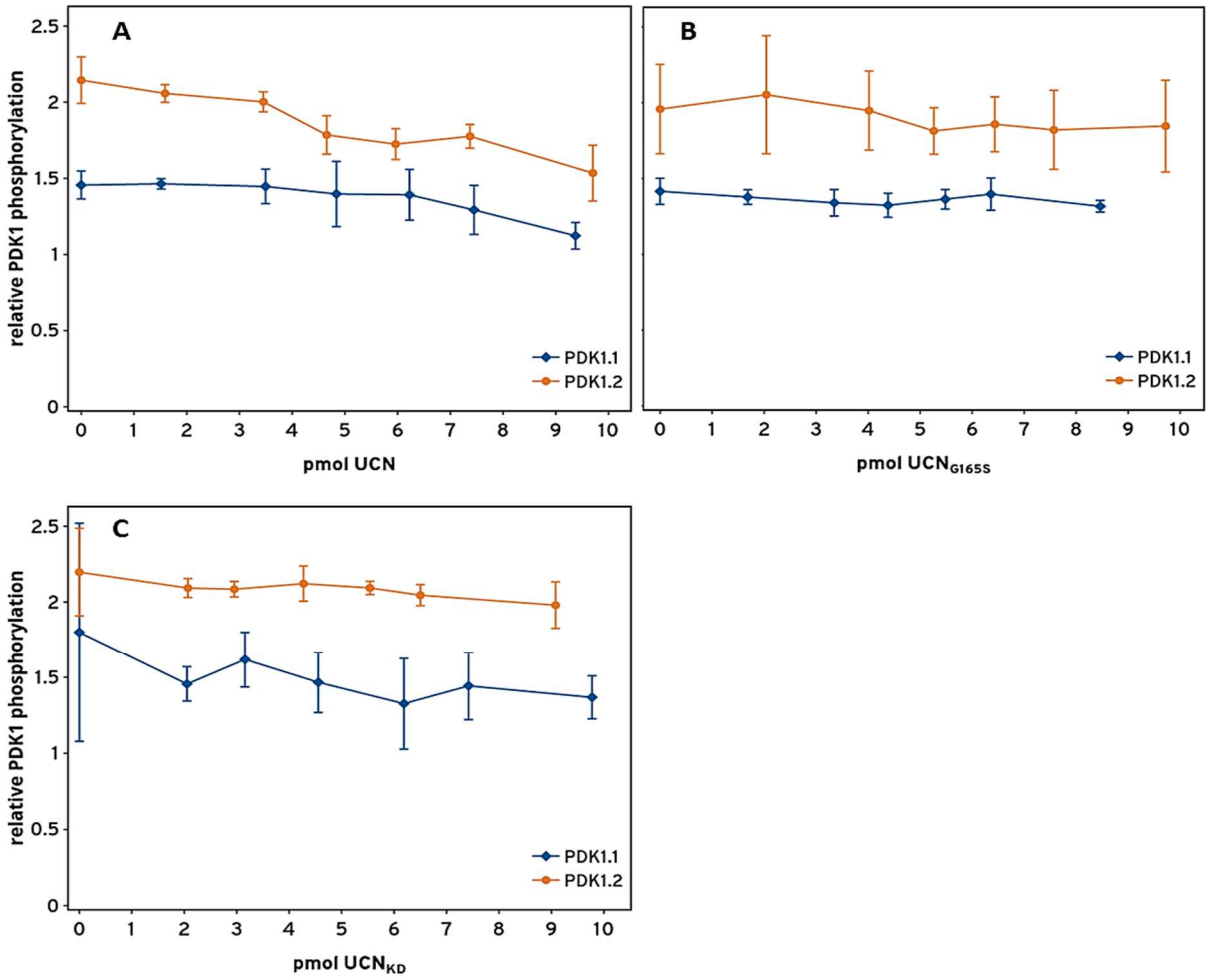

Figure 3-17 Relative PDK1 phosphorylation with respect to UCN$_x$ levels.

PDK1 phosphorylation relative to the CBB input dependent on the level of UCN$_x$ is depicted. Triplicates for each combination shown in Figure 3-16 were measured using ImageJ/Fiji (Schneider et al. 2012, Schindelin et al. 2012, Schindelin et al. 2015). Please note the significant decrease in relative PDK1 phosphorylation dependent on active UCN (upper left; p-values for the highest compared to the lowest level of UCN: p(PDK1.1)=0.021, p(PDK1.2)=0.024). In presence of UCN$_{KD}$ (upper right) or UCN$_{G165S}$ (lower left) no decrease in relative PDK1 phosphorylation was observed. N = 3.

To gain deeper insights in the regulation of UCN, I was interested in detecting the PDK1-dependent UCN phosphorylation sites. Consequently, I performed 'cold' kinase assays and in collaboration with Dr. Fiona Pachl (Chair of Proteomics and Bioanalytics, Prof. Dr. B. Küster, TUM) proteins were analyzed in a liquid chromatography-mass spectrometry/mass spectrometry (LC-MS/MS) approach. Recovery of all peptides of UCN was only 47 – 51% but we were able to identify two phosphorylated serine residues (S233 and S242) within the activation segment of UCN. S242 represents the predicted serine in the T-loop necessarily phosphorylated for activation of the kinase (Figure 3-18). The second detected Ser residue (S233) represents probably the secondary phosphorylation site within the activation segment, which is known to contribute to the catalytic

activity of several AGC kinases (Nolen et al. 2004). The in vitro detected PDK1-dependent phosphorylation sites could be a first cue for PDK1-dependent activation of UCN.

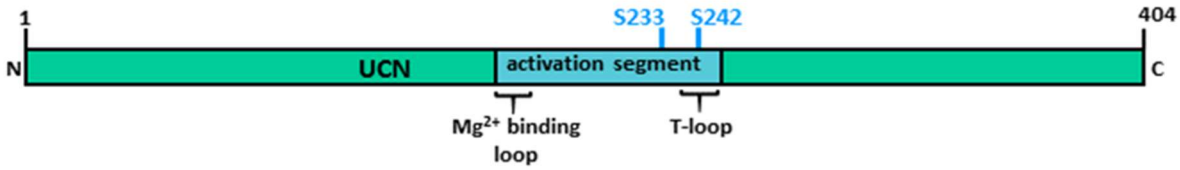

Figure 3-18 PDK1-dependent UCN phosphorylation sites in vitro.

Two phosphorylated serine residues, namely S233 and S242, were detected in a LC-MS/MS approach in collaboration with Dr. Fiona Pachl and Dr. Peng Yu (Chair of Proteomic and Bioanalytics at TUM, Prof. Dr. B. Küster). Both Ser residues are located in the activation segment. S242 represents the conserved activation site in the T-loop.

3.2.3.3 Yeast two-hybrid assay

To substantiate the direct in vitro interactions between the PDK1 proteins and UCN, I performed yeast two-hybrid assays (Y2H). Therefore, I used the protein versions described in Figure 3-13 and section 3.2.3.2. PDK1 versions were fused to the activation domain (AD) and UCN versions were fused to the DNA-binding domain (DB) of the GAL4 transcription factor and co-transformed into yeast strain AH109. As shown in Figure 3-19, only yeast cells transformed with the WT versions of either PDK1 and WT UCN were able to grow on triple drop-out medium (SD-LWH) whereas on double drop-out medium (SD-LW; transformation control) yeast cells co-transformed with any AD – DB combination grew. The results showed that PDK1 (WT) and UCN (WT) proteins directly interact with each other in a Y2H assay. The controls with only AD or DB, respectively, did not grow on SD-LWH.

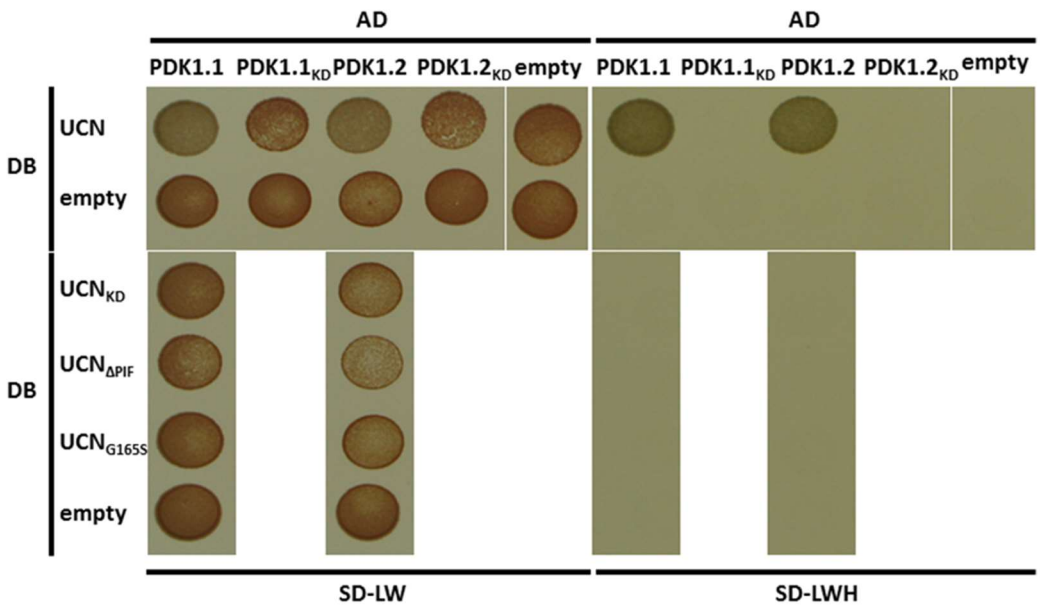

Figure 3-19 Yeast two-hybrid assay of AD:PDK1 versions combined with DB:UCN versions.

DB:UCN was tested with all four versions of PDK1, the other UCN versions were only tested with the wild type versions of PDK1. The left panel depicts yeast growth on transformation control plates (SD-LW), the right panel the interaction control plates (SD-LWH). Please note that only those yeast cells are able to grow on SD-LWH, which were co-transformed with DB:UCN and AD:PDK1.1 or AD:PDK1.2. AD: activation domain of GAL4 TF; DB: DNA-binding domain of GAL4 TF; SD-LW: SD medium lacking Leu and Trp (transformation control); SD-LWH: SD medium lacking Leu, Trp, and His (interaction control).

3.2.3.4 Bimolecular fluorescence complementation assay in Arabidopsis protoplasts

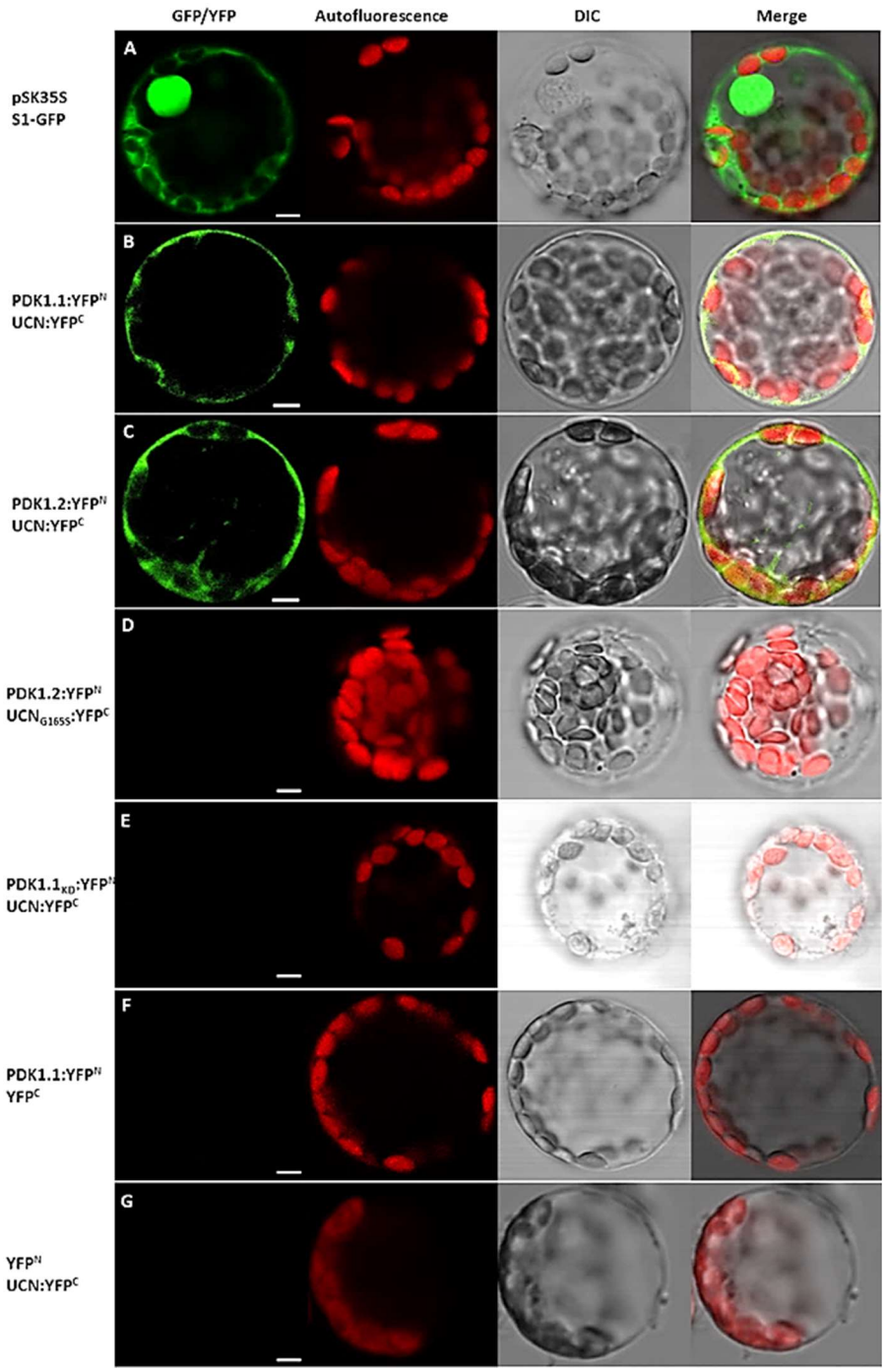

Figure 3-20 Bimolecular fluorescence complementation assays in Arabidopsis mesophyll protoplasts.

Protoplasts were co-transformed with pSPYNE:PDK1$_x$ or pSPYNE$_{ev}$, respectively, and pSPYCE:UCN$_x$ or pSPYCE$_{ev}$, respectively. (A – G) Confocal micrographs depicting GFP/YFP channel, chloroplast autofluorescence, DIC and merge (from left to right). (A) Free GFP. (B – G) BiFC combinations. The combinations are given on the left. Please note that only the WT combinations (B, C) show YFP fluorescence, whereas absence of kinase activity of either interaction partner does not lead to any fluorescence (D, E). Empty vector controls do not show YFP complementation (F, G). For all negative combinations at least 800 protoplasts were inspected. Scale bars: 5 µm.

As a third different and independent method to show direct protein-protein interaction in a plant cell between the studied AGC kinases, I finally employed a bimolecular fluorescence complementation (BiFC; Split-YFP) assay in Arabidopsis mesophyll protoplasts. To this end, we cloned the protein versions described above (Figure 3-13; 3.2.3.2) into vectors pSPYNE or pSPYCE, respectively (Walter et al. 2004). PDK1 versions were fused to the N-terminal part (pSPYNE) and

UCN versions to the C-terminal (pSPYCE) part of YFP. Protoplasts were successfully isolated and transfected with either transfection control, pSK35S-GFP (Figure 3-20 A; gift from Chair of Botany (Prof. Dr. E. Grill), TUM), or different combinations of pSPYNE and pSPYCE (Figure 3-20, B – G), and analyzed using an Olympus FV1000 CLSM. Free GFP of transfection control was detected in the cytosol and the nucleus (A), YFP signals were detected in the cytosol (B, C). I detected YFP fluorescence only for the combinations PDK1.1:YFP^N – UCN:YFP^C and PDK1.2:YFP^N – UCN:YFP^C (Figure 3-20, B and C). All combinations with either a kinase deficient PDK1, a kinase deficient UCN (UCN_{G165S}, UCN_{KD}, $UCN_{KD/\Delta PIF}$) or a PIF-deleted UCN ($UCN_{\Delta PIF}$ and $UCN_{KD/\Delta PIF}$) did not exhibit any YFP signals (Figure 3-20, D and E; two examples are shown). The used negative controls, in which only YFP^C in combination with PDK1:YFP^N or only YFP^N in combination with UCN:YFP^C were combined, all showed no signal (Figure 3-20, F and G). This study in plant cells substantiates the beforehand executed studies in yeast and in vitro. I can clearly show that both PDK1 proteins interact with UCN in at least three independent assays (in vitro, in yeast, and in plant cells).

3.2.4 Relationship between *PDK1* and *ATS*

The negative regulation of PDK1 by UCN mimics the similar inhibition of ATS by UCN (Enugutti et al. 2012, Enugutti and Schneitz 2013). This raises the question how UCN, ATS and PDK1 relate to each other. In order to address this issue, I started to investigate the relationship between PDK1 and ATS. The *ATS* activation tagging line *sk21-D* described by Gao et al. (2010) overexpresses *ATS* in its normal expression domain. This leads to mild *ucn-1*-like protrusions in the integuments (Enugutti and Schneitz 2013). The combination *sk21-D ucn-1* results in an enhanced outgrowth (Enugutti and Schneitz 2013). In a first experiment, I crossed the sk21-D line with the *pdk1* KO lines described in section 3.1.3, and I analyzed double homozygous F3 offspring. I analyzed 346 ovules for *pdk1.1 sk21-D*, and 367 ovules for *pdk1.2 sk21-D*. Whereas 21 of 306 (6.8%) homozygous *sk21-D* ovules showed protrusion formation, none of the analyzed ovules in *pdk1 sk21-D* exhibited any protrusions (Figure 3-21). This genetic finding relates *ATS* to *PDK1* and suggests that PDK1 activity is required for protrusion formation in *ATS* overexpressors.

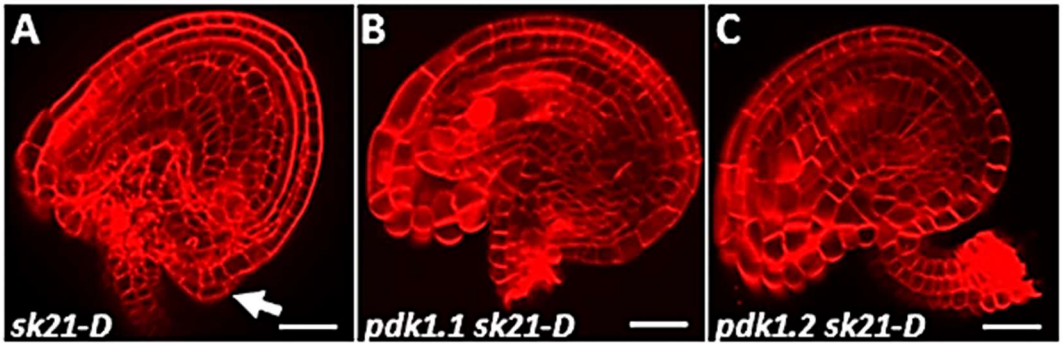

Figure 3-21 Confocal micrographs of mature ovules of (A) *sk21-D*, (B) *pdk1.1 sk21-D,* and (C) *pdk1.2 sk21-D.*

Ovules were stained according to the mPS-PI protocol (Truernit et al. 2008). Please note the protrusion in A (arrow) and absence of protrusions in B and C. Scale bars: 20 µm.

Since PDK1:EGFP localizes to the cytosol and to the PM, and ATS:YFP was only found to be present in the nucleus, direct in planta interaction between PDK1 and ATS is unlikely. In vitro kinase assays showed a very weak phosphorylation of ATS by PDK1 (not shown) but I could not confirm this interaction in BiFC assays in protoplasts (Figure 3-24, K). How exactly PDK1 and ATS relate to each other in planar growth control remains to be determined (see discussion, section 4.2.1).

3.3 UCN phosphorylates serine residues of ATS in vitro

UCN was shown to directly repress the transcription factor ATS (Enugutti et al. 2012, Enugutti and Schneitz 2013). I was interested to shed more light onto this interaction. Therefore, I performed 'cold' kinase assays, in which I incubated either GST:UCN or GST:UCN$_{G165S}$ with a thioredoxin-6xHis tagged ATS(Trx:6xHis:ATS). Subsequently, the proteins were digested with trypsin (or pepsin) and analyzed in a LC-MS/MS approach for detection of potential phosphosites (performed in collaboration with Dr. Fiona Pachl and Dr. Peng Yu from the Chair of Proteomics and Bioanalytics, Prof. Dr. B. Küster, TUM). Unfortunately, recovery of ATS peptides was not satisfactory in three different approaches (trypsin or pepsin digestion, use of an inclusion list). Three phospho-serine residues were detected within the recovered peptides (S13, S92, S211; Figure 3-22). Peptides, which could not be recovered in MS analysis, contain another seven serine residues whose phospho-status remains unknown.

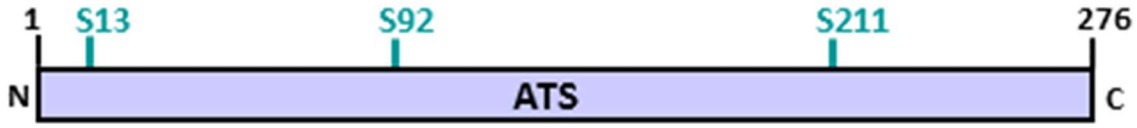

Figure 3-22 ATS phosphosites determined in a LC-MS/MS approach.

Three phosphorylated serine residues, namely S13, S92 and S211, were detected in a LC-MS/MS approach in collaboration with Dr. Fiona Pachl and Dr. Peng Yu (Chair of Proteomic and Bioanalytics at TUM, Prof. Dr. B. Küster). Unfortunately, ATS peptides harboring another seven Ser residues could not be recovered.

3.3.1 UCN still phosphorylates ATS-phosphomutants

Since we were not able to detect the remaining peptides in different approaches, I decided to substitute the three detected phospho-serine residues with alanine residues (phospho-mutants) to test if UCN still interacts with those mutant proteins. Figure 3-23 shows that recombinant GST:UCN is able to phosphorylate recombinant Thioredoxin (Trx):6xHis:ATS (lane 1) as well as all ATS-phosphomutants (single mutants in lanes 3 – 5; double mutants in lanes 7 – 9; and triple phosphomutant in lane 10). I did not detect any obvious differences in phosphorylation intensity of those mutants compared to WT ATS. Other serine residues in the peptides not recovered seem to be phosphorylation targets for UCN in vitro as well.

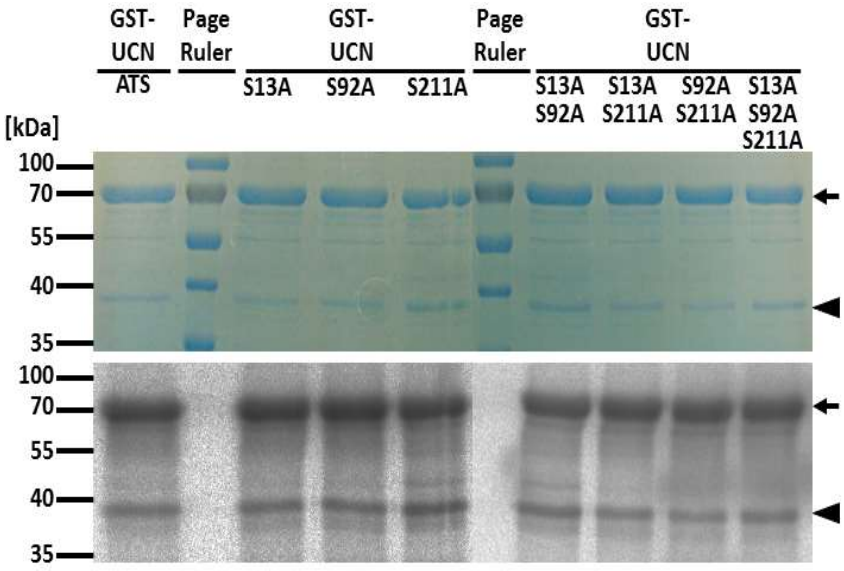

Figure 3-23 UCN-mediated phosphorylation of ATS-phosphomutants.

CBB gel and autoradiogram of active UCN combined with different phosphomutants of ATS. S13, S92 and S211 were mutated to alanines. Lane 1 shows UCN with ATS WT version, lanes 3 – 5 UCN with the single phosphomutants, lanes 7 – 9 the double mutants and lane 10 the triple phosphomutant. Please note that UCN phosphorylates all ATS mutants. Arrows indicate UCN, arrowheads ATS.

3.3.2 UCN interacts with ATS-phosphomutants in plant cells

In order to test the relevance of the detected phospho-serine residues, I transformed Arabidopsis mesophyll protoplasts with BiFC constructs as described in section 3.2.3.4 using WT ATS and its phosphomutants fused to YFP^N and UCN versions fused to YFP^C. As shown in Figure 3-24 (A and J), neither ATS:YFP^N nor UCN:YFP^C display any YFP fluorescence complemented with only YFP^C or YFP^N, respectively (negative control). As published by Enugutti et al. (2012), ATS:YFP^N together with UCN:YFP^C gives a YFP signal in the nucleus (B). To elucidate if substitutions of the three ATS serine residues have any impact on the interaction with UCN, I tested all ATS single,

double and triple phosphomutants fused to YFP^N in combination with UCN:YFP^C (Figure 3-24, C – I). All these combinations depict the same behavior as the WT proteins showing YFP fluorescence exclusively in the nucleus. These results support the above-shown in vitro data meaning that either the detected phosphosites are an in vitro artifact or that UCN phosphorylates other residues besides the discovered ones.

Furthermore, I have tested if PDK1-related UCN mutations/deletions still lead to interactions with ATS (Figure 3-24, L – O). Here, I show that UCN ATS interaction in protoplasts is not PIF-dependent (L) but on UCN kinase activity (M – O). Without UCN PIF motif the YFP fluorescence still localized to the nucleus (L) but three kinase deficient UCN versions fused to YFP^C in combination with ATS:YFP^N did not display any fluorescence complementation (M – O). Since the PIF motif is supposed to be only crucial for the interaction between UCN and PDK1, no impact of PIF deletion on ATS UCN interaction was assumed. Additionally, I wanted to know whether ATS interacts directly with PDK1. In more than 800 protoplasts inspected, I was not able to detect any YFP fluorescence, neither in the nucleus nor in the cytosol Figure 3-24, K).

Taken together, UCN directly represses ATS and PDK1 presumably in a similar posttranslational fashion. However, since a *pdk1* knockout rescues not only the integuments but also the flowers, PDK1 repression appears more global in comparison to ATS. Identification of PDK1 as a regulator of planar growth is a major breakthrough regarding the understanding of the UCN-mediated molecular mechanism coordinating cell division and growth in ovule integuments and other floral organs.

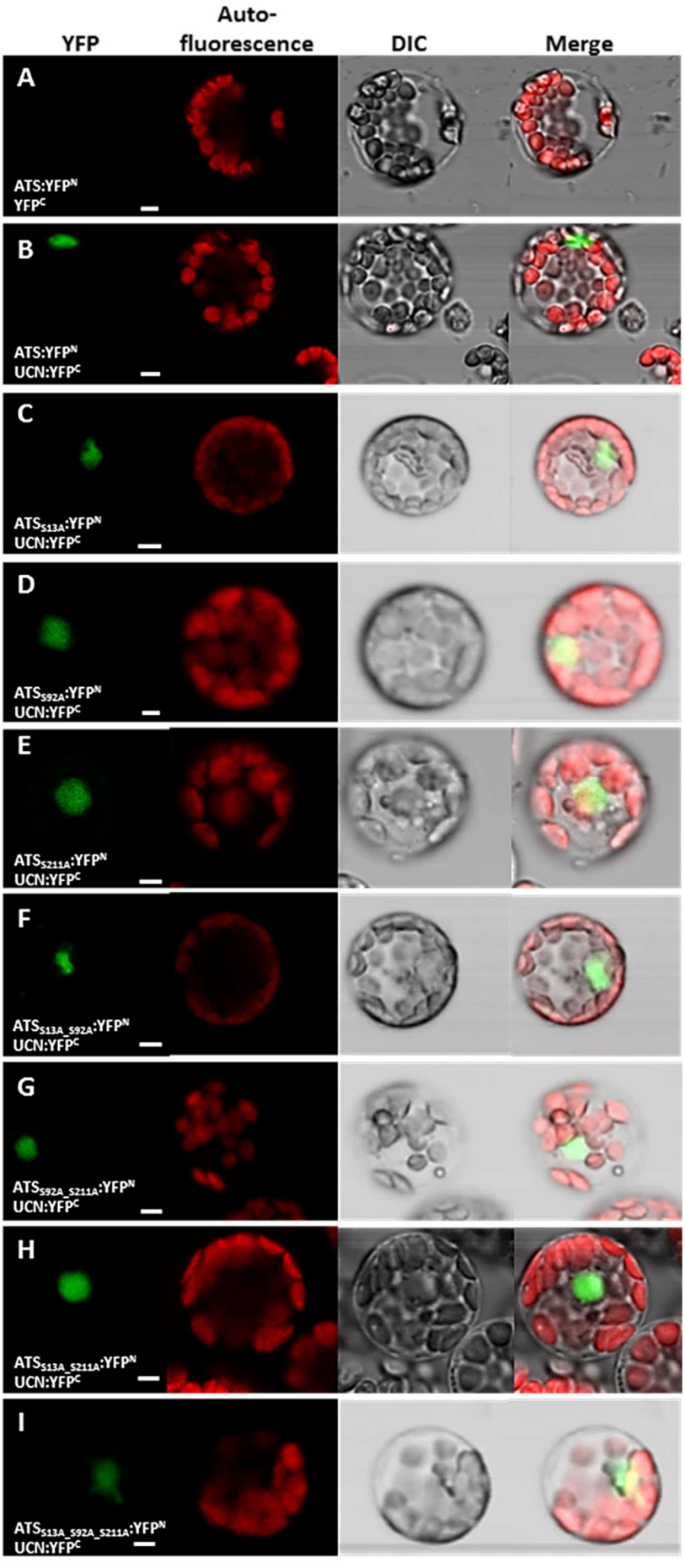

Figure 3-24 Bimolecular fluorescence complementation assays between UCN_x, PDK1 and ATS phosphomutants in Arabidopsis mesophyll protoplasts.

Protoplasts were co-transformed with pSPYNE:$PDK1_x$, pSPYNE:ATS, or $pSPYNE_{ev}$, respectively, and pSPYCE:UCN_x, pSPYCE:ATS, or $pSPYCE_{ev}$, respectively. (A – G) Confocal micrographs depicting YFP channel, chloroplast autofluorescence, DIC and merge (from left to right). (A + J) Negative controls. (B – I, K – O) BiFC combinations. The combinations are given on the left. Please note that all ATS phosphomutants with UCN show YFP signals in the nuclei (C - I), whereas absence of UCN kinase activity (M – O) does not lead to any fluorescence. The UCN PIF motif is not necessary for the interaction with ATS (L). Empty vector controls do not show YFP complementation (A, J). For all negative combinations at least 800 protoplasts were inspected. Scale bars: 5 µm. Figure continues on next page.

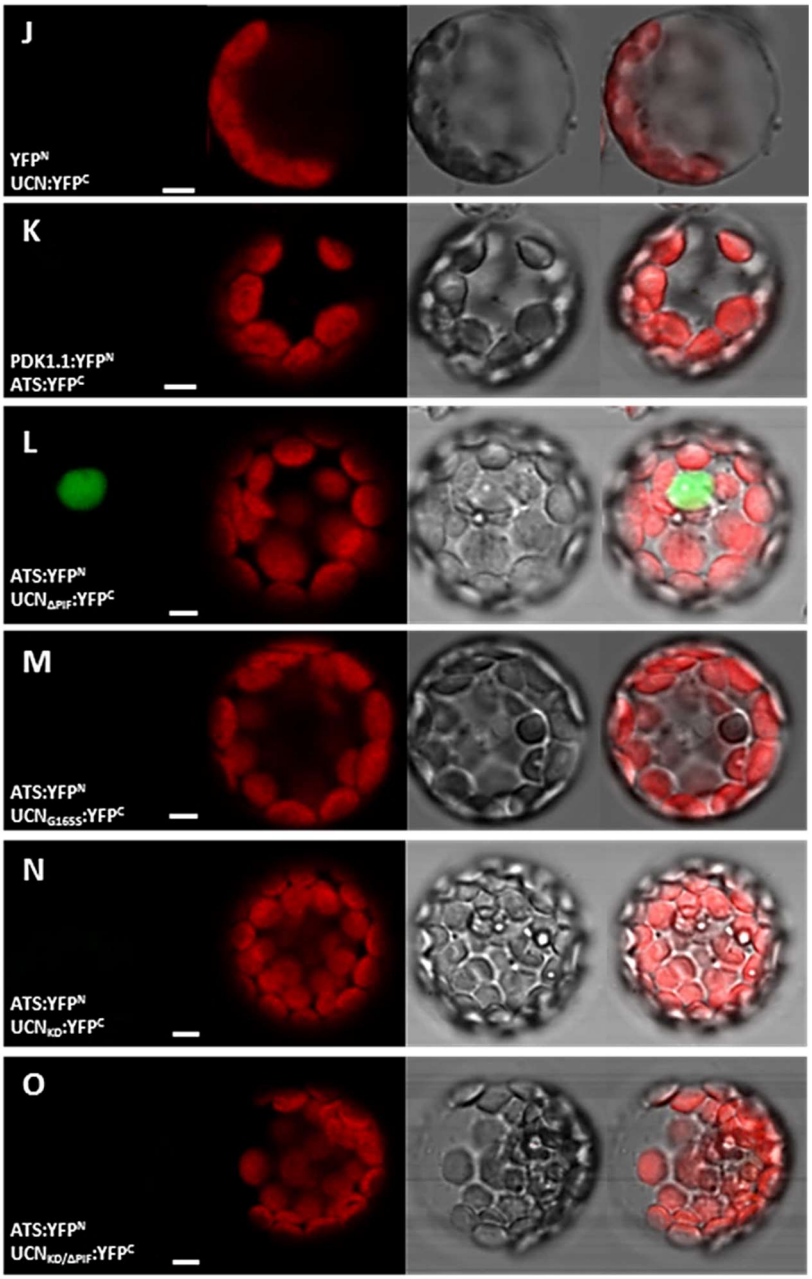
J
YFP^N
UCN:YFP^C
K
PDK1.1:YFP^N
ATS:YFP^C
L
ATS:YFP^N
UCN_ΔPIF:YFP^C
M
ATS:YFP^N
UCN_G165S:YFP^C
N
ATS:YFP^N
UCN_KD:YFP^C
O
ATS:YFP^N
UCN_KD/ΔPIF:YFP^C

3.4 Generation of novel *ucn* alleles

Unfortunately, the second *ucn* allele (*ucn-10*) displaying strong *ucn-1*-like phenotypes has been lost. Moreover, the null allele *ucn-2* in Col-0 background exhibits morphological *ucn-1*-like phenotypes only under short day conditions. Therefore, I decided to utilize the CRISPR/Cas9 system to generate novel *ucn* alleles in order to obtain at least one additional independent *ucn* mutant allele. Therefore, I made use of the system developed by Wang et al. (2015), in which an egg cell specific promoter (*pEC1.2*) controls *Cas9* expression. The advantage of an egg cell specific over constitutive promoters (e.g., *pCaMV35S, pUBQ10*) is the occurrence of homozygous or trans-heterozygous mutations already in T1 generation rather than a genetic mosaic. Here, I present a novel *ucn* mutant, which I named *ucn-11*.

3.4.1 Approach

In order to try to mimic the *ucn-10* allele (D122N), I designed a single guide RNA (sgRNA) binding to the region +346 to +365 of the *UCN* coding sequence. The destination vector pHEE401 containing this sgRNA under control of the *U6-26* promoter and the plant optimized *Cas9* coding sequence under control of *pEC1.2* was transformed into L*er* and Col-0 WT plants. Subsequently, I phenotypically analyzed the resulting T1 generation and sequenced the target region of three T1 plants (L*er* background) showing a mild *ucn-1*-like phenotype.

3.4.2 Characterization of *ucn-11*

Phenotypic analysis of the resulting independent T1 plants suggested that three of them might contain a mutation in the *UCN* gene. In order to evaluate whether these three plants harbor a desired mutation, I sequenced the region of interest. For one plant, I obtained a mutated sequence besides the WT sequence indicating heterozygosity. The other two plants showed WT sequence. Subsequently, I cloned the amplicon featuring into pJET1.2/blunt and transformed the resulting vector into *E.coli*. Subsequently, I sequenced four clones. One of them contained a sequence distinct from WT sequence. This sequence depicted a single adenine insertion at position +386 leading eventually to a STOP codon at position +391 to +393 (Figure 3-25), and resulting in a protein of only 130 instead of 404 AA. The predicted mutant protein lacks the whole activation segment, the complete second kinase subdomain and 40 AA of kinase subdomain 1

making it most likely an inactive kinase. Molecular characterization of *ucn-11* needs to be performed in more detail.

The resulting phenotype is displayed in Figure 3-25. Compared to *ucn-1* (Figure 3-25, C), the novel *ucn-11* mutant shows weaker but conspicuous protrusions in ovules and floral distortion (Figure 3-25, B). To date, I have obtained more CRISPR-mediated mutants for other target regions of *UCN* and for the *PDK1* genes in L*er* background, which need to be analyzed pheno- and genotypically.

To conclude, the utilized CRISPR/Cas9 system is functional and sufficient to obtain mutants in different target regions and results in expected phenotypes in case of *UCN.*

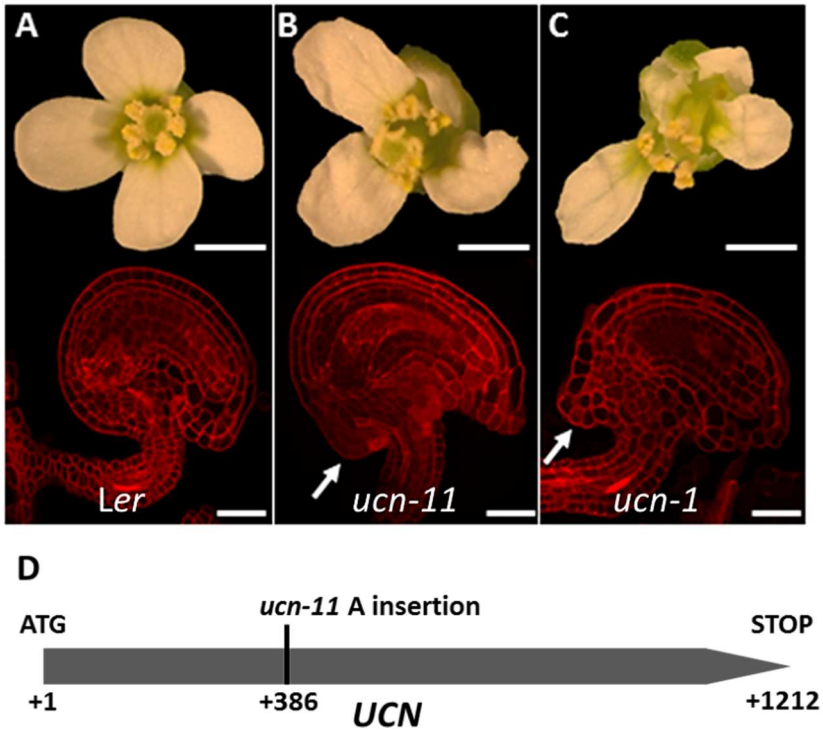

Figure 3-25 Stereo- and confocal micrographs depicting *ucn-11* phenotype, and *UCN* gene structure.

The upper panel depicts stereo-micrographs of flowers, the lower panel confocal micrographs of mPS-PI stained mature ovules. (A) L*er* WT, (B) *ucn-11*, and (C) *ucn-1* phenotypes. Please note distorted flower and ovule protrusion (arrow) in *ucn-11* and *ucn-1*. Scale bars: (flowers) 1 mm; (ovules) 20 µm. (D) Gene structure of *UCN* with CRISPR/Cas9 induced *ucn-11* single A insertion.

4 DISCUSSION

The spatiotemporal orchestration of proliferation and elongation is of paramount importance for the maintenance of distinct cell layers and tissue morphogenesis. Aberrant behavior of molecular components of this process can result in tumor formation (Weinberg 2014). Among various central cell cycle regulators in animals, several members of the AGC kinase family play key roles in tumor formation and cancer (Pearce et al. 2010). The most prominent AGC kinase with respect to the formation of tumors and cancerogenesis in animals is PDK1 (Gagliardi et al. 2017). By contrast, plants have evolved mechanisms that seem to maintain tissue architecture more robustly, as they appear relatively resistant to spontaneous or hereditary genetic tumor formation. The rigid cell wall that immobilizes plant cells prevents plants from developing cancer (Doonan and Sablowski 2010). Thus, the control of tissue architecture maintenance in plants is considered to vary from that in animals (Dodueva et al. 2007, Doonan and Sablowski 2010).

4.1 PDK1s – AGC master regulators of development?

AGC kinases play pivotal roles in animals as well as in plants. Many of them are involved in important developmental processes. Animal PDK1 is known as the master regulator of AGC kinase signaling by transducing signals from phospholipids as secondary messenger to the downstream AGC kinase targets, which subsequently initialize signaling pathways. *PDK1* genes are present in all eukaryotic kingdoms of life (Zegzouti et al. 2006a, Zegzouti et al. 2006b, Dittrich and Devarenne 2012), and plant PDK1 proteins are strongly conserved among angiosperms (Figure 3-2). PDK1 functions in animals, especially in mammals, in a more crucial fashion compared to Arabidopsis. Despite a broad expression range throughout development and tissues (Figure 3-3, Figure 3-6; sections 3.1.2, 3.1.4), Arabidopsis *PDK1* functions seem to be involved in specific developmental tasks, such as root hair growth (Anthony et al. 2004, supplemental Figure 7-3). Overexpression of *PDK1* results in strongly affected root hair growth (supplemental Figure 7-3; Anthony et al. (2004)) and aberrant floral organ development including petals and ovules (Figure 3-10). Here, I present a functional analysis of PDK1 with respect to different aspects of plant development and to *UCN* signaling.

4.1.1 Do other kinases substitute for the PDK1s?

Since double knockout *pdk1.1 pdk1.2* plants show a very mild phenotype (Camehl et al. (2011), this study), the question was raised whether other kinases substitute PDK1's vital role (Zhang and McCormick 2009, Zulawski et al. 2014). By contrast, *PDK1* downregulation by 90% in mice led to 40 – 50% overall size reduction, and the knockout of *PDK1* resulted in abortion of the embryos at day 9.5 of embryo development (Lawlor et al. 2002), the double knockdown of tomato *PDK1s* is lethal as well (Devarenne et al. 2006), and *Physcomitrella patens PDK1* KO mosses exhibit strong developmental phenotypes and are severely impaired in abiotic stress resistance (Dittrich and Devarenne 2012). This leads to the hypothesis that the functions of *PDK1* in different species have evolved to distinct extents. In some species, *PDK1* is of essential importance for survival of the organism (Lawlor et al. 2002, Devarenne et al. 2006); in others the impact is more or less limited to distinct aspects of development (Matsui et al. 2010, Camehl et al. 2011, Dittrich and Devarenne 2012). The data regarding the nature of PDK1 proteins in plants show that they share common features (an activation segment including the Mg^{2+}-binding site and the T-loop) and are very similar in size (Figure 3-2). The third predicted PDK1 (Zulawski et al. 2014) does not show any of these features (supplemental Figure 7-3). This clearly indicates that there is no evidence for At2g20050 representing a PDK1-like protein, and unfortunately, the authors of this study do not explain how and why they claim that At2g20050 should represent PDK1.3.

Accordingly, the question about the presence of other kinases substituting PDK1 function in pivotal processes of Arabidopsis development remain unanswered. In this study, I was also not able to find a good candidate as PDK1 substituent. BLAST approaches at NCBI and literature research were not sufficient to reveal any adequate candidate kinase.

Taking AGC kinase regulation in animals into account, the mammalian TARGET OF RAPAMYCIN (mTOR) kinase homolog could be involved in AGC kinase regulation in Arabidopsis as well (Figure 4-1). In mammals, TOR forms at least two functionally and structurally distinct complexes, mTORC1 and mTORC2 (Wullschleger et al. 2006, Laplante and Sabatini 2012, Cornu et al. 2013). The RAPTOR-mTOR complex (mTORC1) consists of several proteins including RAPTOR (regulatory associate protein of target of rapamycin), and is rapamycin sensitive. The second complex, mTORC2, which contains, among others, the RICTOR (rapamycin-insensitive companion of mTOR) protein, regulates spatial cell growth, by controlling cytoskeleton structure and polarity via phosphorylation of the AGC kinase Akt/PKB (Wullschleger et al. 2006, Laplante and Sabatini 2012, Cornu et al. 2013). Moreover, mTORC2 was shown to act as the elusive "PDK2" in the

regulation of Akt/PKB signaling (Sarbassov et al. 2005). In plants, the presence of a conserved and functional TORC1 complex was shown (Mahfouz et al. 2006, Moreau et al. 2012, Xiong and Sheen 2012, Xiong et al. 2013, Xiong and Sheen 2014). Although the presence of a TORC2 complex in plants has not been reported so far, it is hypothesized in several studies and reviews (Díaz-Troya et al. 2008, Moreau et al. 2010, Dobrenel et al. 2011, Moreau et al. 2012, Robaglia et al. 2012, Xiong and Sheen 2014). Arabidopsis *tor* mutants are embryo lethal, revealing the paramount importance of the TOR kinase as well in plants (Menand et al. 2002, Ren et al. 2012). Manipulating TOR kinase activity results in alterations in growth and development from embryogenesis to senescence (Menand et al. 2002, Deprost et al. 2007, Ren et al. 2011, Ren et al. 2012, Xiong and Sheen 2012, Caldana et al. 2013, Xiong et al. 2013).

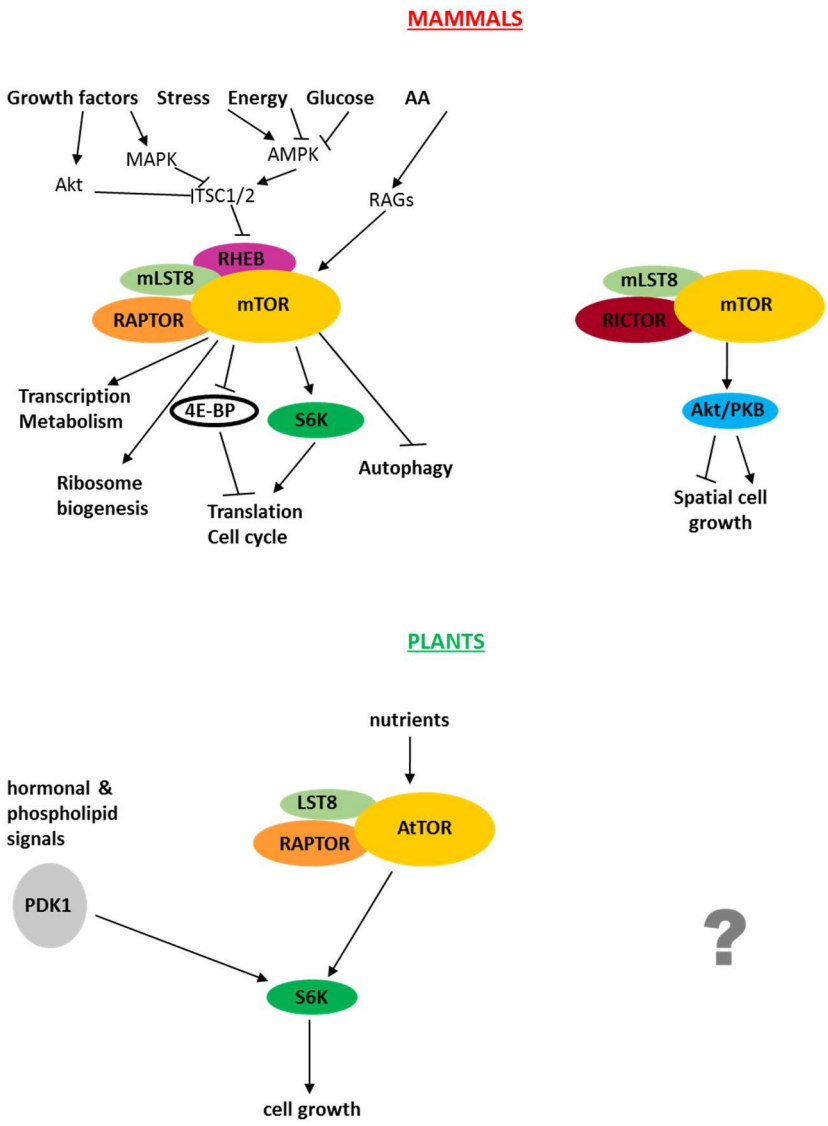

Figure 4-1 Simplified models of TOR signaling pathways in animals and plants.
The mammalian mTORC1 (left) consisting of mTOR, RAPTOR, mLST8 and RHEB controls various aspects of cellular processes. The mTORC2 (top right) consisting of mTOR, RICTOR and mLST8 controls spatial cell growth by regulating cytoskeleton structure and polarity via Akt/PKB phosphorylation. In plants, only a TORC1 equivalent (bottom left) has been described so far. Here, TORC1 regulates cell growth by activating S6K together with PDK1. The presence of a TORC2 equivalent (bottom right) remains unknown. Adapted from Bögre et al. (2003), and Xiong and Sheen (2014).

4.1.2 PDK1 kinases control polarity in plant development

The AGC kinase PDK1 is involved in different aspects of plant development. In Arabidopsis, the most striking phenotypes I observed in overexpression lines rather than in knockout lines (Figure 3-4, Figure 3-10). As discussed above, *pdk1* double knockouts display very mild phenotypes but overexpressors for either PDK1 exhibit interesting phenotypes regarding floral organ development and root hair growth (supplemental Figure 7-4; Anthony et al. (2004). Root hairs in *PDK1$_{OX}$* show one to several branches or ballooning indicating polarity defects, and *pdk1* double KO lines are slightly impaired in root hair elongation. Anthony et al. (2004) demonstrated that OXI1/AGC2-1 is involved in root hair growth in a PA-PDK1-dependent manner. Thus, PDK1 might be required for correct polar growth. Polar growth is predominantly regulated via small RAC/ROP GTPases (Yalovsky et al. 2008). These small molecular switches control polar growth by cycling from an inactive GDP-bound state at the flanks of the tip to an active GTP-bound state at the apex of the tip-growing cell such as root hairs, pollen tubes or trichomes. For this regulation, other proteins are required, e.g. GAPs (GTPase-activating proteins), which catalyze the GTP-hydrolyzing activity of the GTPase; GDIs (GDP dissociation inhibitors), which are responsible to keep the non-plasma membrane-anchored GTPase in the inactive state. GEFs (Guanine nucleotide exchange factors), which are required to activate the inactive form by exchanging GDP for GTP. GDFs (GDI-displacement factor) are responsible to remove the GDI from the GDP-bound GTPase in order to facilitate binding to the membrane and replacing GDP by GTP, and downstream effectors, which are the targets of the active GTPase (reviewed, among others, in Kost (2008). In several studies, PDK1 was shown to be directly or indirectly involved in Rho GTPase signaling in animals (Flynn et al. 2000, Coleman et al. 2004, Pinner and Sahai 2008), and in plant innate immunity (Trusov et al. 2010). Similar PDK1-dependent mechanisms involving small RAC/ROP GTPases could explain the root hair phenotypes. PDK1 might regulate a downstream AGC kinase, which in turn interferes directly or indirectly with the tip-growth control machinery. Further experiments are required to elucidate the role of PDK1 in the control of tip-growth.

Furthermore, the *PDK1* transcripts and PDK1 proteins are abundant in all tissues during all developmental steps suggesting global functions of the PDK1s (Figures 3-3, 3-5, 3-8, 3-9). Interestingly, PDK1.2 localizes besides the cytosol as well to the plasma membrane of root cells in a polar fashion (apical-basal; Figure 3-9). Zegzouti et al. (2006a) demonstrated that PINOID (PID) interacts in vivo with PDK1, and that PDK1 increases PID activity. The polar localization of PDK1 might be due to the polar localization of the PIN localization modulators PID and D6PK (Zourelidou

et al. 2014), but PDK1 cannot play an important role in the recruitment and activation because *pdk1* double knockout plants do not show any phenotypes related to the disruption of polar auxin transport.

4.2 The role of *PDK1* in *UCN* signaling

I demonstrated that a single *pdk1* knockout is capable of restoring the *ucn-1* phenotype to 80 – 90% of the WT control (Figure 3-7). It was important to analyze high numbers of ovules because the homozygous offspring resulting from crossings between Col-0 and *ucn-1* (and reciprocal) rescue the *ucn-1* phenotype by about 20%. Initially, I was concerned that the genetic Col-0 background is responsible for the reduction of ovules depicting the *ucn-1* phenotype rather than the *pdk1* knockout. Subsequently, I analyzed more than 30,000 ovules in total. I analyzed three independent crossings for each combination (and reciprocal combinations), and three independent plants of homozygous F3 progeny of each crossing combination (Table 7-2 in supplement). In addition, *PDK1* overexpression lines exhibit an interesting *unicorn*-like phenotype in petals and ovule integuments (Figure 3-10). These results clearly indicate a role for *PDK1* in the control of planar growth and floral organ shape. PDK1 functions in animals and plants are similar but different. In animals, almost all AGC kinases are PDK1-dependent (Pearce et al. 2010). By contrast, the activity of several plant AGCVIII kinases is significantly increased by PDK1 in vitro but does not rely on the presence of PDK1 (Anthony et al. 2004, Devarenne et al. 2006, Zegzouti et al. 2006a, Enugutti et al. 2012). Additionally, at least in the species *Arabidopsis thaliana* and *Oryza sativa* (rice) the knockout of *PDK1* does not cause a dramatic phenotype (Matsui et al. 2010, Camehl et al. 2011) whereas in other species such as mouse and tomato loss of *PDK1* is lethal (Lawlor et al. 2002, Devarenne et al. 2006). One could ask whether *PDK1* is of any importance in Arabidopsis. The answer is obviously ‘yes’ although PDK1 functions in Arabidopsis seem to be more restricted to regulatory pathways of only some AGC kinases compared to other plant species and animals.

In animals, strong evidence is present that PDK1 is a major regulator of proliferation and growth. It has been demonstrated that overexpression of the *PDK1* gene or hyperactivity of the PDK1 protein is frequently involved in tumorigenesis via the AGC kinase Akt/PKB (Vivanco and Sawyers 2002, Carpten et al. 2007). Frequent amplification of the *PDK1* locus was shown in castration-resistant prostate cancer and lymph node metastases (Choucair et al. 2012), and *PDK1*

overexpression is related to acute myeloid leukemia (Zabkiewicz et al. 2014), melanoma (Scortegagna et al. 2014), hepatocellular carcinoma (Wang et al. 2016), and gastric cancer, in which the level of abundant PDK1 protein negatively correlates with patient prognosis (Bai et al. 2016). I showed that the expression levels of either *PDK1* in Arabidopsis correlate positively with the abundance of ovule protrusions up to certain levels (Figure 3-11). Thus, similarities between animal and plant *PDK1s* can be drawn. *PDK1* seems to be an important factor in animal and plant tumorigenesis. Interestingly, tumor formation in plants is usually related to alterations in cytokinin and auxin homeostasis (Morris 1986, Ulmasov et al. 1999, Remington et al. 2004, Doehlemann et al. 2008) but the *ucn*-induced protrusion formation is independent of auxin and cytokinin (Enugutti and Schneitz 2013). Accordingly, PDK1, with respect to *UCN* signaling, acts most likely independently of the before-mentioned hormones. In addition, *PDK1* function in floral organs is certainly not whorl- but organ-specific, since it affects the architecture of second whorl petals, the development of which is controlled by class A, B and E homeotic genes, and ovule architecture within the fourth whorl regulated by class C, D and E TFs. More evidence is provided by the fact that *PDK1's* influence on floral organ development is most probably *UCN*-dependent, for which organ- and not whorl-specificity was shown by Enugutti and Schneitz (2013). Additionally, I provide evidence for a direct posttranslational PDK1 suppression mediated by UCN (Figures 3-10, 3-15 – 3-18). The genetics indicate that *UCN* is a negative regulator of *PDK1* (Figure 3-10), and active UCN is able to repress PDK1 activity in vitro (Figure 3-18). Since only active UCN is able to repress PDK1 in vitro, I propose a model in which PDK1 activates UCN, and UCN subsequently represses PDK1 in a negative feedback loop (Figure 4-2). Since PDK1 has been suggested to be constitutively active (Belham et al. 1999, Peterson and Schreiber 1999) PDK1 repression by another AGC kinase exhibits a unique feature. Although I have observed more interactions in vitro, the in vivo interaction data show clearly that UCN and PDK1 interact directly with each other in a kinase activity- and PIF-dependent manner.

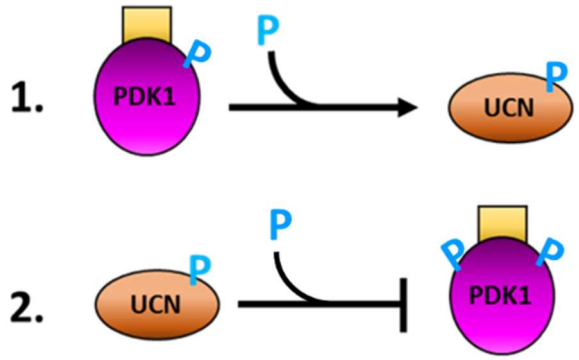

Figure 4-2 Negative feedback loop of UCN activation and PDK1 repression.

In a first step, PDK1 activates UCN through phosphorylation, and the activated UCN represses PDK1 through phosphorylation in a second step. P indicates phosphate.

4.2.1 How does *PDK1* relate to *ATS* with respect to *UCN* signaling?

UNICORN was shown to suppress ectopic outgrowth in Arabidopsis ovule integuments by directly repressing the KANADI TF ATS. PDK1 behaves similar to ATS. Thus, I was interested in elucidating whether *PDK1* regulates *ATS*. Therefore, I crossed the activation tagging line *sk21-D* (Gao et al. 2010*)*, which overexpresses *ATS* in its own expression domain and therefore exhibits protrusions on ovule integuments (Enugutti et al. 2012, Enugutti and Schneitz 2013), with *pdk1.1* and *pdk1.2* KO lines. Interestingly, the homozygous offspring of these crossings showed no protrusion formation.

Next, I wanted to know whether PDK1 and ATS proteins could interact directly. In vitro kinase assays first revealed very weak PDK1-dependent phosphorylation of ATS but BiFC assays in protoplast (Figure 3-24 K) could not support direct interaction. With respect to the subcellular localization of PDK1 in the cytosol/at the plasma membrane and ATS in the nucleus (Figures 3-5, 3-6, and 3-24), direct interaction most probably does not occur. Thus, I propose a model, in which ATS positively influences the transcription of an unknown gene, the gene product of which is positively regulated directly or indirectly by PDK1. Both the PDK1 proteins contribute to the activation of UCN but are not necessary in planta. I gained evidence for PDK1-dependent activation of UCN by phosphorylation site determination in UCN_{KD} proteins co-incubated with PDK1.1 or PDK1.2, respectively (Figure 3-18). In collaboration with Dr. Fiona Pachl and Dr. Peng Yu (Chair of Proteomics and Bioanalytics, Prof. Dr. B. Küster, TUM), I determined two serine residues (S233 and S242) as in vitro target sites phosphorylated by both PDK1s. Interestingly, Dr. Julia Mergner (Chair of Proteomics and Bioanalytics, Prof. Dr. B. Küster, TUM) obtained the same serine residues in a large scale phosphoproteome analysis of in vivo samples (personal communication). These findings indicate that PDK1 is able to activate UCN, and that the in vitro detected phosphorylation sites are not in vitro artifacts. These two serine residues are located in the activation segment of UCN. S242 represents the conserved Ser in the T-loop, the phosphorylation of which is essential for the activation of the kinase. S233 represents an additional conserved phosphorylation site in the activation segment, which is phosphorylated upon T-loop phosphorylation in a second step (Bögre et al. 2003, Pearce et al. 2010).

To gain further insights, these phosphorylation sites should be mutated to either Ala (phosphomutants) or Asp/Glu (phosphomimetics). Subsequently, the different combinations of the mutated UCN versions should be tested in different assays for interaction with PDK1 and ATS (kinase assays, MST measurements, Y2H, BiFC) as well as transformed into different genotypes

(WT, *ucn-1, ucn-11, ucn-2, ats-3* and *pdk1 ucn-1* double mutants). The auto- and trans-activated UCN is translocated into the nucleus where it represses ATS that activates the expression of *X,* which I named *RHINO* (*RNO*) for the phenotypical relationship between unicorns and rhinoceroses. *RNO* mRNA is translated within the cytosol into protein RNO, the activity of which is positively regulated by the PDK1s. The hypothetical protein RNO in turn is a positive regulator of periclinal and/or a negative regulator of anticlinal cell division. Besides ATS suppression in the nucleus, UCN represses the PDK1 proteins in the cytoplasm and/or at the plasma membrane (Figure 4-3). Hence, I suppose a regulatory feedback between the three AGC kinases, UCN on the one and the two PDK1 proteins on the other hand. Loss-of-function of one of the *PDK1* genes is sufficient to restore the *ucn* phenotype almost to WT. Thus, either both PDK1 activities are needed for downstream signaling or we deal with a quantitative effect. Activation of the downstream effector(s) by only one PDK1 in both cases is not sufficient to result in the respective phenotype.

4.2.2 PDK1 as a global player in UCN signaling

Since ATS is restricted to the ovules, PDK1 is involved in the UCN-mediated repression of ectopic growth in a more global fashion. Loss of one of the two *PDK1* genes in *ucn-1* background rescues not only the integument phenotype but also the floral phenotype, i.e. aberrant growth in petals and stamina, and the overall morphological defects of the flower (Figure 3-7). These results indicate, together with the *PDK1* overexpression phenotypes (Figure **3-10**), that PDK1 is part of *UCN* signaling in those floral organs, in which *UCN* controls organ architecture. Thus, I extended the above-introduced model of UCN-dependent regulation to other floral organs. The second model for the hypothetical molecular mechanism coordinating organ architecture in a UCN-dependent manner represents almost the same as described above for integument development. I just replaced the KANADI TF ATS by an unknown transcription factor named W (which might be a TF of the KANADI family as well). UCN is auto- and trans-activated by PDK1 in the cytosol/at the plasma membrane, and subsequently translocated to the nucleus where it represses W. The TF W is a positive regulator of *RNO* expression. The RNO protein is trans-activated by PDK1 in the cytosol/at the PM. UCN in turn negatively regulates PDK1 activity despite the hypothesis that PDK1 is due to its auto-activating ability constitutively active (Zhang and McCormick 2009). Here I present genetic and biochemical data obviously showing that PDK1 can be repressed by at least one AGCVIII kinase (Figures 3-9 and 3-16). The in vitro results I gained from the kinase assays in Figure 3-16 support a negative regulation of PDK1 by UCN. In a next step, the UCN-dependent

PDK1 phosphorylation sites need to be determined in order to gain deeper insights how UCN represses PDK1.

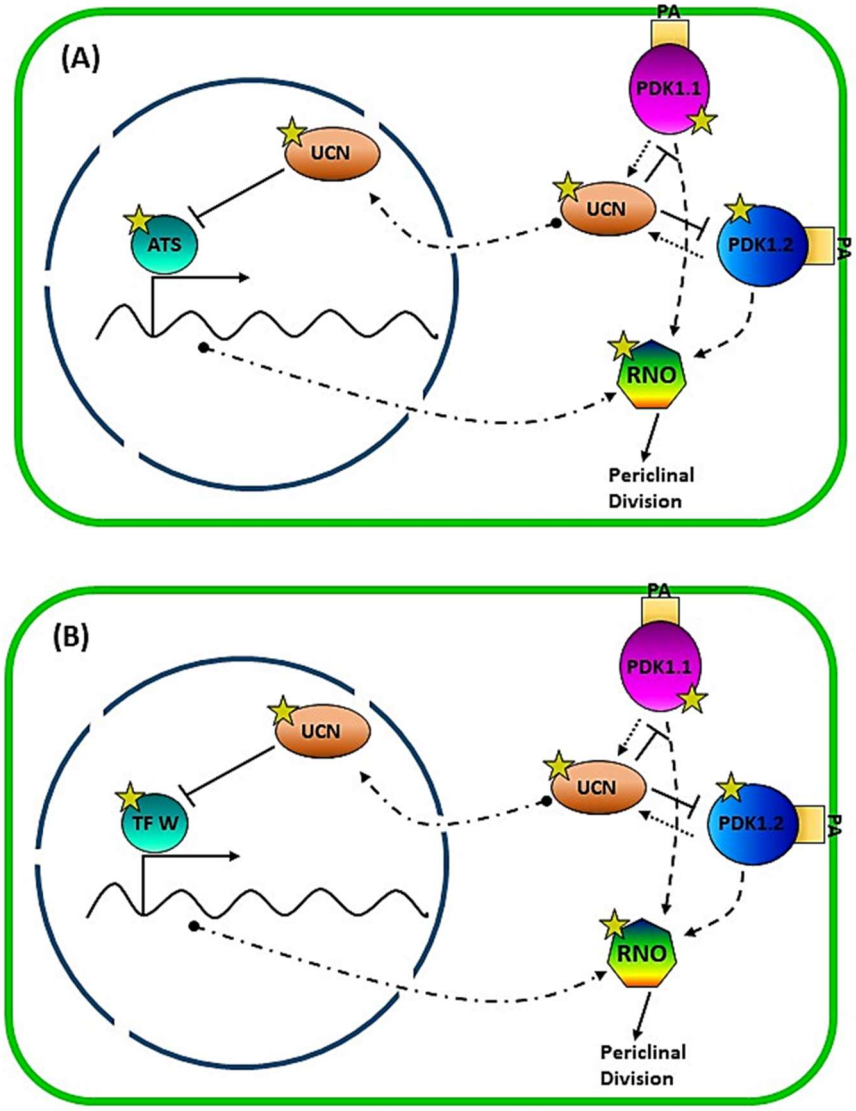

Figure 4-3 Hypothetical model of the molecular mechanisms underlying the *UCN* signaling pathway in the control of planar growth.

(A) Cartoon depicting the proposed molecular mechanism in the control of ovule integument architecture. UCN is activated in the cytosol, is translocated into the nucleus, where it represses ATS, which controls the expression of *RHINO (RNO).* The RNO protein is activated by PDK1.1 and PDK1.2 in the cytosol and induces periclinal divisions. (B) The same proposed molecular mechanism for the repression of ectopic growth in other floral organs. ATS is replaced by a yet unknown transcription factor W. Stars indicate phosphorylation. *PA* phosphatidic acid. Dotted arrows between PDK1 and UCN are not proven. Dash-dotted arrows indicate movement, and dashed arrows indicate a proposed PDK1-mediated activation of the unknown factor RNO.

4.3 UCN-ATS interaction

In order to gain more insights into the UCN-dependent ATS regulation, I performed cold kinase assays, and the peptides resulting from protease (trypsin and pepsin, respectively) digestion were analyzed in LC-MS/MS approaches in collaboration with Dr. Fiona Pachl and Dr. Peng Yu (Chair of Proteomics and Bioanalytics, Prof. Dr. B. Küster, TUM). Although the recovery of the peptides was not complete, I obtained three phosphorylated Ser residues, namely S13, S92 and S211, reproducibly. Since changes in the experimental approach (using a different protease, application of an inclusion list) did not result in better recovery of the ATS peptides, I decided to generate Ser to Ala substitutions to obtain potential phospho-mutants of ATS. Testing all possible combinations of single, double and triple S to A substitutions in kinase and BiFC assays revealed that the detected phospho-serines are not sufficient. This might have different reasons. On the one hand, the in vitro phosphorylation sites might result from in vitro artifacts. On the other hand, the peptides that have not been recovered contain seven additional Ser residues, which might be of relevance regarding UCN-mediated ATS repression by phosphorylation. Therefore, one could try to analyze ATS phosphorylation sites in floral plant tissue of WT and *unicorn* mutants.

4.4 CRISPR/CAS9 mediated genetic engineering – a powerful tool for the generation of novel mutants

In order to generate a second *ucn* allele in L*er* WT background, I made use of the CRISPR/Cas9 system using an egg cell specific promoter (*pEC1.2*) to drive *Cas9* expression (Wang et al. 2015). As described in section 3.4, I obtained one mutant so far that was named *ucn-11*. In principle, the used *Streptococcus pyogenes* Cas9 introduces double strand break (DSB) next to its PAM sequence (NGG), which needs to be adjacent to the target region. The repair of the introduced DSB by non-homologous end-joining (NHEJ) causes errors, which can be detected as deletions, insertions, and substitutions. Using an egg cell specific promoter has the major advantage over constitutive active promoter such as *pCaMV-35S*, *pUBQ* or *p16* that *Cas9* is exclusively expressed in the egg cell. Therefore, homozygous and trans-heterozygous mutants are expected already in T1 generation rather than a mosaic. I targeted a region of the *UCN* gene close to the lost *ucn-10* substitution (D122N) in order to try to mimic this mutation. I analyzed around 100 T1 plants phenotypically, and three of them showed a mild *ucn-1*-like floral phenotype.

Subsequent sequencing revealed that one of them carries an insertion of a single adenine at position +386 leading eventually to a STOP codon at position +391 to +393. This leads maximally to a protein of 130 instead of 404 AA, which in turn – if present and stable – lacking the whole activation segment, 40 AA of kinase subdomain 1, and the complete second kinase subdomain making it certainly an inactive kinase fragment. I observed in homozygous T2 offspring *unicorn* phenotypes in ovules, petals and overall floral architecture (see Figure 3-25), leading to the assumption that the used CRISPR/Cas9 system provided by Wang et al. (2015) is suitable for genome editing in my hands. To date, additional lines are in the pipeline for targeting the *UCN* gene directly downstream of the START codon in order to generate true null mutants in L*er* and Col-0, as well as in *pdk1* single and double insertion lines. Moreover, I decided to knock out the *PDK1* genes (single and double KO) in *ucn* mutant backgrounds and L*er* WT.

5 CONCLUSION

Organ architecture relies on spatiotemporal orchestration of proliferation, division plane determination and growth. Arabidopsis ovule integuments comprise excellent model tissues for studying planar growth control. The AGCVIII kinase UCN was demonstrated to be of paramount importance in the suppression of ectopic growth in floral organs (Enugutti et al. 2012). Furthermore, UCN-mediated direct repression of the KANADI transcription factor ATS was shown to be crucial for ectopic growth suppression. Besides ATS, no other components of the *UCN* signaling pathway have been identified so far.

3-PHOSPHOINOSITIDE-DEPENDENT KINASE 1 (PDK1) represents a major upstream regulator of AGC kinase signaling in animals, and for some AGC kinases as well in plants. Surprisingly, *pdk1.1 pdk1.2* double loss-of-function lines in Arabidopsis exhibit a quite mild phenotype but already a single *pdk1* loss-of-function in *ucn-1* rescues the *ucn* phenotype, which leads to the assumption that either both PDK1 activities are needed for activation of the downstream signaling or a simple quantitative effect leads to the phenotypical restoration. In fact, (over)expression of one *PDK1* in *pdk1.1 pdk1.2* double loss-of-function background is sufficient to compensate for the phenotype. Overexpression of one *PDK1* in WT background has the ability to phenocopy the *ucn-1* phenotype but to a lesser extent. Since PDK1 repression has not been shown so far, UCN-mediated PDK1 repression represents a novel and unique feature in AGC kinase regulation.

Since PDK1 and ATS were not supposed to interact directly due to their spatial separation (cytosol/plasma membrane vs. nucleus), and indeed, in BiFC assays in Arabidopsis protoplasts I could not observe YFP complementation indicating that these two proteins are strictly separated within the cell. Therefore, I propose a speculative model of the molecular mechanism underlying the *UCN* signaling pathway coordinating integument and floral organ architecture (Figure 4-3). The UCN kinase interacts with both PDK1 proteins in the cytosol and/or at the plasma membrane. Upon auto- and PDK1-dependent trans-phosphorylation, UCN is capable of entering the nucleus and repressing (i) ATS in ovule integuments; and (ii) an unknown transcription factor (maybe another KANADI TF) in petals for instance. In turn, these transcription factors, without being phosphorylated by UCN, activate the expression of another unexposed component I named *RHINO* (*RNO*). The RNO protein in turn is positively regulated by PDK1, which in turn is repressed by UCN.

UCN shares similarities with some animal AGC kinases and tumor-suppressors, e.g. Akt/PKB. *AtPDK1* shares common features with mammalian *PDK1s*, especially that PDK1 promotes protrusion formation in response to overexpression.

The overall analysis reveals that tumor or protrusion formation exhibits common characteristics between mammals and plants. PDK1 and at least one other AGC kinase are involved in this process in both kingdoms. Nevertheless, more components, especially *RNO*, need to be unraveled to gain a better understanding of the molecular mechanism underlying this process. The mechanism I propose shares some similarities with mechanisms described for AGC kinase-dependent growth control in animals (Akt/PKB; Warts/LATS). PDK1 seems to act as a master regulator that promotes cell proliferation across kingdoms.

In addition, further experiments are needed to completely understand the role of PDK1 in *UCN* signaling. Subcellular localization of PDK1:EGFP fusion proteins in *ucn-1* background are necessary to determine if the absence of functional UCN influences PDK1 distribution. Moreover, UCN S233/S242 phosphomutants need to be generated and analyzed in planta.

6 REFERENCES

ABRASH EB AND BERGMANN DC. 2009. Asymmetric Cell Divisions: A View from Plant Development. Developmental Cell 16: 783-796.

AHUJA M. 1998. Genetic tumors in Nicotiana and other plants. The Quarterly review of biology 73: 439-462.

AHUJA MR. 1965. Genetic Control of Tumor Formation in Higher Plants. The Quarterly Review of Biology 40: 329-340.

AMBROSE JC AND CYR R. 2008. Mitotic Spindle Organization by the Preprophase Band. Molecular Plant 1: 950-960.

ANGENENT GC AND COLOMBO L. 1996. Molecular control of ovule development. Trends in plant science 1: 228-232.

ANTHONY RG, HENRIQUES R, HELFER A, MÉSZÁROS T, RIOS G, TESTERINK C, MUNNIK T, DEÁK M, KONCZ C AND BÖGRE L. 2004. A protein kinase target of a PDK1 signalling pathway is involved in root hair growth in Arabidopsis. The EMBO Journal 23: 572-581.

ANTHONY RG, KHAN S, COSTA J, PAIS MS AND BÖGRE L. 2006. The Arabidopsis Protein Kinase PTI1-2 Is Activated by Convergent Phosphatidic Acid and Oxidative Stress Signaling Pathways Downstream of PDK1 and OXI1. Journal of Biological Chemistry 281: 37536-37546.

ARMSTRONG W. 1995. To be or not to be a gall. Pacific Horticulture 56: 39-45.

ASCENCIO-IBÁÑEZ JT, SOZZANI R, LEE T-J, CHU T-M, WOLFINGER RD, CELLA R AND HANLEY-BOWDOIN L. 2008. Global analysis of Arabidopsis gene expression uncovers a complex array of changes impacting pathogen response and cell cycle during geminivirus infection. Plant physiology 148: 436-454.

BAI X, LI P, XIE Y, GUO C, SUN Y, XU Q AND ZHAO D. 2016. Overexpression of 3-phosphoinositide-dependent protein kinase-1 is associated with prognosis of gastric carcinoma. Tumor Biology 37: 2333-2339.

BAKER SC, ROBINSON-BEERS K, VILLANUEVA JM, GAISER JC AND GASSER CS. 1997. Interactions among Genes Regulating Ovule Development in Arabidopsis Thaliana. Genetics 145: 1109-1124.

BAUD S, BELLEC Y, MIQUEL M, BELLINI C, CABOCHE M, LEPINIEC L, FAURE JD AND ROCHAT C. 2004. gurke and pasticcino3 mutants affected in embryo development are impaired in acetyl-CoA carboxylase. EMBO reports 5: 515-520.

BAYER EM, SMITH RS, MANDEL T, NAKAYAMA N, SAUER M, PRUSINKIEWICZ P AND KUHLEMEIER C. 2009. Integration of transport-based models for phyllotaxis and midvein formation. Genes & Development 23: 373-384.

BECHTOLD N, ELLIS J AND PELLETIER G. 1993. In planta Agrobacterium mediated gene transfer by infiltration of adult Arabidopsis thaliana plants. Comptes rendus de l'Académie des sciences Série 3, Sciences de la vie 316: 1194-1199.

BEEMSTER GT, FIORANI F AND INZE D. 2003. Cell cycle: the key to plant growth control? Trends in plant science 8: 154-158.

BELHAM C, WU S AND AVRUCH J. 1999. Intracellular signalling: PDK1–a kinase at the hub of things. Current biology 9: R93-R96.

BENJAMINS R, AMPUDIA CSG, HOOYKAAS PJJ AND OFFRINGA R. 2003. PINOID-Mediated Signaling Involves Calcium-Binding Proteins. Plant Physiology 132: 1623-1630.

BENJAMINS R, QUINT A, WEIJERS D, HOOYKAAS P AND OFFRINGA R. 2001. The PINOID protein kinase regulates organ development in Arabidopsis by enhancing polar auxin transport. Development 128: 4057-4067.

BESSON S AND DUMAIS J. 2011. Universal rule for the symmetric division of plant cells. Proceedings of the National Academy of Sciences 108: 6294-6299.

BIRD DM AND KOLTAI H. 2000. Plant parasitic nematodes: habitats, hormones, and horizontally-acquired genes. Journal of Plant Growth Regulation 19: 183-194.

BLAKESLEE A AND SATINA S. 1947. Ovular tumors associated with hybrid embryos in Datura. Science (New York, NY) 105: 633-633.

BLECKMANN A AND DRESSELHAUS T. 2016. Fluorescent whole-mount RNA in situ hybridization (F-WISH) in plant germ cells and the fertilized ovule. Methods 98: 66-73.

BÖGRE L, OKRÉSZ L, HENRIQUES R AND ANTHONY RG. 2003. Growth signalling pathways in Arabidopsis and the AGC protein kinases. Trends in plant science 8: 424-431.

BRAND U, FLETCHER JC, HOBE M, MEYEROWITZ EM AND SIMON R. 2000. Dependence of Stem Cell Fate in Arabidopsis on a Feedback Loop Regulated by CLV3 Activity. Science 289: 617-619.

BRAUN AC. 1972. The relevance of plant tumor systems to an understanding of the basic cellular mechanisms underlying tumorigenesis. Prog Exp Tumor Res 15: 165-187.

BRAUN AC 1975. Plant tumors. Biology of Tumors: Surfaces, Immunology, and Comparative Pathology: Springer, p. 411-427.

BREFORT T, DOEHLEMANN G, MENDOZA-MENDOZA A, REISSMANN S, DJAMEI A AND KAHMANN R. 2009. Ustilago maydis as a pathogen. Annual review of phytopathology 47: 423-445.

BUSCH W ET AL. 2010. Transcriptional Control of a Plant Stem Cell Niche. Developmental Cell 18: 841-853.

CALDANA C, LI Y, LEISSE A, ZHANG Y, BARTHOLOMAEUS L, FERNIE AR, WILLMITZER L AND GIAVALISCO P. 2013. Systemic analysis of inducible target of rapamycin mutants reveal a general metabolic switch controlling growth in Arabidopsis thaliana. The Plant Journal 73: 897-909.

CAMEHL I, DRZEWIECKI C, VADASSERY J, SHAHOLLARI B, SHERAMETI I, FORZANI C, MUNNIK T, HIRT H AND OELMULLER R. 2011. The OXI1 kinase pathway mediates Piriformospora indica-induced growth promotion in Arabidopsis. PLoS Pathog 7: e1002051.

CARPTEN JD, FABER AL, HORN C, DONOHO GP, BRIGGS SL, ROBBINS CM, HOSTETTER G, BOGUSLAWSKI S, MOSES TY AND SAVAGE S. 2007. A transforming mutation in the pleckstrin homology domain of AKT1 in cancer. Nature 448: 439.

CHALUPOWICZ L, BARASH I, SCHWARTZ M, ALONI R AND MANULIS S. 2006. Comparative anatomy of gall development on Gypsophila paniculata induced by bacteria with different mechanisms of pathogenicity. Planta 224: 429-437.

CHAMPION A, KREIS M, MOCKAITIS K, PICAUD A AND HENRY Y. 2004. Arabidopsis kinome: after the casting. Functional & Integrative Genomics 4: 163-187.

CHO H-Y, TSENG T-S, KAISERLI E, SULLIVAN S, CHRISTIE JM AND BRIGGS WR. 2007. Physiological Roles of the Light, Oxygen, or Voltage Domains of Phototropin 1 and Phototropin 2 in Arabidopsis. Plant Physiology 143: 517-529.

CHOUCAIR KA, GUÉRARD K-P, EJDELMAN J, CHEVALIER S, YOSHIMOTO M, SCARLATA E, FAZLI L, SIRCAR K, SQUIRE JA AND BRIMO F. 2012. The 16p13. 3 (PDPK1) genomic gain in prostate cancer: a potential role in disease progression. Translational oncology 5: 453-460.

CHUNG SK AND PARISH RW. 1995. Studies on the promoter of the Arabidopsis thaliana cdc2a gene. FEBS letters 362: 215-219.

CLOUGH SJ AND BENT AF. 1998. Floral dip: a simplified method for Agrobacterium-mediated transformation of Arabidopsis thaliana. Plant J 16.

COEN ES AND MEYEROWITZ EM. 1991. The war of the whorls: genetic interactions controlling flower development. Nature 353: 31-37.

COEN O, FIUME E, XU W, DE VOS D, LU J, PECHOUX C, LEPINIEC L AND MAGNANI E. 2017. Developmental patterning of the sub-epidermal integument cell layer in Arabidopsis seeds. Development (Cambridge, England) 144: 1490-1497.

COLEMAN ML, MARSHALL CJ AND OLSON MF. 2004. RAS and RHO GTPases in G1-phase cell-cycle regulation. Nature reviews Molecular cell biology 5: 355.

CORNU M, ALBERT V AND HALL MN. 2013. mTOR in aging, metabolism, and cancer. Current opinion in genetics & development 23: 53-62.

CUCINOTTA M, COLOMBO L AND ROIG-VILLANOVA I. 2014. Ovule development, a new model for lateral organ formation. Frontiers in Plant Science 5.

CURTIS MD AND GROSSNIKLAUS U. 2003. A gateway cloning vector set for high-throughput functional analysis of genes in planta. Plant physiology 133: 462-469.

DE MEUTTER J, TYTGAT T, WITTERS E, GHEYSEN G, VAN ONCKELEN H AND GHEYSEN G. 2003. Identification of cytokinins produced by the plant parasitic nematodes Heterodera schachtii and Meloidogyne incognita. Molecular Plant Pathology 4: 271-277.

DE SMET I AND BEECKMAN T. 2011. Asymmetric cell division in land plants and algae: the driving force for differentiation. Nat Rev Mol Cell Biol 12: 177-188.

DEAK M, KISS GB, KONCZ C AND DUDITS D. 1986. Transformation of Medicago by Agrobacterium mediated gene transfer. Plant Cell Reports 5: 97-100.

DEMIDOV D, HESSE S, TEWES A, RUTTEN T, FUCHS J, KARIMI ASHTIYANI R, LEIN S, FISCHER A, REUTER G AND HOUBEN A. 2009. Aurora1 phosphorylation activity on histone H3 and its cross-talk with other post-translational histone modifications in Arabidopsis. The Plant Journal 59: 221-230.

DEPROST D, YAO L, SORMANI R, MOREAU M, LETERREUX G, NICOLAÏ M, BEDU M, ROBAGLIA C AND MEYER C. 2007. The Arabidopsis TOR kinase links plant growth, yield, stress resistance and mRNA translation. EMBO reports 8: 864-870.

DESVOYES B, RAMIREZ-PARRA E, XIE Q, CHUA N-H AND GUTIERREZ C. 2006. Cell type-specific role of the retinoblastoma/E2F pathway during Arabidopsis leaf development. Plant Physiology 140: 67-80.

DEVARENNE TP, EKENGREN SK, PEDLEY KF AND MARTIN GB. 2006. Adi3 is a Pdk1-interacting AGC kinase that negatively regulates plant cell death. The EMBO Journal 25: 255-265.

DEVOS S, VISSENBERG K, VERBELEN JP AND PRINSEN E. 2005. Infection of Chinese cabbage by Plasmodiophora brassicae leads to a stimulation of plant growth: impacts on cell wall metabolism and hormone balance. New phytologist 166: 241-250.

DHONUKSHE P ET AL. 2010. Plasma membrane-bound AGC3 kinases phosphorylate PIN auxin carriers at TPRXS(N/S) motifs to direct apical PIN recycling. Development 137: 3245-3255.

DÍAZ-TROYA S, PÉREZ-PÉREZ ME, FLORENCIO FJ AND CRESPO JL. 2008. The role of TOR in autophagy regulation from yeast to plants and mammals. Autophagy 4: 851-865.

DISSMEYER N AND SCHNITTGER A 2011. The Age of Protein Kinases. In*:* DISSMEYER, N AND SCHNITTGER, A (Eds.) Plant Kinases: Methods and Protocols, Totowa, NJ: Humana Press, p. 7-52.

DITTA G, PINYOPICH A, ROBLES P, PELAZ S AND YANOFSKY MF. 2004. The SEP4 gene of Arabidopsis thaliana functions in floral organ and meristem identity. Current Biology 14: 1935-1940.

DITTRICH ACN AND DEVARENNE TP. 2012. Characterization of a PDK1 Homologue from the Moss Physcomitrella patens. Plant Physiology 158: 1018-1033.

DOBRENEL T, MARCHIVE C, SORMANI R, MOREAU M, MOZZO M, MONTANÉ M-H, MENAND B, ROBAGLIA C AND MEYER C 2011. Regulation of plant growth and metabolism by the TOR kinase. Portland Press Limited.

DODUEVA IE, FROLOVA NV AND LUTOVA LA. 2007. Plant tumorigenesis: different ways for shifting systemic control of plant cell division and differentiation. . Transgen Plant J 1: 17-38.

DOEHLEMANN G, WAHL R, HORST RJ, VOLL LM, USADEL B, POREE F, STITT M, PONS-KÜHNEMANN J, SONNEWALD U AND KAHMANN R. 2008. Reprogramming a maize plant: transcriptional and metabolic changes induced by the fungal biotroph Ustilago maydis. The Plant Journal 56: 181-195.

DOONAN JH AND SABLOWSKI R. 2010. Walls around tumours - why plants do not develop cancer. Nat Rev Cancer 10: 794-802.

DREWS GN, LEE D AND CHRISTENSEN CA. 1998. Genetic analysis of female gametophyte development and function. The Plant Cell 10: 5-17.

DUHR S AND BRAUN D. 2006. Why molecules move along a temperature gradient. Proceedings of the National Academy of Sciences 103: 19678-19682.

EBEL C, MARICONTI L AND GRUISSEM W. 2004. Plant retinoblastoma homologues control nuclear proliferation in the female gametophyte. Nature 429: 776.

EMERY JF, FLOYD SK, ALVAREZ J, ESHED Y, HAWKER NP, IZHAKI A, BAUM SF AND BOWMAN JL. 2003. Radial Patterning of Arabidopsis Shoots by Class III HD-ZIP and KANADI Genes. Current Biology 13: 1768-1774.

ENUGUTTI B, KIRCHHELLE C, OELSCHNER M, TORRES RUIZ RA, SCHLIEBNER I, LEISTER D AND SCHNEITZ K. 2012. Regulation of planar growth by the Arabidopsis AGC protein kinase UNICORN. Proc Natl Acad Sci U S A 109: 15060-15065.

ENUGUTTI B, KIRCHHELLE C AND SCHNEITZ K. 2013. On the genetic control of planar growth during tissue morphogenesis in plants. Protoplasma 250: 651-661.

ENUGUTTI B AND SCHNEITZ K. 2013. Genetic analysis of ectopic growth suppression during planar growth of integuments mediated by the Arabidopsis AGC protein kinase UNICORN. BMC Plant Biol 13: 2.

ESHED Y, BAUM SF AND BOWMAN JL. 1999. Distinct Mechanisms Promote Polarity Establishment in Carpels of Arabidopsis. Cell 99: 199-209.

ESHED Y, BAUM SF, PEREA JV AND BOWMAN JL. 2001. Establishment of polarity in lateral organs of plants. Current Biology 11: 1251-1260.

ESHED Y, IZHAKI A, BAUM SF, FLOYD SK AND BOWMAN JL. 2004. Asymmetric leaf development and blade expansion in Arabidopsis are mediated by KANADI and YABBY activities. Development 131: 2997-3006.

FAURE J-D, VITTORIOSO P, SANTONI V, FRAISIER V, PRINSEN E, BARLIER I, VAN ONCKELEN H, CABOCHE M AND BELLINI C. 1998. The PASTICCINO genes of Arabidopsis thaliana are involved in the control of cell division and differentiation. Development 125: 909-918.

FAVARO R, PINYOPICH A, BATTAGLIA R, KOOIKER M, BORGHI L, DITTA G, YANOFSKY MF, KATER MM AND COLOMBO L. 2003. MADS-box protein complexes control carpel and ovule development in Arabidopsis. The Plant Cell 15: 2603-2611.

FERNANDO W, ZHANG J, CHEN C, REMPHREY W, SCHURKO A AND KLASSEN G. 2005. Molecular and morphological characteristics of Apiosporina morbosa, the causal agent of black knot in Prunus spp. Canadian journal of plant pathology 27: 364-375.

FLETCHER JC, BRAND U, RUNNING MP, SIMON R AND MEYEROWITZ EM. 1999. Signaling of Cell Fate Decisions by CLAVATA3 in Arabidopsis Shoot Meristems. Science 283: 1911-1914.

FLYNN P, MELLOR H, CASAMASSIMA A AND PARKER PJ. 2000. Rho GTPase control of protein kinase C-related protein kinase activation by 3-phosphoinositide-dependent protein kinase. Journal of Biological Chemistry 275: 11064-11070.

FRANK M, GUIVARC'H A, KRUPKOVÁ E, LORENZ-MEYER I, CHRIQUI D AND SCHMÜLLING T. 2002. TUMOROUS SHOOT DEVELOPMENT (TSD) genes are required for co-ordinated plant shoot development. The Plant Journal 29: 73-85.

FREELING M AND HAKE S. 1985. Developmental genetics of mutants that specify knotted leaves in maize. Genetics 111: 617-634.

FULTON L, BATOUX M, VADDEPALLI P, YADAV RK, BUSCH W, ANDERSEN SU, JEONG S, LOHMANN JU AND SCHNEITZ K. 2009. DETORQUEO, QUIRKY, and ZERZAUST represent novel components involved in organ development mediated by the receptor-like kinase STRUBBELIG in Arabidopsis thaliana. PLoS Genet 5: e1000355.

GAGLIARDI PA, PULIAFITO A AND PRIMO L. 2017. PDK1: At the crossroad of cancer signaling pathways. Seminars in Cancer Biology.

GAO P, LI X, CUI D, WU L, PARKIN I AND GRUBER MY. 2010. A new dominant Arabidopsis transparent testa mutant, *sk21-D*, and modulation of seed flavonoid biosynthesis by KAN4. Plant Biotechnol J 8: 979-993.

GASSER CS, BROADHVEST J AND HAUSER BA. 1998. GENETIC ANALYSIS OF OVULE DEVELOPMENT. Annual Review of Plant Physiology and Plant Molecular Biology 49: 1-24.

GELVIN SB. 2003. Agrobacterium-mediated plant transformation: the biology behind the "Gene-Jockeying" tool. Microbiology and molecular biology reviews 67: 16-37.

GLICKMANN E, GARDAN L, JACQUET S, HUSSAIN S, ELASRI M, PETIT A AND DESSAUX Y. 1998. Auxin production is a common feature of most pathovars of Pseudomonas syringae. Molecular plant-microbe interactions 11: 156-162.

GOTO K AND MEYEROWITZ EM. 1994. Function and regulation of the Arabidopsis floral homeotic gene PISTILLATA. Genes & Development 8: 1548-1560.

GROSSNIKLAUS U AND SCHNEITZ K. 1998. The molecular and genetic basis of ovule and megagametophyte development. Seminars in Cell & Developmental Biology 9: 227-238.

GRUNEWALD W AND FRIML J. 2010. The march of the PINs: developmental plasticity by dynamic polar targeting in plant cells. The EMBO Journal 29: 2700-2714.

HABERER G, ERSCHADI S AND TORRES-RUIZ RA. 2002. The Arabidopsis gene PEPINO/PASTICCINO2 is required for proliferation control of meristematic and non-meristematic cells and encodes a putative anti-phosphatase. Development genes and evolution 212: 542-550.

HALDER G AND JOHNSON RL. 2011. Hippo signaling: growth control and beyond. Development 138: 9-22.

HAMANT O, HEISLER MG, JÖNSSON H, KRUPINSKI P, UYTTEWAAL M, BOKOV P, CORSON F, SAHLIN P, BOUDAOUD A AND MEYEROWITZ EM. 2008. Developmental patterning by mechanical signals in Arabidopsis. science 322: 1650-1655.

HANLEY-BOWDOIN L, SETTLAGE SB AND ROBERTSON D. 2004. Reprogramming plant gene expression: a prerequisite to geminivirus DNA replication. Molecular Plant Pathology 5: 149-156.

HARASHIMA H AND SCHNITTGER A. 2010. The integration of cell division, growth and differentiation. Current opinion in plant biology 13: 66-74.

HARRAR Y, BELLEC Y, BELLINI C AND FAURE J-D. 2003. Hormonal control of cell proliferation requires PASTICCINO genes. Plant physiology 132: 1217-1227.

HEISLER MG, OHNO C, DAS P, SIEBER P, REDDY GV, LONG JA AND MEYEROWITZ EM. 2005. Patterns of Auxin Transport and Gene Expression during Primordium Development Revealed by Live Imaging of the Arabidopsis Inflorescence Meristem. Current Biology 15: 1899-1911.

HOOPER CM, CASTLEDEN IR, TANZ SK, ARYAMANESH N AND MILLAR AH. 2017. SUBA4: the interactive data analysis centre for Arabidopsis subcellular protein locations. Nucleic Acids Research 45: D1064-D1074.

HOOPER CM, TANZ SK, CASTLEDEN IR, VACHER MA, SMALL ID AND MILLAR AH. 2014. SUBAcon: a consensus algorithm for unifying the subcellular localization data of the Arabidopsis proteome. Bioinformatics 30: 3356-3364.

HOWDEN AJM, SALEK M, MIGUET L, PULLEN M, THOMAS B, KNIGHT MR AND SWEETLOVE LJ. 2011. The phosphoproteome of Arabidopsis plants lacking the oxidative signal-inducible1 (OXI1) protein kinase. New Phytologist 190: 49-56.

IRISH VF. 2010. The flowering of Arabidopsis flower development. The Plant Journal 61: 1014-1028.

JACK T, BROCKMAN LL AND MEYEROWITZ EM. 1992. The homeotic gene APETALA3 of Arabidopsis thaliana encodes a MADS box and is expressed in petals and stamens. Cell 68: 683-697.

JERABEK-WILLEMSEN M, WIENKEN CJ, BRAUN D, BAASKE P AND DUHR S. 2011. Molecular Interaction Studies Using Microscale Thermophoresis. Assay and Drug Development Technologies 9: 342-353.

JOFUKU KD, DEN BOER B, VAN MONTAGU M AND OKAMURO JK. 1994. Control of Arabidopsis flower and seed development by the homeotic gene APETALA2. The Plant Cell 6: 1211-1225.

JUAREZ MT, KUI JS, THOMAS J, HELLER BA AND TIMMERMANS MCP. 2004. microRNA-mediated repression of rolled leaf1 specifies maize leaf polarity. Nature 428: 84-88.

JUSTICE RW, ZILIAN O, WOODS DF, NOLL M AND BRYANT PJ. 1995. The Drosophila tumor suppressor gene warts encodes a homolog of human myotonic dystrophy kinase and is required for the control of cell shape and proliferation. Genes & development 9: 534-546.

KANNAN N, HASTE N, TAYLOR SS AND NEUWALD AF. 2007. The hallmark of AGC kinase functional divergence is its C-terminal tail, a cis-acting regulatory module. Proceedings of the National Academy of Sciences of the United States of America 104: 1272-1277.

KAWABE A, MATSUNAGA S, NAKAGAWA K, KURIHARA D, YONEDA A, HASEZAWA S, UCHIYAMA S AND FUKUI K. 2005. Characterization of plant Aurora kinases during mitosis. Plant Molecular Biology 58: 1-13.

KELLEY DR, ARREOLA A, GALLAGHER TL AND GASSER CS. 2012. ETTIN (ARF3) physically interacts with KANADI proteins to form a functional complex essential for integument development and polarity determination in Arabidopsis. Development 139: 1105-1109.

KELLEY DR, SKINNER DJ AND GASSER CS. 2009. Roles of Polarity Determinants in Ovule Development. The Plant journal : for cell and molecular biology 57: 1054-1064.

KERSTETTER RA, BOLLMAN K, TAYLOR RA, BOMBLIES K AND POETHIG RS. 2001. KANADI regulates organ polarity in Arabidopsis. Nature 411: 706-709.

KILIAN J, WHITEHEAD D, HORAK J, WANKE D, WEINL S, BATISTIC O, D'ANGELO C, BORNBERG-BAUER E, KUDLA J AND HARTER K. 2007. The AtGenExpress global stress expression data set: protocols, evaluation and model data analysis of UV-B light, drought and cold stress responses. The Plant Journal 50: 347-363.

KIRCHHELLE C. 2012. Functional analysis of the Arabidopsis AGC kinase UCN. M.Sc., TU München.

KOST B. 2008. Spatial control of Rho (Rac-Rop) signaling in tip-growing plant cells. Trends in cell biology 18: 119-127.

KOSTOFF D. 1939. Abnormal mitosis in tobacco plants forming hereditary tumours. Nature 144: 599.

KRIZEK BA. 1999. Ectopic expression of AINTEGUMENTA in Arabidopsis plants results in increased growth of floral organs. Developmental Genetics 25: 224-236.

KRIZEK BA AND EADDY M. 2012. AINTEGUMENTA-LIKE6 regulates cellular differentiation in flowers. Plant Molecular Biology 78: 199-209.

KRIZEK BA AND FLETCHER JC. 2005. Molecular mechanisms of flower development: an armchair guide. Nature reviews Genetics 6: 688.

KRUPKOVÁ E, IMMERZEEL P, PAULY M AND SCHMÜLLING T. 2007. The TUMOROUS SHOOT DEVELOPMENT2 gene of Arabidopsis encoding a putative methyltransferase is required for cell adhesion and co-ordinated plant development. The Plant Journal 50: 735-750.

KRUPKOVÁ E AND SCHMÜLLING T. 2009. Developmental consequences of the tumorous shoot development1 mutation, a novel allele of the cellulose-synthesizing KORRIGAN1 gene. Plant molecular biology 71: 641-655.

KUDO H, UYEDA I AND SHIKATA E. 1991. Viruses in the phytoreovirus genus of the Reoviridae family have the same conserved terminal sequences. Journal of General Virology 72: 2857-2866.

KURIHARA D, MATSUNAGA S, KAWABE A, FUJIMOTO S, NODA M, UCHIYAMA S AND FUKUI K. 2006. Aurora kinase is required for chromosome segregation in tobacco BY-2 cells. The Plant Journal 48: 572-580.

LAPLANTE M AND SABATINI DM. 2012. mTOR signaling in growth control and disease. Cell 149: 274-293.

LAWLOR MA, MORA A, ASHBY PR, WILLIAMS MR, MURRAY-TAIT V, MALONE L, PRESCOTT AR, LUCOCQ JM AND ALESSI DR. 2002. Essential role of PDK1 in regulating cell size and development in mice. The EMBO Journal 21: 3728-3738.

LEE J, KIM D-M, LIM Y AND PAI H-S. 2004. The shooty callus induced by suppression of tobacco CHRK1 receptor-like kinase is a phenocopy of the tobacco genetic tumor. Plant cell reports 23: 397-403.

LEIBFRIED A, TO JPC, BUSCH W, STEHLING S, KEHLE A, DEMAR M, KIEBER JJ AND LOHMANN JU. 2005. WUSCHEL controls meristem function by direct regulation of cytokinin-inducible response regulators. Nature 438: 1172-1175.

LEON-KLOOSTERZIEL KM, KEIJZER CJ AND KOORNNEEF M. 1994. A Seed Shape Mutant of Arabidopsis That Is Affected in Integument Development. The Plant Cell 6: 385-392.

LIPKA E, HERRMANN A AND MUELLER S. 2015. Mechanisms of plant cell division. Wiley Interdisciplinary Reviews: Developmental Biology 4: 391-405.

LIPPINCOTT JA AND LIPPINCOTT BB. 1975. The genus Agrobacterium and plant tumorigenesis. Annu Rev Microbiol 29: 377-405.

LUDWIG C 1856. Diffusion zwischen ungleich erwärmten Orten gleich zusammengesetzter Lösung. Aus der KK Hof-und Staatsdruckerei, in Commission bei W. Braumüller, Buchhändler des KK Hofes und der K. Akademie der Wissenschaften.

MACMAHON B, COLE P AND BROWN J. 1973. Etiology of Human Breast Cancer: A Review 2. Journal of the National Cancer Institute 50: 21-42.

MAHFOUZ MM, KIM S, DELAUNEY AJ AND VERMA DPS. 2006. Arabidopsis TARGET OF RAPAMYCIN Interacts with RAPTOR, Which Regulates the Activity of S6 Kinase in Response to Osmotic Stress Signals. The Plant Cell 18: 477-490.

MANDEL MA, GUSTAFSON-BROWN C, SAVIDGE B AND YANOFSKY MF. 1992. Molecular characterization of the Arabidopsis floral homeotic gene APETALA1. Nature 360: 273-277.

MANNING G, WHYTE DB, MARTINEZ R, HUNTER T AND SUDARSANAM S. 2002. The Protein Kinase Complement of the Human Genome. Science 298: 1912-1934.

MANSFIELD SG AND BRIARTY LG. 1991. Early embryogenesis in Arabidopsis thaliana. II. The developing embryo. Canadian Journal of Botany 69: 461-476.

MARTIN FW. 1966. Frosty spot. A developmental disturbance of the tomato leaf. Annals of Botany 30: 701-709.

MATSUI H, MIYAO A, TAKAHASHI A AND HIROCHIKA H. 2010. Pdk1 Kinase Regulates Basal Disease Resistance Through the OsOxi1–OsPti1a Phosphorylation Cascade in Rice. Plant and Cell Physiology 51: 2082-2091.

MAURER M, SU T, SAAL LH, KOUJAK S, HOPKINS BD, BARKLEY CR, WU J, NANDULA S, DUTTA B AND XIE Y. 2009. 3-Phosphoinositide–dependent kinase 1 potentiates upstream lesions on the phosphatidylinositol 3-kinase pathway in breast carcinoma. Cancer research 69: 6299-6306.

MCABEE JM, HILL TA, SKINNER DJ, IZHAKI A, HAUSER BA, MEISTER RJ, VENUGOPALA REDDY G, MEYEROWITZ EM, BOWMAN JL AND GASSER CS. 2006. ABERRANT TESTA SHAPE encodes a KANADI family member, linking polarity determination to separation and growth of Arabidopsis ovule integuments. The Plant Journal 46: 522-531.

MCCONNELL JR AND BARTON MK. 1998. Leaf polarity and meristem formation in Arabidopsis. Development 125: 2935-2942.

MCCONNELL JR, EMERY J, ESHED Y, BAO N, BOWMAN J AND BARTON MK. 2001. Role of PHABULOSA and PHAVOLUTA in determining radial patterning in shoots. Nature 411: 709-713.

MENAND B, DESNOS T, NUSSAUME L, BERGER F, BOUCHEZ D, MEYER C AND ROBAGLIA C. 2002. Expression and disruption of the Arabidopsis TOR (target of rapamycin) gene. Proceedings of the National Academy of Sciences 99: 6422-6427.

MIKSCHE JP AND JOHN AMB. 1965. Development of Vegetative and Floral Meristems of Arabidopsis thaliana. American Journal of Botany 52: 533-537.

MINEYUKI Y, MARC J AND PALEVITZ BA. 1991. Relationship Between the Preprophase Band, Nucleus and Spindle in Dividing Allium Cotyledon Cells. Journal of Plant Physiology 138: 640-649.

MINEYUKI Y AND PALEVITZ BA. 1990. Relationship between preprophase band organization, F-actin and the division site in Allium. Fluorescence and morphometric studies on cytochalasin-treated cells. J Cell Sci: 283-295.

MIZUKAMI Y AND FISCHER RL. 2000. Plant organ size control: AINTEGUMENTA regulates growth and cell numbers during organogenesis. Proceedings of the National Academy of Sciences 97: 942-947.

MODRUSAN Z, REISER L, FELDMANN KA, FISCHER RL AND HAUGHN GW. 1994. Homeotic Transformation of Ovules into Carpel-like Structures in Arabidopsis. The Plant Cell 6: 333-349.

MORA A, KOMANDER D, VAN AALTEN DMF AND ALESSI DR. 2004. PDK1, the master regulator of AGC kinase signal transduction. Seminars in Cell & Developmental Biology 15: 161-170.

MOREAU M, AZZOPARDI M, CLÉMENT G, DOBRENEL T, MARCHIVE C, RENNE C, MARTIN-MAGNIETTE M-L, TACONNAT L, RENOU J-P AND ROBAGLIA C. 2012. Mutations in the Arabidopsis homolog of LST8/GβL, a partner of the target of rapamycin kinase, impair plant growth, flowering, and metabolic adaptation to long days. The Plant Cell 24: 463-481.

MOREAU M, SORMANI R, MENAND B, VEIT B, ROBAGLIA C AND MEYER C. 2010. The TOR complex and signaling pathway in plants. The enzymes 27: 285-302.

MORRIS RO. 1986. Genes specifying auxin and cytokinin biosynthesis in phytopathogens. Annual Review of Plant Physiology 37: 509-538.

MOUILLE G, RALET MC, CAVELIER C, ELAND C, EFFROY D, HÉMATY K, MCCARTNEY L, TRUONG HN, GAUDON V AND THIBAULT JF. 2007. Homogalacturonan synthesis in Arabidopsis thaliana requires a Golgi-localized protein with a putative methyltransferase domain. The Plant Journal 50: 605-614.

MURATA T AND WADA M. 1991. Effects of centrifugation on preprophase-band formation in Adiantum protonemata. Planta 183(3).

NAGAR S, PEDERSEN TJ, CARRICK KM, HANLEY-BOWDOIN L AND ROBERTSON D. 1995. A geminivirus induces expression of a host DNA synthesis protein in terminally differentiated plant cells. The Plant Cell 7: 705-719.

NAKATA M AND OKADA K. 2013. The Leaf Adaxial-Abaxial Boundary and Lamina Growth. Plants 2: 174-202.

NOLEN B, TAYLOR S AND GHOSH G. 2004. Regulation of protein kinases: controlling activity through activation segment conformation. Molecular cell 15: 661-675.

NUTTALL V AND LYALL L. 1964. Inheritance of neoplastic pod in the pea. Journal of Heredity 55: 184-186.

Ó'MAOILÉIDIGH DS, GRACIET E AND WELLMER F. 2014. Gene networks controlling Arabidopsis thaliana flower development. New Phytologist 201: 16-30.

PAWSON T AND SCOTT JD. 2005. Protein phosphorylation in signaling – 50 years and counting. Trends in Biochemical Sciences 30: 286-290.

PEARCE LR, KOMANDER D AND ALESSI DR. 2010. The nuts and bolts of AGC protein kinases. Nat Rev Mol Cell Biol 11: 9-22.

PEKKER I, ALVAREZ JP AND ESHED Y. 2005. Auxin Response Factors Mediate Arabidopsis Organ Asymmetry via Modulation of KANADI Activity. The Plant Cell 17: 2899-2910.

PELAZ S, DITTA GS, BAUMANN E, WISMAN E AND YANOFSKY MF. 2000. B and C floral organ identity functions require SEPALLATA MADS-box genes. Nature 405: 200.

PELAZ S, TAPIA-LÓPEZ R, ALVAREZ-BUYLLA ER AND YANOFSKY MF. 2001. Conversion of leaves into petals in Arabidopsis. Current Biology 11: 182-184.

PETERSON RT AND SCHREIBER SL. 1999. Kinase phosphorylation: Keeping it all in the family. Current biology 9: R521-R524.

PETRICKA JJ, VAN NORMAN JM AND BENFEY PN. 2009. Symmetry Breaking in Plants: Molecular Mechanisms Regulating Asymmetric Cell Divisions in Arabidopsis. Cold Spring Harbor Perspectives in Biology 1.

PIKE MC, SPICER DV, DAHMOUSH L AND PRESS MF. 1993. Estrogens progestogens normal breast cell proliferation and breast cancer risk. Epidemiologic reviews 15: 17-35.

PIMPRIKAR P. 2012. FUNCTIONAL CHARACTERISATION OF ARABIDOPSIS AGC KINASES 3-PHOSPHOINOSITIDE DEPENDENT KINASE-1 AND TUMOR SUPPRESSOR UNICORN. M.Sc., TU München.

PINNER S AND SAHAI E. 2008. PDK1 regulates cancer cell motility by antagonising inhibition of ROCK1 by RhoE. Nature cell biology 10: 127.

PINON V, PRASAD K, GRIGG SP, SANCHEZ-PEREZ GF AND SCHERES B. 2013. Local auxin biosynthesis regulation by PLETHORA transcription factors controls phyllotaxis in Arabidopsis. Proceedings of the National Academy of Sciences 110: 1107-1112.

PINYOPICH A, DITTA GS, SAVIDGE B AND LILJEGREN SJ. 2003. Assessing the redundancy of MADS-box genes during carpel and ovule development. Nature 424: 85.

PLEßMANN J. 2017. The role of the Arabidopsis AGCVIII kinase UNICORN (UCN) in plant development and flowering time determination. Ph.D., TU München.

RADEMACHER EH AND OFFRINGA R. 2012. Evolutionary Adaptations of Plant AGC Kinases: From Light Signaling to Cell Polarity Regulation. Front Plant Sci 3: 250.

RAVEN PH, EVERT RF AND EICHHORN SE 1992. The Biology of Plants. IAWA Journal, n. 13, 455-455 p.

REINHARDT D, MANDEL T AND KUHLEMEIER C. 2000. Auxin Regulates the Initiation and Radial Position of Plant Lateral Organs. The Plant Cell 12: 507-518.

REINHARDT D, PESCE E-R, STIEGER P, MANDEL T, BALTENSPERGER K, BENNETT M, TRAAS J, FRIML J AND KUHLEMEIER C. 2003. Regulation of phyllotaxis by polar auxin transport. Nature 426: 255-260.

REINHART BJ, WEINSTEIN EG, RHOADES MW, BARTEL B AND BARTEL DP. 2002. MicroRNAs in plants. Genes & Development 16: 1616-1626.

REMINGTON DL, VISION TJ, GUILFOYLE TJ AND REED JW. 2004. Contrasting modes of diversification in the Aux/IAA and ARF gene families. Plant physiology 135: 1738-1752.

REN M, QIU S, VENGLAT P, XIANG D, FENG L, SELVARAJ G AND DATLA R. 2011. Target of rapamycin regulates development and ribosomal RNA expression through kinase domain in Arabidopsis. Plant physiology 155: 1367-1382.

REN M, VENGLAT P, QIU S, FENG L, CAO Y, WANG E, XIANG D, WANG J, ALEXANDER D AND CHALIVENDRA S. 2012. Target of rapamycin signaling regulates metabolism, growth, and life span in Arabidopsis. The Plant Cell 24: 4850-4874.

RHOADES MW, REINHART BJ, LIM LP, BURGE CB, BARTEL B AND BARTEL DP. 2002. Prediction of Plant MicroRNA Targets. Cell 110: 513-520.

RIOU-KHAMLICHI C, HUNTLEY R, JACQMARD A AND MURRAY JA. 1999. Cytokinin activation of Arabidopsis cell division through a D-type cyclin. Science 283: 1541-1544.

ROBAGLIA C, THOMAS M AND MEYER C. 2012. Sensing nutrient and energy status by SnRK1 and TOR kinases. Current opinion in plant biology 15: 301-307.

ROBINSON-BEERS K, PRUITT RE AND GASSER CS. 1992. Ovule Development in Wild-Type Arabidopsis and Two Female-Sterile Mutants. The Plant Cell 4: 1237-1249.

ROMANELLI A, DREISBACH VC AND BLENIS J. 2002. Characterization of Phosphatidylinositol 3-Kinase-dependent Phosphorylation of the Hydrophobic Motif Site Thr389 in p70 S6 Kinase 1. Journal of Biological Chemistry 277: 40281-40289.

ROMANO RA, KANNAN N, KORNEV AP, ALLISON CJ AND TAYLOR SS. 2009. A chimeric mechanism for polyvalent trans-phosphorylation of PKA by PDK1. Protein Science : A Publication of the Protein Society 18: 1486-1497.

ROUDIER F, FEDOROVA E, LEBRIS M, LECOMTE P, GYÖRGYEY J, VAUBERT D, HORVATH G, ABAD P, KONDOROSI A AND KONDOROSI E. 2003. The Medicago species A2-type cyclin is auxin regulated and involved in meristem formation but dispensable for endoreduplication-associated developmental programs. Plant Physiology 131: 1091-1103.

ROUDIER F, GISSOT L, BEAUDOIN F, HASLAM R, MICHAELSON L, MARION J, MOLINO D, LIMA A, BACH L AND MORIN H. 2010. Very-long-chain fatty acids are involved in polar auxin transport and developmental patterning in Arabidopsis. The Plant Cell 22: 364-375.

SAMBROOK J, FRITSCH E AND MANIATIS T. 1989. Molecular cloning: a laboratory manual. Cold Spring Harbor Laboratory Press 2nd Edition.

SAMPATHKUMAR A, KRUPINSKI P, WIGHTMAN R, MILANI P, BERQUAND A, BOUDAOUD A, HAMANT O, JÖNSSON H AND MEYEROWITZ EM. 2014. Subcellular and supracellular mechanical stress prescribes cytoskeleton behavior in Arabidopsis cotyledon pavement cells. Elife 3: e01967.

SANTNER AA AND WATSON JC. 2006. The WAG1 and WAG2 protein kinases negatively regulate root waving in Arabidopsis. The Plant Journal 45: 752-764.

SARBASSOV DD, GUERTIN DA, ALI SM AND SABATINI DM. 2005. Phosphorylation and regulation of Akt/PKB by the rictor-mTOR complex. Science 307: 1098-1101.

SATINA S, BLAKESLEE AF AND AVERY AG. 1940. Demonstration of the Three Germ Layers in the Shoot Apex of Datura by Means of Induced Polyploidy in Periclinal Chimeras. American Journal of Botany 27: 895-905.

SAWA S, WATANABE K, GOTO K, KANAYA E, MORITA EH AND OKADA K. 1999. FILAMENTOUS FLOWER, a meristem and organ identity gene of Arabidopsis, encodes a protein with a zinc finger and HMG-related domains. Genes & Development 13: 1079-1088.

SCHAEFER E, BELCRAM K, UYTTEWAAL M, DUROC Y, GOUSSOT M, LEGLAND D, LARUELLE E, DE TAUZIA-MOREAU M-L, PASTUGLIA M AND BOUCHEZ D. 2017. The preprophase band of microtubules controls the robustness of division orientation in plants. Science 356: 186-189.

SCHALLY AV, COMARU-SCHALLY AM, NAGY A, KOVACS M, SZEPESHAZI K, PLONOWSKI A, VARGA JL AND HALMOS G. 2001. Hypothalamic hormones and cancer. Frontiers in neuroendocrinology 22: 248-291.

SCHINDELIN J ET AL. 2012. Fiji - an Open Source platform for biological image analysis. Nature methods 9: 10.1038/nmeth.2019.

SCHINDELIN J, RUEDEN CT, HINER MC AND ELICEIRI KW. 2015. The ImageJ ecosystem: an open platform for biomedical image analysis. Molecular reproduction and development 82: 518-529.

SCHNEIDER CA, RASBAND WS AND ELICEIRI KW. 2012. NIH Image to ImageJ: 25 years of Image Analysis. Nature methods 9: 671-675.

SCHNEITZ K. 1999. The molecular and genetic control of ovule development. Curr Opin Plant Biol 2: 13-17.

SCHNEITZ K, BALASUBRAMANIAN S AND SCHIEFTHALER U. 1998. Organogenesis in plants: the molecular and genetic control of ovule development. Trends in Plant Science 3: 468-472.

SCHNEITZ K, HULSKAMP M, KOPCZAK SD AND PRUITT RE. 1997. Dissection of sexual organ ontogenesis: a genetic analysis of ovule development in Arabidopsis thaliana. Development 124: 1367-1376.

SCHNEITZ K, HULSKAMP M AND PRUITT RE. 1995. Wild-type ovule development in Arabidopsis thaliana: a light microscope study of cleared whole-mount tissue. The Plant Journal 7: 731-749.

SCHWEIGHOFER A, HIRT H AND MESKIENE I. 2004. Plant PP2C phosphatases: emerging functions in stress signaling. Trends in plant science 9: 236-243.

SCORTEGAGNA M, RULLER C, FENG Y, LAZOVA R, KLUGER H, LI J-L, DE SK, RICKERT R, PELLECCHIA M AND BOSENBERG M. 2014. Genetic inactivation or pharmacological inhibition of Pdk1 delays development and inhibits metastasis of BrafV600E:: Pten−/− melanoma. Oncogene 33: 4330.

SESSIONS A, NEMHAUSER JL, MCCOLL A, ROE JL, FELDMANN KA AND ZAMBRYSKI PC. 1997. ETTIN patterns the Arabidopsis floral meristem and reproductive organs. Development 124: 4481-4491.

SHARP W AND GUNCKEL J. 1969. Physiological comparisons of pith callus with crown-gall and genetic tumors of Nicotiana glauca, N. langsdorffii, and N. glauca-langsdorffii grown in vitro. II. Nutritional physiology. Plant physiology 44: 1073-1079.

SIEBER P, GHEYSELINCK J, GROSS-HARDT R, LAUX T, GROSSNIKLAUS U AND SCHNEITZ K. 2004. Pattern formation during early ovule development in Arabidopsis thaliana. Dev Biol 273: 321-334.

SIEBERER T, HAUSER M-T, SEIFERT GJ AND LUSCHNIG C. 2003. PROPORZ1, a putative Arabidopsis transcriptional adaptor protein, mediates auxin and cytokinin signals in the control of cell proliferation. Current Biology 13: 837-842.

SIEGFRIED KR, ESHED Y, BAUM SF, OTSUGA D, DREWS GN AND BOWMAN JL. 1999. Members of the YABBY gene family specify abaxial cell fate in Arabidopsis. Development 126: 4117-4128.

SKIBBE DS, DOEHLEMANN G, FERNANDES J AND WALBOT V. 2010. Maize tumors caused by Ustilago maydis require organ-specific genes in host and pathogen. Science 328: 89-92.

SMERTENKO A ET AL. 2017. Plant Cytokinesis: Terminology for Structures and Processes. Trends in Cell Biology.

SMITH LG, GREENE B, VEIT B AND HAKE S. 1992. A dominant mutation in the maize homeobox gene, Knotted-1, causes its ectopic expression in leaf cells with altered fates. Development 116: 21-30.

SMITH LM, BOMBLIES K AND WEIGEL D. 2011. Complex evolutionary events at a tandem cluster of Arabidopsis thaliana genes resulting in a single-locus genetic incompatibility. PLoS genetics 7: e1002164.

SORET C 1880. Sur l'etat d'équilibre que prend au point de vue de sa concentration une dissolution saline primitivement homogène dont deux parties sont portées a des températures différentes: Deuxieme note.

ST JOHN A, TAO W, FEI X, FUKUMOTO R, CARCANGIU ML, BROWNSTEIN DG, PARLOW AF, MCGRATH J AND XU T. 1999. Mice deficient of Lats1 develop soft-tissue sarcomas, ovarian tumours and pituitary dysfunction. Nature genetics 21: 182-186.

STREISSLE G AND MARAMOROSCH K. 1963. Reovirus and wound-tumor virus: serological cross reactivity. Science 140: 996-997.

SUSSEX IM. 1954. Experiments on the Cause of Dorsiventrality in Leaves. Nature 174: 351-352.

SZIRAKI I, BALAZS E AND KIRALY Z. 1975. Increased levels of cytokinin and indoleacetic acid in peach leaves infected with Taphrina deformans. Physiological Plant Pathology 5: 45-50.

TAKEUCHI M, KARAHARA I, KAJIMURA N, TAKAOKA A, MURATA K, MISAKI K, YONEMURA S, STAEHELIN LA AND MINEYUKI Y. 2016. Single microfilaments mediate the early steps of microtubule bundling during preprophase band formation in onion cotyledon epidermal cells. Molecular Biology of the Cell 27: 1809-1820.

TANG G, REINHART BJ, BARTEL DP AND ZAMORE PD. 2003. A biochemical framework for RNA silencing in plants. Genes & Development 17: 49-63.

TAVARES S, INÁCIO J AND OLIVEIRA C. 2004. Direct detection of Taphrina deformans on peach trees using molecular methods. European journal of plant pathology 110: 973-982.

TEMSAH M, HANNA L AND SAAD A. 2010. Histological pathogenesis of *Pseudomonas savastanoi* on *Nerium oleander*. Journal of Plant Pathology: 407-413.

THEIßEN G. 2001. Development of floral organ identity: stories from the MADS house. Current opinion in plant biology 4: 75-85.

THEIßEN G, MELZER R AND RÜMPLER F. 2016. MADS-domain transcription factors and the floral quartet model of flower development: linking plant development and evolution. Development 143: 3259-3271.

TILNEY-BASSETT RAE. 1986. Plant chimeras. Edward Arnold, London.

TORRES-RUIZ RA, LOHNER A AND JÜRGENS G. 1996. The GURKE gene is required for normal organization of the apical region in the Arabidopsis embryo. The Plant Journal 10: 1005-1016.

TRUERNIT E, BAUBY H, DUBREUCQ B, GRANDJEAN O, RUNIONS J, BARTHÉLÉMY J AND PALAUQUI J-C. 2008. High-resolution whole-mount imaging of three-dimensional tissue organization and gene expression enables the study of phloem development and structure in Arabidopsis. The Plant Cell 20: 1494-1503.

TRUERNIT E AND HASELOFF J. 2008. Arabidopsis thaliana outer ovule integument morphogenesis: Ectopic expression of KNAT1reveals a compensation mechanism. BMC Plant Biology 8: 35.

TRUSOV Y, JORDÁ L, MOLINA A AND BOTELLA JR 2010. G proteins and plant innate immunity. Integrated G proteins signaling in plants: Springer, p. 221-250.

TURCK F, ZILBERMANN F, KOZMA SC, THOMAS G AND NAGY F. 2004. Phytohormones Participate in an S6 Kinase Signal Transduction Pathway in Arabidopsis. Plant Physiology 134: 1527-1535.

ULMASOV T, HAGEN G AND GUILFOYLE TJ. 1999. Dimerization and DNA binding of auxin response factors. The Plant Journal 19: 309-319.

VADDEPALLI P ET AL. 2014. The C2-domain protein QUIRKY and the receptor-like kinase STRUBBELIG localize to plasmodesmata and mediate tissue morphogenesis in Arabidopsis thaliana. Development 141: 4139-4148.

VADDEPALLI P, SCHOLZ S AND SCHNEITZ K. 2015. Pattern formation during early floral development. Curr Opin Genet Dev 32: 16-23.

VAN DAMME D, DE RYBEL B, GUDESBLAT G, DEMIDOV D, GRUNEWALD W, DE SMET I, HOUBEN A, BEECKMAN T AND RUSSINOVA E. 2011. Arabidopsis α Aurora Kinases Function in Formative Cell Division Plane Orientation. The Plant Cell 23: 4013-4024.

VAN LEEUWEN W, ÖKRÉSZ L, BÖGRE L AND MUNNIK T. 2004. Learning the lipid language of plant signalling. Trends in Plant Science 9: 378-384.

VANDEPUTTE O, ÖDEN S, MOL A, VEREECKE D, GOETHALS K, EL JAZIRI M AND PRINSEN E. 2005. Biosynthesis of auxin by the gram-positive phytopathogen Rhodococcus fascians is controlled by compounds specific to infected plant tissues. Applied and environmental microbiology 71: 1169-1177.

VILLANUEVA JM, BROADHVEST J, HAUSER BA, MEISTER RJ, SCHNEITZ K AND GASSER CS. 1999. INNER NO OUTER regulates abaxial– adaxial patterning in Arabidopsis ovules. Genes & Development 13: 3160-3169.

VIVANCO I AND SAWYERS CL. 2002. The phosphatidylinositol 3-kinase-AKT pathway in human cancer. Nature reviews Cancer 2: 489.

WACHSMAN G, HEIDSTRA R AND SCHERES B. 2011. Distinct cell-autonomous functions of RETINOBLASTOMA-RELATED in Arabidopsis stem cells revealed by the Brother of Brainbow clonal analysis system. The Plant Cell 23: 2581-2591.

WAGNER D, SABLOWSKI RWM AND MEYEROWITZ EM. 1999. Transcriptional Activation of APETALA1 by LEAFY. Science 285: 582-584.

WALTER M ET AL. 2004. Visualization of protein interactions in living plant cells using bimolecular fluorescence complementation. Plant J 40: 428-438.

WANG J, LIU F, AO P, LI X, ZHENG H, WU D, ZHANG N, SHE J, YUAN J AND WU X. 2016. Correlation of PDK1 expression with clinicopathologic features and prognosis of hepatocellular carcinoma. OncoTargets and therapy 9: 5597.

WANG Z-P, XING H-L, DONG L, ZHANG H-Y, HAN C-Y, WANG X-C AND CHEN Q-J. 2015. Egg cell-specific promoter-controlled CRISPR/Cas9 efficiently generates homozygous mutants for multiple target genes in Arabidopsis in a single generation. Genome Biology 16: 144.

WEIGEL D, ALVAREZ J, SMYTH DR, YANOFSKY MF AND MEYEROWITZ EM. 1992. LEAFY controls floral meristem identity in Arabidopsis. Cell 69: 843-859.

WEIGEL D AND NILSSON O. 1995. A developmental switch sufficient for flower initiation in diverse plants. Nature 377: 495-500.

WEINBERG RA 2014. The biology of cancer., n. 2: Garland Science.

WELLER B, ZOURELIDOU M, FRANK L, BARBOSA ICR, FASTNER A, RICHTER S, JÜRGENS G, HAMMES UZ AND SCHWECHHEIMER C. 2017. Dynamic PIN-FORMED auxin efflux carrier phosphorylation at the plasma membrane controls auxin efflux-dependent growth. Proceedings of the National Academy of Sciences 114: E887-E896.

WILLIGE BC ET AL. 2013. D6PK AGCVIII Kinases Are Required for Auxin Transport and Phototropic Hypocotyl Bending in Arabidopsis. The Plant Cell 25: 1674-1688.

WILLIGE BC, OGISO-TANAKA E, ZOURELIDOU M AND SCHWECHHEIMER C. 2012. WAG2 represses apical hook opening downstream from gibberellin and PHYTOCHROME INTERACTING FACTOR 5. Development 139: 4020-4028.

WILSON E. 1965. Pathological histogenesis in oleander tumors induced by Pseudomonas savastanoi. Phytopathology 55: 1244-&.

WILSON E AND MAGIE A. 1964. Systemic invasion of the host plant by the tumor-inducing bacterium, Pseudomonas savastanoi. Phytopathology 54: 576-579.

WULLSCHLEGER S, LOEWITH R AND HALL MN. 2006. TOR signaling in growth and metabolism. Cell 124: 471-484.

XIONG Y, MCCORMACK M, LI L, HALL Q, XIANG C AND SHEEN J. 2013. Glucose-TOR signalling reprograms the transcriptome and activates meristems. Nature 496: 181-186.

XIONG Y AND SHEEN J. 2012. Rapamycin and glucose-target of rapamycin (TOR) protein signaling in plants. Journal of Biological Chemistry 287: 2836-2842.

XIONG Y AND SHEEN J. 2014. The role of target of rapamycin signaling networks in plant growth and metabolism. Plant physiology 164: 499-512.

XU T, WANG W, ZHANG S, STEWART RA AND YU W. 1995. Identifying tumor suppressors in genetic mosaics: the Drosophila lats gene encodes a putative protein kinase. Development 121: 1053-1063.

XUE T, WANG D, ZHANG S, EHLTING J, NI F, JAKAB S, ZHENG C AND ZHONG Y. 2008. Genome-wide and expression analysis of protein phosphatase 2C in rice and Arabidopsis. BMC genomics 9: 550.

YADAV RK, PERALES M, GRUEL J, GIRKE T, JÖNSSON H AND REDDY GV. 2011. WUSCHEL protein movement mediates stem cell homeostasis in the Arabidopsis shoot apex. Genes & Development 25: 2025-2030.

YADAV RK, PERALES M, GRUEL J, OHNO C, HEISLER M, GIRKE T, JÖNSSON H AND REDDY GV. 2013. Plant stem cell maintenance involves direct transcriptional repression of differentiation program. Molecular Systems Biology 9: 654-654.

YALOVSKY S, BLOCH D, SOREK N AND KOST B. 2008. Regulation of Membrane Trafficking, Cytoskeleton Dynamics, and Cell Polarity by ROP/RAC GTPases. Plant Physiology 147: 1527-1543.

YAMAGUCHI N, WINTER CM, WU M-F, KANNO Y, YAMAGUCHI A, SEO M AND WAGNER D. 2014. Gibberellin Acts Positively Then Negatively to Control Onset of Flower Formation in Arabidopsis. Science 344: 638-641.

YAMAGUCHI N, WU M-F, WINTER CARA M, BERNS MARKUS C, NOLE-WILSON S, YAMAGUCHI A, COUPLAND G, KRIZEK BETH A AND WAGNER D. 2013. A Molecular Framework for Auxin-Mediated Initiation of Flower Primordia. Developmental Cell 24: 271-282.

YANG Z, WU Z, LIU T, HAN L, WANG C, YANG B AND ZHENG F. 2014. Upregulation of PDK1 associates with poor prognosis in esophageal squamous cell carcinoma with facilitating tumorigenicity in vitro. Medical oncology 31: 337.

YANOFSKY MF, MA H, BOWMAN JL, DREWS GN, FELDMANN KA AND MEYEROWITZ EM. 1990. The protein encoded by the Arabidopsis homeotic gene agamous resembles transcription factors. Nature 346: 35.

YOO SD, CHO YH AND SHEEN J. 2007. Arabidopsis mesophyll protoplasts: a versatile cell system for transient gene expression analysis. Nat Protoc 2: 1565-1572.

ZABKIEWICZ J, PEARN L, HILLS RK, MORGAN RG, TONKS A, BURNETT AK AND DARLEY RL. 2014. The PDK1 master kinase is over-expressed in acute myeloid leukemia and promotes PKC-mediated survival of leukemic blasts. Haematologica 99: 858-864.

ZEGZOUTI H, ANTHONY RG, JAHCHAN N, BOGRE L AND CHRISTENSEN SK. 2006a. Phosphorylation and activation of PINOID by the phospholipid signaling kinase 3-phosphoinositide-dependent protein kinase 1 (PDK1) in Arabidopsis. Proc Natl Acad Sci U S A 103: 6404-6409.

ZEGZOUTI H, LI W, LORENZ TC, XIE M, PAYNE CT, SMITH K, GLENNY S, PAYNE GS AND CHRISTENSEN SK. 2006b. Structural and Functional Insights into the Regulation of Arabidopsis AGC VIIIa Kinases. Journal of Biological Chemistry 281: 35520-35530.

ZHANG Y, HE J AND MCCORMICK S. 2009. Two Arabidopsis AGC kinases are critical for the polarized growth of pollen tubes. The Plant Journal 58: 474-484.

ZHANG Y AND MCCORMICK S. 2009. AGCVIII kinases: at the crossroads of cellular signaling. Trends in Plant Science 14: 689-695.

ZHONG R AND YE Z-H. 2007. Regulation of HD-ZIP III Genes by MicroRNA 165. Plant Signaling & Behavior 2: 351-353.

ZOURELIDOU M ET AL. 2014. Auxin efflux by PIN-FORMED proteins is activated by two different protein kinases, D6 PROTEIN KINASE and PINOID. eLife 3: e02860.

ZULAWSKI M, SCHULZE G, BRAGINETS R, HARTMANN S AND SCHULZE WX. 2014. The Arabidopsis Kinome: phylogeny and evolutionary insights into functional diversification. BMC Genomics 15: 548.

ZULAWSKI M AND SCHULZE WX 2015. The Plant Kinome. In*:* SCHULZE, WX (Ed.) Plant Phosphoproteomics: Methods and Protocols, New York, NY: Springer New York, p. 1-23.

7 SUPPLEMENT

Table 7-1: Oligonucleotides used in this study. Sequence and purpose are indicated.

Name	5'-sequence-3'	Purpose
PDK1.1_fw EcoRI_new	GGCCGAATTCATGTTGGCAATGGAGAAAGAA	Cloning PDK1.1 CDS into pMal c2x forward
PDK1.1_rev BamHI_new	GGCCGGATCCTCAGCGGTTCTGAAGAGTCTC	Cloning PDK1.1 CDS into pMal c2x reverse
PDK1.2 fw_BamHI_new	GGCCGGATCCATGTTGACAATGGACAAGGAA	Cloning PDK1.2 CDS into pMal c2x forward
PDK1.2_rev_PstI_new	GGATCTGCAGTCAACGGTTTTGAAGAGTTTC	Cloning PDK1.2 CDS into pMal c2x reverse
PDK1.1_fw_BamHI_BiFC	CCCCGGATCCATGTTGGCAATGGAGAAAGAATTT	Cloning PDK1.1 CDS into pSPYCE/pSPYNE forward
PDK1.1_rev_XmaI_BiFC	AAAACCCGGGGCGGTTCTGAAGAGTCTCGAT	Cloning PDK1.1 CDS into pSPYCE/pSPYNE reverse
PDK1.2_fw_BamHI_BiFC	CCCCGGATCCATGTTGACAATGGACAAGGAA	Cloning PDK1.2 CDS into pSPYCE/pSPYNE forward
PDK1.2_rev_KpnI_BiFC	CCCCGGTACCACGGTTTTGAAGAGTTTCGAT	Cloning PDK1.2 CDS into pSPYCE/pSPYNE reverse
UCN_fw_XbaI_BiFC	CCCCTCTAGAATGGAGACAAGACCATCATCATCATC	Cloning UCN into pSPYCE/pSPYNE forward
UCN_dPIF_rev_XmaI_BiFC	AAAACCCGGGCGGATTGTTTTCAGAACACTCGTGC	Cloning UCN_dPIF into pSPYCE/pSPYNE reverse
UCN_rev_XmaI_BiFC	AAAACCCGGGGAAATCAACAAACGGATTGTTTTCAGA	Cloning of UCN into pSPYCE/pSPYNE reverse
SALK_LBb1.3	ATTTTGCCGATTTCGGAAC	Genotyping SALK lines
pdk1.1_SALK_053385_LP	TGGAAGTTTGGTTGATCGAAG	Genotyping pdk1.1-1 SALK_053385
pdk1.1_SALK_053385_RP	ACATTAGCACCGTTGGATGAG	Genotyping pdk1.1-1 SALK_053385
pdk1.1_SALK_113251_LP	TGGTAAGATGCATCAAAAGCC	Genotyping pdk1.1-2 SALK_113251
pdk1.1_SALK_113251_RP	TTACCACGGTTTTGTGAAAGG	Genotyping pdk1.1-2 SALK_113251
SAIL_LB2	GCTTCCTATTATATCTTCCCAAATTACCAATACA	Genotyping SAIL lines
pdk1.2_SAIL_62_G04_LP	CTTACCATGATTTCGAGCTCG	Genotyping pdk1.2-2 SAIL_62_G04
pdk1.2_SAIL_62_G04_RP	TTCAGGAGGAACATATGCAGC	Genotyping pdk1.2-2 SAIL_62_G04
pdk1.2_SAIL_450_B01_LP	CTTGATCAACTCGAACATCCC	Genotyping pdk1.2-3 SAIL_450_B01
pdk1.2_SAIL_450_B01_RP	AACCTTCTGATCCAGCTCCTG	Genotyping pdk1.2-3 SAIL_450_B01
pUBQ10_HindIII_fw	AACCAAGCTTAGCTGCGACGAGTCAGTAATAAACG	Replacing p35S in pMDC43/83 forward
pUBQ10_KpnI_rev	TTCCGGTACCAGATCATGTTAATCAGAAAAACTCAG	Replacing p35S in pMDC43 reverse

pUBQ10_SpeI_rev	CCCCACTAGTTGTTAATCAGAAAAACTCAG	Replacing p35S in pMDC83 reverse
p16_HindIII_fw	AACCAAGCTTAGCTGTGGAACCATCTTTTGGGTTCC	Replacing p35S in pMDC43/83 forward
p16_KpnI_rev	TTCCGGTACCAGATCGACCACGCCGTCGTAGATGAG	Replacing p35S in pMDC43 reverse
p16_SpeI_rev	CCCCACTAGTCCACGCCGTCGTAGATGAG	Replacing p35S in pMDC83 reverse
pPDK1.2_fw_attB1	GGGGACAAGTTTGTACAAAAAAGCAGGCTATGGGTTTTCCACCTTGAGGC	Cloning pPDK1.2::gPDK1.2 into pMDC43 forward
PDK1.2_rev_attB2	GGGGACCACTTTGTACAAGAAAGCTGGGTTACGGTTTTGAAGAGTTTCG	Cloning pPDK1.2::gPDK1.2 into pMDC43 reverse
PDK1.1sense_CDS_F	TAATACGACTCACTATAGGGATGTTGGCAATGGAGAAAG	PDK1.1 in situ sense probe forward
PDK1.1sense_CDS_R	TCAGCGGTTCTGAAGAGTC	PDK1.1 in situ sense probe reverse
PDK1.1as_CDS_F	ATGTTGGCAATGGAGAAAG	PDK1.1 in situ antisense probe forward
PDK1.1as_CDS_R	TAATACGACTCACTATAGGGTCAGCGGTTCTGAAGAGTC	PDK1.1 in situ antisense probe reverse
PDK1.2sense_CDS_F	TAATACGACTCACTATAGGGATGTTGACAATGGACAAGG	PDK1.2 in situ sense probe forward
PDK1.2sense_CDS_R	TCAACGGTTTTGAAGAGTT	PDK1.2 in situ sense probe reverse
PDK1.2as_CDS_F	ATGTTGACAATGGACAAGG	PDK1.2 in situ antisense probe forward
PDK1.2as_CDS_R	TAATACGACTCACTATAGGGTCAACGGTTTTGAAGAGTT	PDK1.2 in situ antisense probe reverse
At4g33380(qRT)_F	TGAAGGAGAGGAAGAGCCTGAGGAA	Reference gene 1 forward qRT-PCR
At4g33380(qRT)_R	CCCCATCTCACTGCAGCACCAC	Reference gene 1 reverse qRT-PCR
At2g28390(qRT)_F	AGATTGCAGGGTACGCCTTGAGG	Reference gene 2 forward qRT-PCR
At2g28390(qRT)_R	ACACGCATTCCACCTTCCGCG	Reference gene 2 reverse qRT-PCR
At5g46630(qRT)_F	CCAAATGGAATTTCAGGTGCCAATG	Reference gene 3 forward qRT-PCR
At5g46630(qRT)_R	CAATGCGTACCTTGAGAAAACGAAC	Reference gene 3 reverse qRT-PCR
PDK1.2_(qRT)_fw	TCGCCTTTAAGGCTCCTCAGG	PDK1.2 forward qRT-PCR
PDK1.2_(qRT)_rev	CCATGATCTTCAAGGCATACACAG	PDK1.2 reverse qRT-PCR
PDK1.1(qRT)_fw2	AACGGTGCTAATGTTTCTAGAAGC	PDK1.1 forward qRT-PCR
PDK1.1(qRT)_rev	CAGTTTCCTTCTTCTTTGCCCTAAC	PDK1.1 reverse qRT-PCR

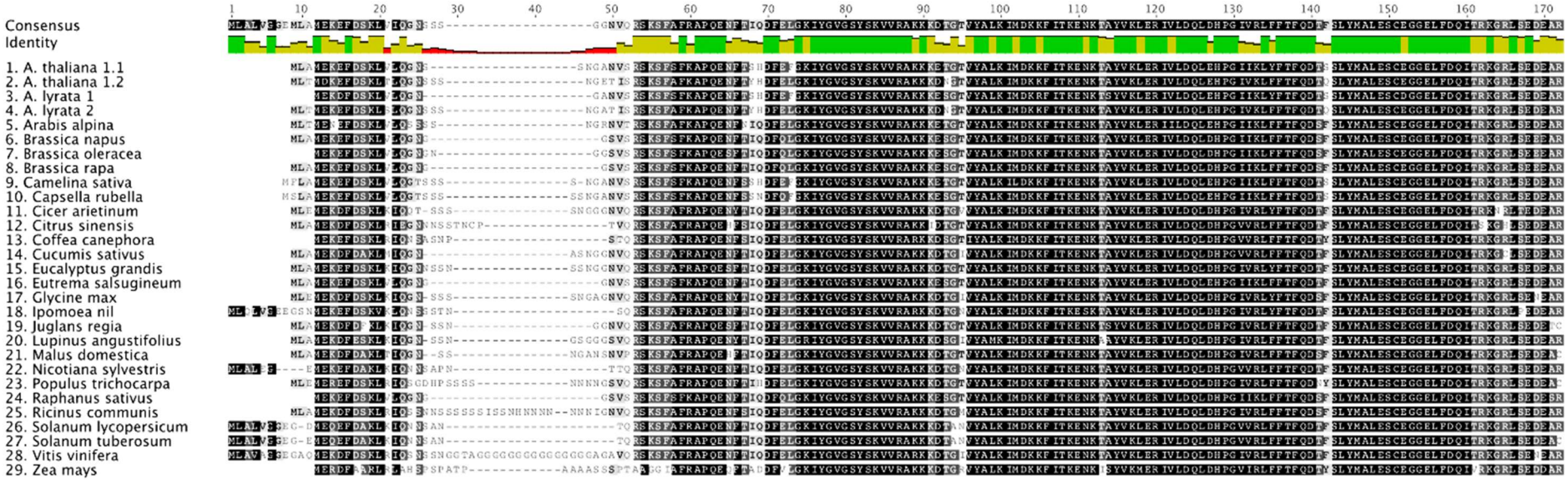

Figure 7-1 Alignment of 29 PDK1 protein sequences of 27 different plant species.

Black bars indicate identity or high similarity, grey bars similarity, and light grey bars little similarity. The brighter the grey value the less similar are the sequences. Lines show gaps. Alignment was performed in Geneious software using ClustalW algorithm with BLSM62 matrix. Sequences are continued on the next page.

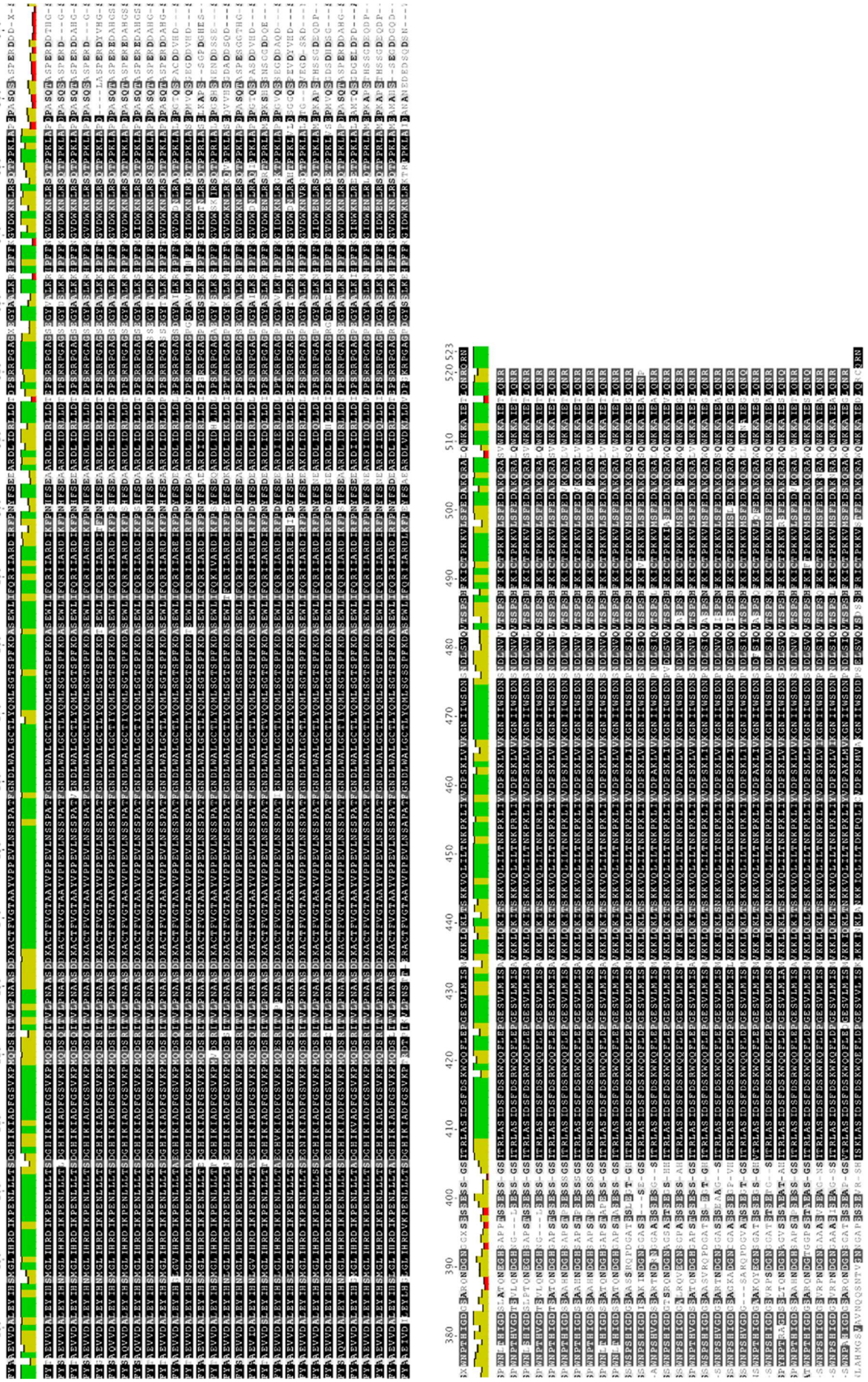

Table 7-2 Absolute and relative values of *ucn-1* (L*er*), *ucn-1* (Col-0), and *pdk1 ucn-1* ovule phenotypes.

Three individuals of three independent crosses for each combination were analyzed.

ucn-1 L*er* homozygous ucn-1 F3					*Ler ucn-1* homozygous ucn-1 F3				
		Cross 1	Cross 2	Cross 3			Cross 1	Cross 2	Cross 3
Plant 1	0 protrusions	17	25	18	Plant 1	0 protrusions	20	34	17
	1 protrusion	146	247	199		1 protrusion	167	238	127
	2 protrusion	29	44	32		2 protrusion	27	38	19
	> 2 protrusions	6	8	10		> 2 protrusions	3	4	2
	N	198	324	259		N	217	314	165
	% zero	8.59	7.72	6.95		% zero	9.22	10.83	10.30
	% one	73.74	76.23	76.83		% one	76.96	75.80	76.97
	% two	14.65	13.58	12.36		% two	12.44	12.10	11.52
	% > two	3.03	2.47	3.86		% > two	1.38	1.27	1.21
Plant 2	0 protrusions	14	24	25	Plant 2	0 protrusions	23	40	13
	1 protrusion	136	233	208		1 protrusion	158	270	92
	2 protrusion	24	38	40		2 protrusion	24	36	13
	> 2 protrusions	5	8	5		> 2 protrusions	3	5	1
	N	179	303	278		N	208	351	119
	% zero	7.82	7.92	8.99		% zero	11.06	11.40	10.92
	% one	75.98	76.90	74.82		% one	75.96	76.92	77.31
	% two	13.41	12.54	14.39		% two	11.54	10.26	10.92
	% > two	2.79	2.64	1.80		% > two	1.44	1.42	0.84
Plant 3	0 protrusions	21	11	12	Plant 3	0 protrusions	28	39	34
	1 protrusion	186	104	124		1 protrusion	196	263	209
	2 protrusion	38	19	21		2 protrusion	36	37	31
	> 2 protrusions	7	4	4		> 2 protrusions	4	5	5
	N	252	138	161		N	264	344	279
	% zero	8.33	7.97	7.45		% zero	10.61	11.34	12.19
	% one	73.81	75.36	77.02		% one	74.24	76.45	74.91
	% two	15.08	13.77	13.04		% two	13.64	10.76	11.11
	% > two	2.78	2.90	2.48		% > two	1.52	1.45	1.79
Total	N	629	765	698	Total	N	689	1009	563
	0 protrusions	52	60	55		0 protrusions	71	113	64
	1 protrusion	468	584	531		1 protrusion	521	771	428
	2 protrusion	91	101	93		2 protrusion	87	111	63
	> 2 protrusions	18	20	19		> 2 protrusions	10	14	8
	% zero	8.27	7.84	7.88		% zero	10.30	11.20	11.37
	% one	74.40	76.34	76.07		% one	75.62	76.41	76.02
	% two	14.47	13.20	13.32		% two	12.63	11.00	11.19
	% > two	2.86	2.61	2.72		% > two	1.45	1.39	1.42

ucn-1 Col-0 homozygous F3					Col-0 *ucn-1* homozygous F3				
		Cross 1	Cross 2	Cross 3			Cross 1	Cross 2	Cross 3
Plant 1	0 protrusions	42	54	41	Plant 1	0 protrusions	89	47	52
	1 protrusion	139	239	152		1 protrusion	241	146	158
	2 protrusion	14	21	18		2 protrusion	20	16	14
	> 2 protrusions	2	2	2		> 2 protrusions	2	1	2
	N	197	316	213		N	352	210	226
	% zero	21.32	17.09	19.25		% zero	25.28	22.38	23.01
	% one	70.56	75.63	71.36		% one	68.47	69.52	69.91
	% two	7.11	6.65	8.45		% two	5.68	7.62	6.19
	% > two	1.01	0.62	0.77		% > two	0.57	0.48	0.88
Plant 2	0 protrusions	39	59	81	Plant 2	0 protrusions	76	57	67
	1 protrusion	140	215	243		1 protrusion	188	162	178
	2 protrusion	13	24	26		2 protrusion	20	15	15
	> 2 protrusions	2	3	3		> 2 protrusions	3	2	1
	N	194	301	353		N	287	236	261
	% zero	20.10	19.60	22.95		% zero	26.48	24.15	25.67
	% one	72.16	71.43	68.84		% one	65.51	68.64	68.20
	% two	6.70	7.97	7.37		% two	6.97	6.36	5.75
	% > two	1.03	1.00	0.85		% > two	1.05	0.85	0.38
Plant 3	0 protrusions	68	74	17	Plant 3	0 protrusions	37	99	87
	1 protrusion	243	255	68		1 protrusion	102	271	244
	2 protrusion	18	19	6		2 protrusion	10	26	21
	> 2 protrusions	4	2	0		> 2 protrusions	1	4	3
	N	333	350	91		N	150	400	355
	% zero	20.42	21.14	18.68		% zero	24.67	24.75	24.51
	% one	72.97	72.86	74.73		% one	68.00	67.75	68.73
	% two	5.41	5.43	6.59		% two	6.67	6.50	5.92
	% > two	1.20	0.57	0		% > two	0.67	1.00	0.85
Total	N	724	967	657	Total	N	789	846	842
	0 protrusions	149	187	139		0 protrusions	202	203	206
	1 protrusion	522	709	463		1 protrusion	531	579	580
	2 protrusion	45	64	50		2 protrusion	50	57	50
	> 2 protrusions	8	7	5		> 2 protrusions	6	7	6
	% zero	20.58	19.34	21.16		% zero	25.60	24.00	24.47
	% one	72.10	73.32	70.47		% one	67.30	68.44	68.88
	% two	6.22	6.62	7.61		% two	6.34	6.74	5.94
	% > two	1.10	0.72	0.76		% > two	0.76	0.83	0.71

Continued on next page.

pdk1.1-1 ucn-1 homozygous F3

		Cross 1	Cross 2	Cross3
Plant1	0 protrusions	181	197	223
	1 protrusion	37	43	51
	% rescue	83.03	82.08	81.39
Plant2	0 protrusions	212	164	256
	1 protrusion	43	35	53
	% rescue	83.14	82.41	82.85
Plant3	0 protrusions	238	222	253
	1 protrusion	57	41	50
	% rescue	80.68	84.41	83.50
total	N	768	702	886
	0 protrusions	631	583	732
	1 protrusion	137	119	154
	Mean rescue %	82.16	83.05	82.62
	STDEV.P	1.13	1.03	0.88

pdk1.1-2 ucn-1 homozygous F3

		Cross 1	Cross 2	Cross3
Plant1	0 protrusions	234	111	199
	1 protrusion	59	23	53
	% rescue	79.86	82.84	78.97
Plant2	0 protrusions	191	283	306
	1 protrusion	40	57	82
	% rescue	82.68	83.24	78.87
Plant3	0 protrusions	265	325	297
	1 protrusion	58	90	56
	% rescue	82.04	78.31	84.14
total	N	847	889	993
	0 protrusions	690	719	802
	1 protrusion	157	170	191
	Mean rescue %	81.46	80.88	80.77
	STDEV.P	1.21	2.23	2.46

ucn-1 pdk1.1-1 homozygous F3

		Cross 1	Cross 2	Cross3
Plant1	0 protrusions	220	233	146
	1 protrusion	59	52	48
	% rescue	78.85	81.75	75.26
Plant2	0 protrusions	169	252	188
	1 protrusion	37	78	53
	% rescue	82.04	76.36	78.01
Plant3	0 protrusions	203	228	201
	1 protrusion	58	64	59
	% rescue	77.78	78.08	77.31
total	N	746	907	695
	0 protrusions	592	713	535
	1 protrusion	154	194	160
	Mean rescue %	79.36	78.61	76.98
	STDEV.P	1.81	2.25	1.17

ucn-1 pdk1.1-2 homozygous F3

		Cross 1	Cross 2	Cross3
Plant1	0 protrusions	195	223	271
	1 protrusion	53	60	67
	% rescue	78.63	78.80	80.18
Plant2	0 protrusions	230	162	313
	1 protrusion	62	43	93
	% rescue	78.77	79.02	77.09
Plant3	0 protrusions	158	286	236
	1 protrusion	50	81	64
	% rescue	75.96	77.93	78.67
total	N	748	855	1044
	0 protrusions	583	671	820
	1 protrusion	165	184	224
	Mean rescue %	77.94	78.48	78.54
	STDEV.P	1.29	0.47	1.26

pdk1.2-2 ucn-1 homozygous F3

		Cross 1	Cross 2	Cross3
Plant1	0 protrusions	233	249	262
	1 protrusion	16	23	29
	% rescue	93.57	91.54	90.03
Plant2	0 protrusions	282	208	296
	1 protrusion	26	28	26
	% rescue	91.56	88.14	91.93
Plant3	0 protrusions	263	191	248
	1 protrusion	19	28	21
	% rescue	93.26	87.21	92.19
total	N	839	727	882
	0 protrusions	778	648	806
	1 protrusion	61	79	76
	Mean rescue %	92.73	89.13	91.38
	STDEV.P	0.89	1.86	0.96

pdk1.2-3 ucn-1 homozygous F3

		Cross 1	Cross 2	Cross3
Plant1	0 protrusions	321	274	341
	1 protrusion	30	25	38
	% rescue	91.45	91.64	89.97
Plant2	0 protrusions	264	263	148
	1 protrusion	35	31	17
	% rescue	88.29	89.46	89.70
Plant3	0 protrusions	276	309	217
	1 protrusion	28	36	27
	% rescue	90.79	89.57	88.93
total	N	954	938	788
	0 protrusions	861	846	706
	1 protrusion	93	92	82
	Mean rescue %	90.25	90.19	89.59
	STDEV.P	1.36	1.00	0.44

ucn-1 pdk1.2-2 homozygous F3

		Cross 1	Cross 2	Cross3
Plant1	0 protrusions	308	261	346
	1 protrusion	38	40	53
	% rescue	89.02	86.71	86.72
Plant2	0 protrusions	237	229	136
	1 protrusion	36	29	19
	% rescue	86.81	88.76	87.74
Plant3	0 protrusions	188	246	211
	1 protrusion	27	29	23
	% rescue	87.44	89.45	90.17
total	N	834	834	788
	0 protrusions	733	736	693
	1 protrusion	101	98	95
	Mean rescue %	87.89	88.25	87.94
	STDEV.P	0.93	1.16	1.45

ucn-1 pdk1.2-3 homozygous F3

		Cross 1	Cross 2	Cross3
Plant1	0 protrusions	134	246	287
	1 protrusion	24	40	52
	% rescue	84.81	86.01	84.66
Plant2	0 protrusions	269	268	308
	1 protrusion	36	39	42
	% rescue	88.20	87.30	88.00
Plant3	0 protrusions	364	294	265
	1 protrusion	51	40	32
	% rescue	87.71	88.02	89.23
total	N	878	927	986
	0 protrusions	767	808	860
	1 protrusion	111	119	126
	Mean rescue %	87.36	87.16	87.22
	STDEV.P	1.50	0.83	1.93

Continued on next page.

	Col-0	Ler	*ucn-1/-* Ler	Ler *ucn-1/-*	*ucn-1/-* Col-0	Col-0 *ucn-1/-*		
0 protrusions	231	264	167	248	475	611		
1 protrusion	0	0	1583	1720	1694	1690		
2 protrusions	0	0	285	261	159	157		
> 2protrusions	0	0	57	32	20	19		
N	231	264	2092	2261	2348	2477		
			ucn-1 (Ler)		ucn-1 (Col-0)			
0 total	231	264	415		1086			
1 total	0	0	3303		3384			
2 total	0	0	546		316			
> 2 total	0	0	89		39			
N total	231	264	4353		4825			
% 0	100	100	9.533654951		22.50777202			
% 1	0	0	75.87870434		70.13471503			
% 2	0	0	12.54307374		6.549222798			
% >2	0	0	2.044566965		0.808290155			

	pdk1.1-1 ucn-1	*ucn-1 pdk1.1-1*	*pdk1.1-2 ucn-1*	*ucn-1 pdk1.1-2*	*pdk1.2-2 ucn-1*	*ucn-1 pdk1.2-2*	*pdk1.2-3 ucn-1*	*ucn-1 pdk1.2-3*
0 protrusions	1946	1840	2211	2074	2232	2162	2413	2435
1 protrusion	410	508	518	573	216	294	267	356
2 protrusions	0	0	0	0	0	0		0
> 2protrusions	0	0	0	0	0	0		0
N	2356	2348	2729	2647	2448	2456	2680	2791
	pdk1.1 ucn-1				***pdk1.2 ucn-1***			
0 total	8071				9242			
1 total	2009				1133			
2 total	0				0			
> 2 total	0				0			
N total	10080				10375			
% 0	80.06944444				89.07951807			
% 1	19.93055556				10.92048193			
% 2	0				0			
% >2	0				0			
	Σ =30,128							

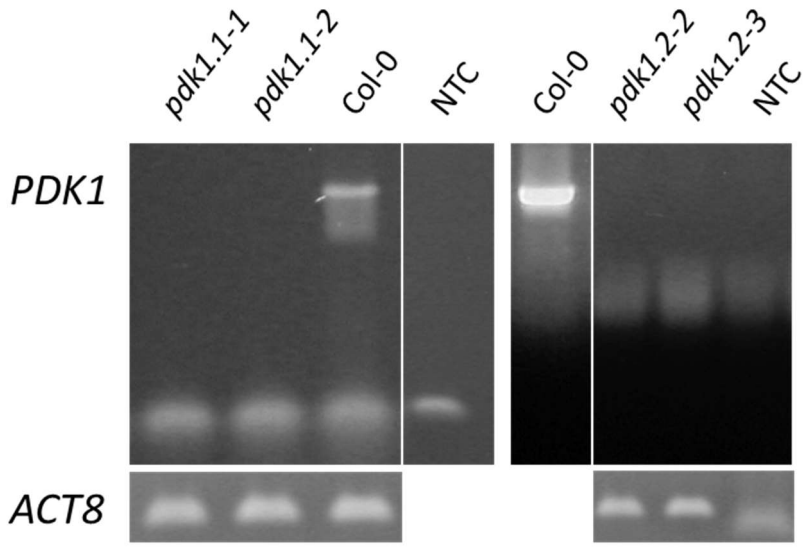

Figure 7-2 *PDK1.1, PDK1.2* and *ACT8* transcript amounts in *pdk1* T-DNA lines and Col-0.

The *pdk1* T-DNA lines do not contain the respective *PDK1* transcripts. *ACTIN8* was used as a control.

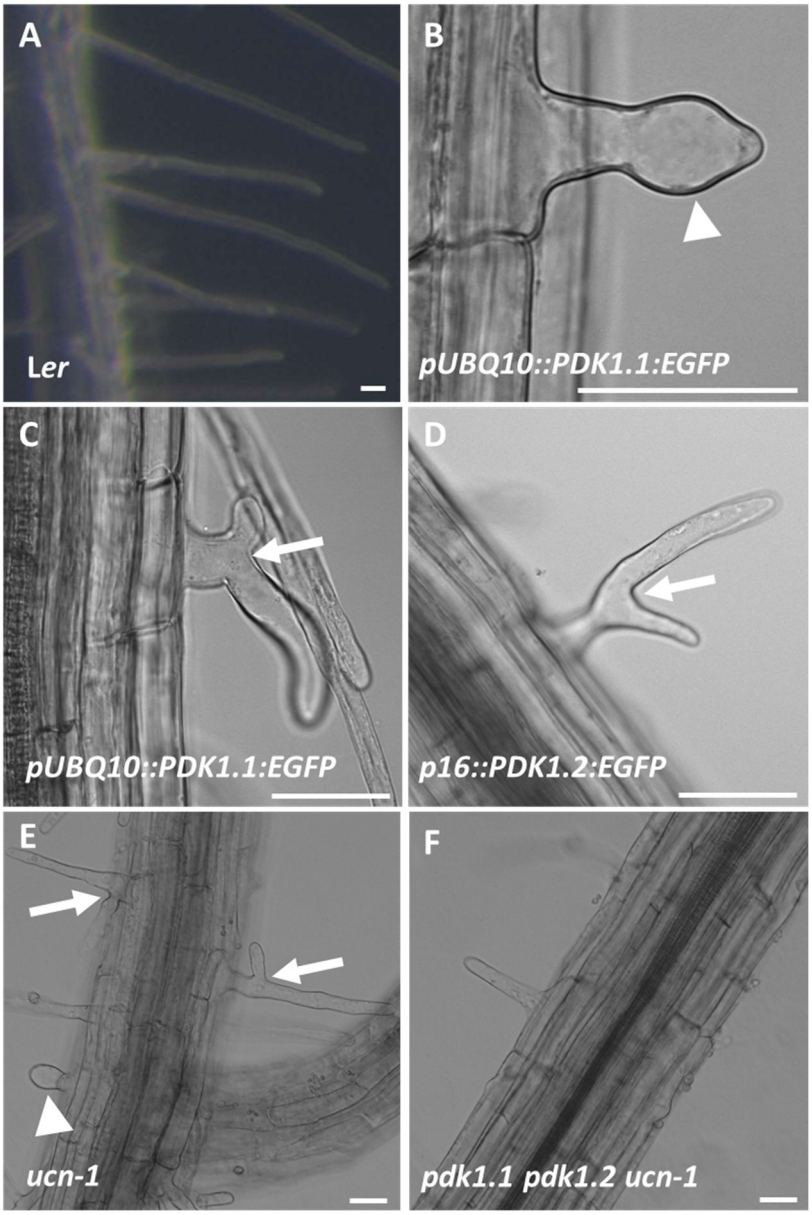

Figure 7-3 Root hair phenotypes.

Light micrographs of root hairs. (A) Phase contrast depicting L*er* root hairs. (B – F) DIC images. (B – D) Three independent *PDK1* overexpressors. (E) *ucn-1* and (F) *pdk1.1 pdk1.2 ucn-1* triple mutant. Please note aberrant root hair polarity in B – E. Arrows indicate branching, arrowheads ballooning of the root hairs. The *pdk1* knockout rescues branching and ballooning of *ucn-1*. Scale bars: 20 µm.

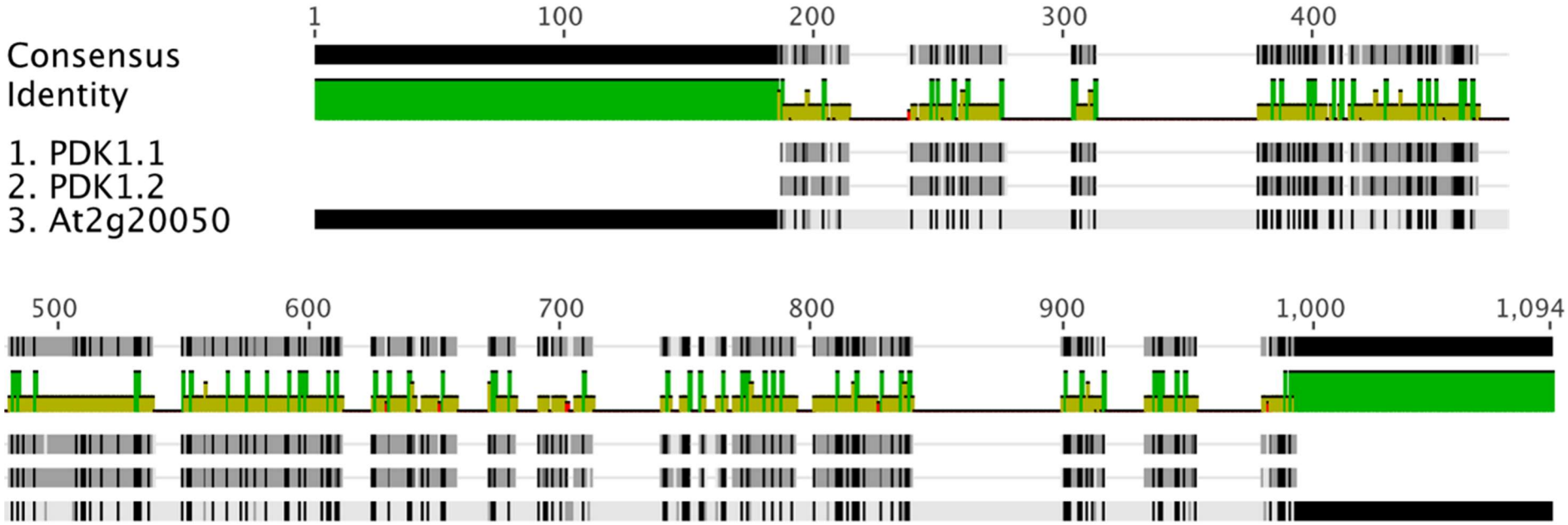

Figure 7-4 Protein alignment of PDK1.1, PDK1.2, and At2g20050.

The alignment was performed using ClustalW algorithm and BLOSUM62 matrix in Geneious software. The brighter the grey value the less similar are the sequences. Lines represent gaps. Please note that the black bars (AA 1 – 187, and 993 - 1094) are unique to At2g20050. The protein sequence analysis reveals that At2g20050 does not represent a third Arabidopsis PDK1, as claimed by Zulawski et al. (2014).

8 DANKSAGUNG

Zunächst möchte ich meinem Doktorvater Prof. Dr. Kay Schneitz herzlich für die Möglichkeit danken, dieses faszinierende Thema bearbeitet haben zu können. Außerdem für seine Unterstützung in vielerlei Hinsicht, sowie den Input durch wissenschaftliche Diskussionen und Anregungen. Kay hat mir die Möglichkeit gegeben, an einem spannenden Thema eigenverantwortlich zu arbeiten und den Grundstein für meine Karriere zu legen. Vielen Dank!

Des Weiteren danke ich Frau Prof. Dr. Brigitte Poppenberger-Sieberer für die Übernahme des Zweitgutachtens, und Herrn Prof. Dr. Erwin Grill für die Bereitschaft den Vorsitz der Kommission zu übernehmen.

Ich danke der gesamten AG Schneitz und ehemaligen Mitgliedern, mit denen man sich austauschen, Probleme erörtern oder einfach mal ein Bier trinken konnte. Besonderer Dank gilt unseren Technischen Assistentinnen Regina und Katrin für die Laborорganisation, Pflanzenpflege, viele Stunden, Tage und Wochen des Klonierens und *In-situ*-Hybridisierens. Außerdem danke ich Prasad, Janys und Ajeet für anregenden wissenschaftlichen Austausch und Unterstützung, und allen anderen Mitgliedern des SNZ-Labs für die gute Arbeitsatmosphäre. Besonders möchte ich Susanna hervorheben, die durch ihre direkte, erfrischende Art seit Frühjahr 2016 als Sekretärin neuen Schwung mitgebracht hat, und für das ein oder andere Päuschen ;).

Außerdem danke ich den Mitarbeiterinnen und Mitarbeitern der Lehrstühle für Botanik und Systembiologie der Pflanzen für die gemeinsame Nutzung von Geräten und eine gute Arbeitsatmosphäre.

Außerordentlich dankbar und zufrieden bin ich damit, dass ich durch das Zusammentreffen mit einigen Menschen am Institut mittlerweile gute Freunde gewonnen habe, die ich nicht mehr missen möchte. Danke liebe *Botany Allstars and Friends*. Manche Menschen, die man im Leben trifft, vergisst man auch wieder, andere hinterlassen Spuren und Erinnerungen fürs ganze Leben. Namentlich sind hier zu nennen: Katha, mit der mich seit über 15 Jahren eine tiefe Freundschaft verbindet, die bisher trotz der großen räumlichen Distanz alles überdauert hat. Katja, Vio und Georg, mit denen ich seit Beginn des Biostudiums vor ziemlich genau 10 Jahren durch dick und dünn gehe und die immer für mich da sind. Co und co., die aus der Erlanger Zeit übriggeblieben sind. Steffi, Teresa, Moritz und meiner WG, die Freising von einem Kaff, in dem ich nicht sein wollte, zu einem Zuhause gemacht haben.

Meiner Familie, insbesondere meinen Eltern, bin ich sehr dankbar, dass sie mich immer unterstützt haben und es erst durch sie möglich geworden ist, dass ich jetzt hier sitze und meine Doktorarbeit mit dieser Danksagung beende.

Zum Wohle!

9 CURRICULUM VITAE

Persönliche Angaben

1.	Nachname	Scholz
2.	Vorname	Sebastian
3.	Geburtsdatum	23.06.1987
4.	Geburtsort	Siegen
5.	Staatsangehörigkeit	Deutsch

6. Ausbildung und Beruf

seit 11/2012	Wissenschaftlicher Mitarbeiter, Professur für Entwicklungsbiologie der Pflanzen, TU München, Emil-Ramann-Str. 4, 85354 Freising.
10/2010 – 09/2012	Studium der Zell- und Molekularbiologie, Friedrich-Alexander-Universität Erlangen-Nürnberg. Abschluss: Master of Science (M.Sc.)
10/2007 – 09/2010	Studium der Biologie (bis 03/2009 in Verbindung mit Chemie), FAU Erlangen-Nürnberg. Abschluss: Bachelor of Science (B.Sc.)
10/2006 – 09/2007	Studium der Humanmedizin, FAU Erlangen-Nürnberg
23.06.2006	Allgemeine Hochschulreife (Abitur), Gymnasium Schloss Wittgenstein
7. Titel der Dissertation	Regulatory feedback between AGC kinases coordinating Arabidopsis ovule integument growth.
8. Betreuer	Prof. Dr. Kay Schneitz
9. Publikationen	1. LE BAIL A, SCHOLZ S, AND KOST B. 2013. Evaluation of reference genes for RT qPCR analyses of structure-specific and hormone regulated gene expression in *Physcomitrella patens* gametophytes. PloS one 8: e70998. 2. VADDEPALLI P, SCHOLZ S, AND SCHNEITZ K. 2015. Pattern formation during early floral development. Curr Opin Genet Dev 32: 16-23.